Upper upper Albian (Mortoniceras rostratum Zone) cephalopods from Clansayes (Drôme, south-eastern France).

Romain Jattiot, Jens Lehmann, Benjamin Latutrie, Amane Tajika, Emmanuelle Vennin, Pauline Vuarin, Arnaud Brayard, Emmanuel Fara, Vincent Trincal

Acta Geologica Polonica, Vol. 72 (2022), No. 2, pp. 187–233
DOI: 10.24425/agp.2021.139308

Upper upper Albian (*Mortoniceras rostratum* Zone) cephalopods from Clansayes (Drôme, south-eastern France)

ROMAIN JATTIOT[1,*], JENS LEHMANN[1], BENJAMIN LATUTRIE[2], AMANE TAJIKA[3, 4], EMMANUELLE VENNIN[5], PAULINE VUARIN[6], ARNAUD BRAYARD[5], EMMANUEL FARA[5] and VINCENT TRINCAL[7]

[1] *Fachbereich 5 Geowissenschaften, Universität Bremen, Klagenfurter Strasse 4, 28357, Bremen, Germany. E-mail: jattiot@uni-bremen.de*

[2] *La Grange, 9003 En Cros, route de Garrigues, 81500, Lavaur, France. E-mail: benjamin.latutrie@gmail.com*

[3] *Division of Paleontology (Invertebrates), American Museum of Natural History, Central Park West 79th Street, New York, NY, 10024, USA. E-mail: atajika@amnh.org*

[4] *University Museum, University of Tokyo, Hongo 7-3-1, Bunkyo-ku, Tokyo, 113-0033, Japan*

[5] *UMR CNRS 6282 Biogéosciences, Université Bourgogne Franche-Comté, 6 Boulevard Gabriel, F-21000 Dijon, France. E-mails: emmanuelle.vennin@u-bourgogne.fr, arnaud.brayard@u-bourgogne.fr, emmanuel.fara@u-bourgogne.fr*

[6] *Université de Lyon, Université Lyon 1, CNRS, Laboratoire de Biométrie et Biologie Évolutive UMR 5558, F-69622 Villeurbanne, France.*

[7] *LMDC, INSAT/UPS Génie Civil, 135 Avenue de Rangueil, 31077 Toulouse cedex 04, France.*

** Corresponding author*

ABSTRACT:

Jattiot, R., Lehmann, J., Latutrie, B., Tajika, A., Vennin, E., Vuarin, P., Brayard, A., Fara, E. and Trincal, V. 2022. Upper upper Albian (*Mortoniceras rostratum* Zone) cephalopods from Clansayes (Drôme, south-eastern France). *Acta Geologica Polonica*, **72** (2), 187–233. Warszawa.

We document an upper upper Albian (*Mortoniceras rostratum* Zone) cephalopod assemblage from Clansayes (Drôme, south-eastern France). Although fossils are rare in local exposures and in the single sampled level, a decade of intensive fossil collecting yielded 290 ammonite and 5 nautilid specimens. In total, we describe 1 species of nautilid and 24 species (within 17 genera) of ammonites, including 13 heteromorphs. Only two of these ammonite taxa were previously recorded from the upper upper Albian at Clansayes, which demonstrates the value of this fauna with regard to taxonomy, palaeobiology and palaeobiogeography. Based on morphological and biometric analyses performed on an extensive material (104 specimens), we discriminate two species for the heteromorphic ammonite genus *Mariella* Nowak, 1916 within the *Mortoniceras rostratum* Zone. In addition, we investigate shell chirality patterns in *Mariella* from the late Albian of southern France. Upon comparison of the Clansayes material with older material from the immediately underlying upper Albian *Mortoniceras fallax* Zone at the neighbouring Salazac locality, we identify an increase in the proportion of sinistral specimens. This observed increase in the frequency of sinistral *Mariella* specimens may hypothetically be part of a global evolutionary pattern, considering that nearly all documented younger Cenomanian *Mariella* (and more generally Cenomanian turrilitids) are sinistral.

Key words: Ammonites; Cretaceous; Upper Albian; Taxonomy; South-eastern France; Shell chirality.

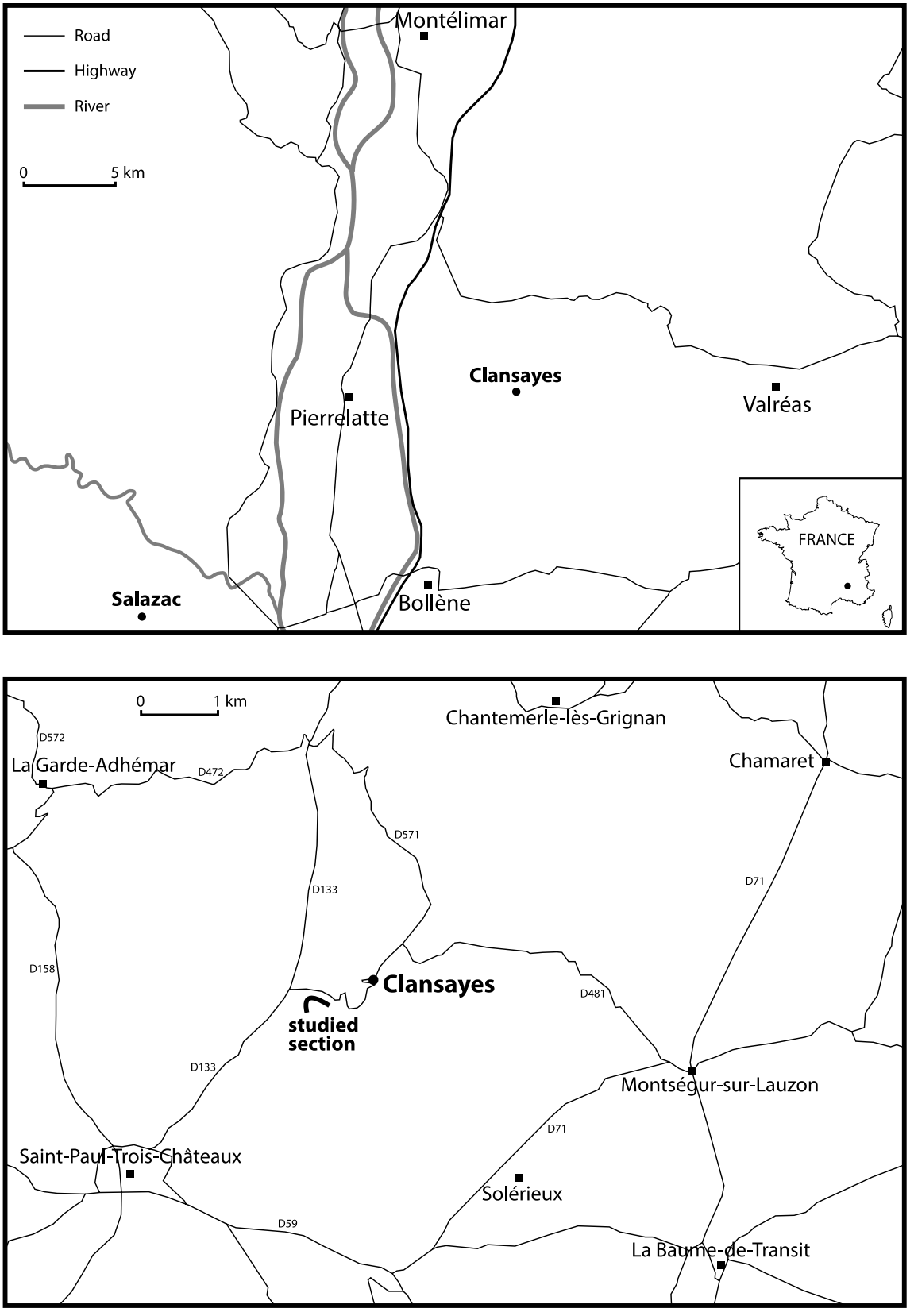

Text-fig. 1. Location of the studied section near Clansayes, Drôme, France.

INTRODUCTION

Owing to their rich and diverse fossil content, Lower Cretaceous strata of south-eastern France have been the focus of considerable work (e.g., for the Albian, Hébert and Munier-Chalmas 1875; Jacob 1905, 1907; Breistroffer 1936, 1940a, b, 1947; Scholz 1973; Delanoy and Latil 1988; Wright and Kennedy 1994; Kennedy and Delamette 1994a, b; Latil 1989, 1994; Gale *et al*. 1996, 2011; Amédro and Robaszynski 2000; Kennedy *et al*. 2000, 2014, 2017; Amédro 2002, 2008; Herrle and Mutterlose 2003; Kennedy and Latil 2007; Joly and Delamette 2008; Robaszynski *et al*. 2008; Petrizzo *et al*. 2012; Jattiot *et al*. 2021). A classical ammonite level is located in the vicinity of the Clansayes village (Drôme; Text-fig. 1) and was initially studied in the early 20th century (Jacob 1905). Based on a few specimens from this level, Breistroffer (1947) defined a new substage representing the upper Aptian, namely the 'Clansayesien'. Although the use of the 'Clansayesien' substage in the stratigraphical nomenclature remains somewhat controversial (Debelmas *et al*. 2004), this ammonite horizon and its biostratigraphic interpretation by Breistroffer (1947) significantly influenced subsequent works pertaining to European ammonite zonation around the Aptian–Albian boundary (e.g., Owen 1984a, b, 1999).

Apart from those related to this classical, now inaccessible, 'Clansayesien' horizon, reports of ammonites from the Clansayes locality are rare. To our knowledge, this includes only the works by Sornay (1950) and Debelmas *et al*. (2004) who documented a total of four upper upper Albian taxa from glauconitic sandstones that crop out in the Clansayes area, namely '*Anisoceras* cf. *perarmatum*' Pictet and Campiche, 1861, '*Pervinquiera* aff. *Rostrata*' (J. Sowerby, 1817), '*Stoliczkaia* sp.' and '*Mortoniceras inflatum*' (J. Sowerby, 1818). However, these taxonomical identifications are not supported by any illustrations and therefore need a reinvestigation. In turn, until now, upper upper Albian ammonites from this locality were virtually unknown.

A decade of intensive sampling within a single level from an upper upper Albian section southwest of the Clansayes village (Text-fig. 1) yielded a rich cephalopod fauna (including 290 ammonites, studied herein), indicative of the *Mortoniceras* (*Subschloenbachia*) *rostratum* Zone (Text-fig. 2). Based on this material, we carry out a thorough taxonomical work including classical descriptive documentation as well as morphological and biometric analyses performed on selected subdatasets, notably the heteromorphic genera *Hamites* Parkinson, 1811 and *Mariella* Nowak, 1916. Additionally, we reconstruct the depositional environments of this locality and integrate our interpretations into a broader, more regional framework to better understand the palaeoecological structuration at that time.

	Ammonite zones and subzones	
Cenomanian (pars)	*Mantelliceras mantelli*	*Mantelliceras saxbii*
		Sharpeiceras schlueteri
		Neostlingoceras carcitanense
	Arrhaphoceras briacense	
upper upper Albian «Vraconnian»	*Mortoniceras perinflatum*	
	Mortoniceras rostratum	
	Mortoniceras fallax	
upper Albian (s. s.)	*Mortoniceras inflatum*	
	Mortoniceras pricei	
	Dipoloceras cristatum	

Text-fig. 2. European upper upper Albian ammonite zonal succession (modified after Amédro and Matrion 2014; Reboulet *et al*. 2018).

GEOLOGICAL AND STRATIGRAPHIC SETTINGS

The Clansayes area is part of the sandy glauconitic peripheral domains of the Vocontian Trough composed of deep pelagic facies (Bréhéret 1997; Ferry 1999). The preserved deposits of the Albian succession show significant changes in thickness and facies, which reflect synsedimentary tectonics (Ferry 1999, 2017). The Clansayes area is located between the proximal Salazac area (see Jattiot *et al*. 2021) and a transitional domain of maximum subsidence related to fault dynamic in the Marcoule area (Amédro 2008; Text-fig. 3). As proposed by Ferry and Rubino (1988) and Ferry (1999), this thick glauconitic sandstone succession results from successive Albian transgressions.

Biostratigraphy

Kennedy and Latil (2007), Kennedy *et al*. (2008), Amédro and Matrion (2014) and Reboulet *et al*. (2018) recognised the following zonal sequence for the upper

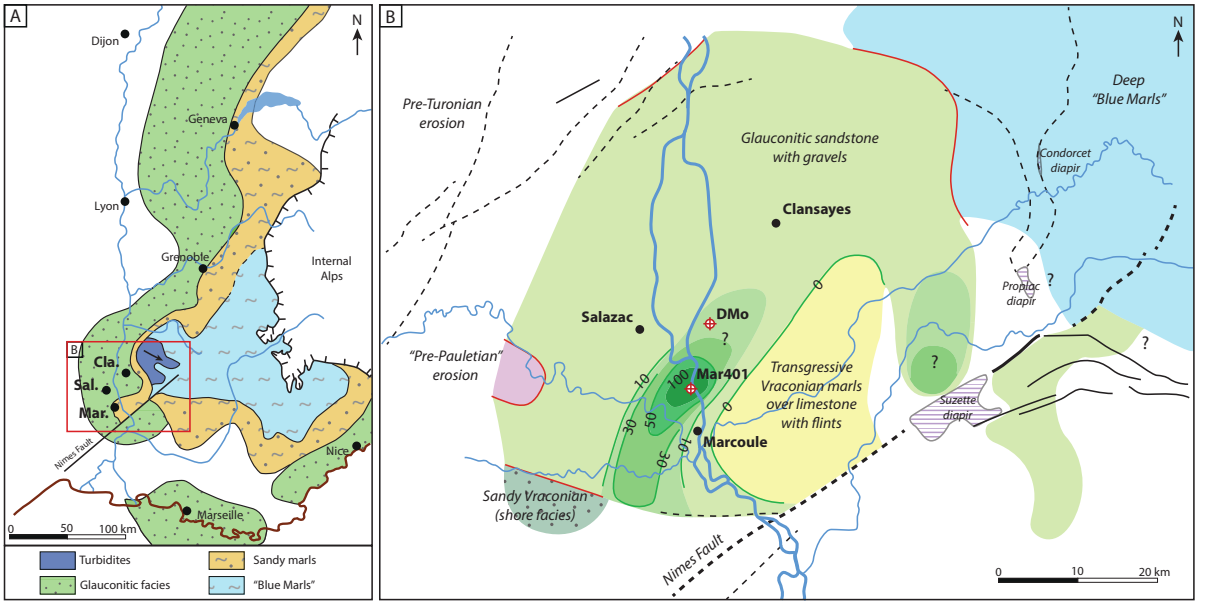

Text-fig. 3. Geological setting of the study area. A – Main domains of sedimentation in southern France during the latest Albian (modified after Ferry 1999, 2017 and Amédro 2008) and position of the Clansayes, Salazac and Marcoule localities. B – Palaeogeographic reconstitution of the Albian succession (DMo and Mar401 correspond to the Marcoule drillings; modified after Ferry 2017), light to dark green shades show the increasing subsidence of the basin with a transition from glauconitic sandstone to sandy marls (see Text-fig. 3A for facies distribution). Abbreviations: Cla., Clansayes; Sal., Salazac; Mar., Marcoule.

upper Albian in Europe: *Mortoniceras* (*Mortoniceras*) *fallax* Zone, *Mortoniceras* (*Subschloenbachia*) *rostratum* Zone, *Mortoniceras* (*Subschloenbachia*) *perinflatum* Zone and *Arrhaphoceras* (*Arrhaphoceras*) *briacense* Zone (from oldest to youngest; Text-fig. 2). This sequence corresponds to the classic *Stoliczkaia dispar* Zone of previous authors (e.g., Latil 1994) and to the 'Vraconnian' *sensu* Amédro (2008).

Lithostratigraphy

The Clansayes area shows a thick glauconite-rich sandstone succession passing upward into bioturbated sandstone layers characterised by the presence of ammonites indicative of the *Mortoniceras* (*S.*) *rostratum* Zone. This succession records a vertical evolution from Unit 1 to 3 (Text-fig. 4).

Unit 1 (Text-fig. 4) consists mainly of bioturbated sandy marls with small-scale (10-20 cm thick) sequences composed of medium-size sandstones, with some pebbles and flat pebbles resting on erosive base, and cross-stratified to rippled sands passing upward into massive fine-grained sandstones to siltstones with intense bioturbation. The pluri-cm thick layers are composed of complex-stratified beds, swaley-cross stratification and ripples often showing a fining upward sequence. These deposits are related to currents and waves and the presence of fine sand and silt on top of them is considered as highly-bioturbated suspension after storm events.

Unit 2 (Text-fig. 4) shows an increase in grain size with thin gravel lags, and a decrease in bioturbation intensity. These quartz sandstones with low bedding preserved are characterised by wavy erosion surfaces, marked by thin lags of coarse sands to gravels. Sorting of sandstones is often poor with quartz forming thin lenses of patchy distribution. Bioturbation is abundant in some intervals and the coarser intervals are frequently cemented. These cementation events are restricted to the coarsest beds due to their high primary porosity. The erosion surfaces which separate individual packages are marked by gravel lags and shallow channels and can be explained by major storm events (Arnott and Southard 1990). These current-dominated sandstones are attributed to moderate-energy deep shoreface. Units 1 and 2 are considered as a distal succession by comparison with the clastic shallow water succession observed at Salazac (Jattiot *et al*. 2021) and as a transition towards the subsiding area of Marcoule, characterised by deeper marls (Text-fig. 3). Whereas Salazac area records thick cross-bedding and coarse sandy

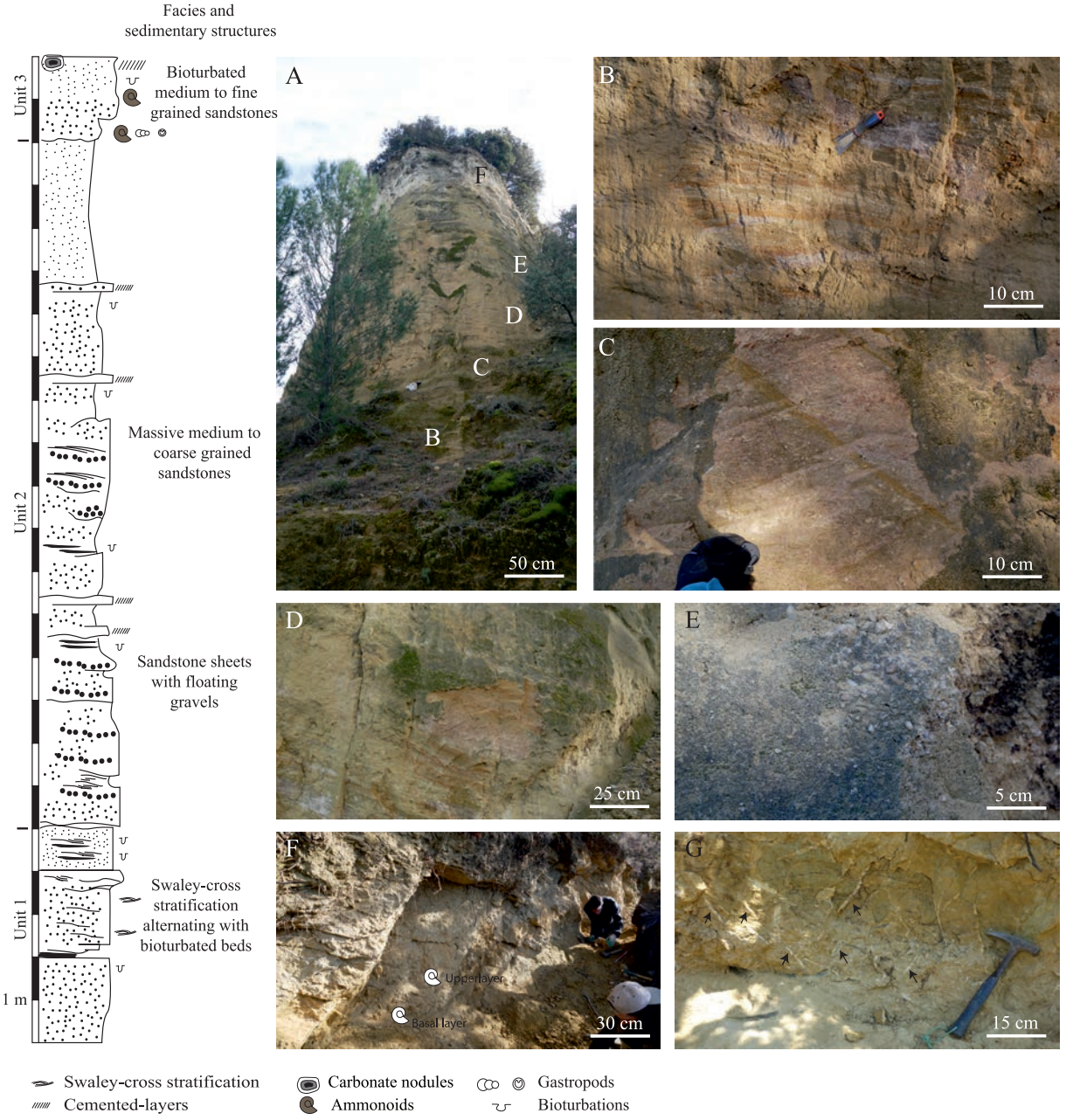

Text-fig. 4. Lithostratigraphy of the Clansayes section. A – Facies and sedimentary structures of the Clansayes section subdivided into three successive lithological units; Unit 3 being characterised by the two studied fossil-rich layers. B – Mud-drapes and reworked clay-flakes in small-scale cross-bedded sandstones (and swaley-cross stratification; Unit 1). C – Poorly sorted sandstones with bioturbation recalling *Macaronichnus* isp. (top of Unit 1). D – Massive medium grain sandstones (Unit 2). E – Massive sandstones sheets with floating gravels in storm-induced deposits (Unit 2). F – Fossiliferous basal and upper layers embedded in a bioturbated sandstone, passing vertically to a bioturbated fine to medium-grained sandstone (Unit 3). G – Dense ophiomorphid bioturbations (black arrows) in Unit 3.

deposits deposited on a proximal ramp, the Clansayes succession is characterised by a distal prograding shelf margin wedge above the storm wave base as indicated by the presence of storm-induced deposits. The unidirectional oblique stratification observed at Salazac may result from an oceanic north-Tethyan current (Rubino and Delamette 1985; Ferry and Rubino 1988). At Clansayes, successive shallowing

and coarsening sandstone successions are interpreted as progradation deltaic sequences (Elliott 1974).

Unit 3 (Text-fig. 4) is a sandy unit showing two major fossiliferous layers embedded in a bioturbated sandstone. The basal layer of Unit 3 rests on an erosion base and is composed of fragmented and complete ammonites, gastropods and bivalves associated with mud-clasts and gravels. The upper layer, corresponding to a local accumulation, yields more or less complete, larger ammonites, and it passes vertically to a bioturbated fine to medium grain sandstone. Bioturbations consist in sparse to dense, vertical to oblique, occasionally bifurcating and locally cross-cutting shafts with an irregular mud lining and sand fill. Their diameters range from 5 to 100 mm but are usually close to 10 mm. These ophiomorphid structures can be tentatively assigned to *Ophiomorpha* cf. *nodosa* Lundgren, 1891. There is no sedimentological evidence for condensation or mixing of faunas; ammonites from both fossiliferous layers are indicative of the *Mortoniceras* (*S.*) *rostratum* Zone.

The basal fossiliferous layer of Unit 3 is considered as resulting from the same process related to the deposition of the coarse sandstones with gravels and phosphatic nodules at Salazac (Jattiot *et al*. 2021). This fossiliferous layer is interpreted as transgressive deposits on top of a shelf margin wedge (Ferry 1999; Amédro 2008) associated with the transport of large quantities of sand from the coast to a distal ramp. The upper fossiliferous layer of this unit is interpreted as resulting from storm-induced events.

From a taphonomical point of view, two types of selective preservation occur within Unit 3. The basal layer yields well-preserved, non-distorted, small and brownish ammonites. As a general rule, larger ammonites are preserved as fragments in this layer. Conversely, the upper layer contains only notably large ammonites preserved as significantly worn, orangish-yellowish internal moulds. Most specimens are deformed, crushed to various degrees. Inner whorls are systematically heavily crushed or absent. The accompanying fauna, extremely poorly preserved, is depauperate in small-size individuals. At the transition between the two layers, specimens display an intermediate preservation.

MATERIAL AND METHODS

All examined fossils are from Clansayes and were retrieved from a single level (comprising two fossiliferous layers) representing the *Mortoniceras* (*S.*) *rostratum* Zone (see above).

Studied specimens are deposited in the collections of the Université de Bourgogne, Géologie Dijon (UBGD), France. The dataset includes 290 studied ammonites (Supplementary Appendix available only in online version), of which the *Mariella* and *Hamites* specimens were used for quantitative morphological and biometric analyses. The dataset on *Mariella* coiling (dextral or sinistral) was extended by including additional Clansayes specimens (N = 55) from a private collection. Each set of measurements for coiled ammonites includes classical geometric parameters of the ammonoid conch such as shell diameter (D), and corresponding whorl height (H), whorl width (W) and umbilical diameter (U). In addition to the three classical ratios H/D, W/D and U/D, the ratio W/H is also used as a descriptor of the whorl section. Regarding heteromorphic ammonites, the number of tubercles in each row per whorl in *Mariella,* as well as the number of ribs in a distance equal to maximum preserved whorl height (= rib index) in *Hamites*, were determined whenever possible. Additionally, we defined a visual index representing tubercle strength for each *Mariella* specimen. This index is scored from 1 to 5, 1 corresponding to barely conspicuous tubercles and 5 to markedly prominent tubercles. The preservation of specimens precluded in most cases examination of suture lines. Because most ammonite specimens from Clansayes are moderately preserved only (the surface of the internal moulds is often significantly worn), we used different main light positions for the photographs. This is to highlight important ornamental features barely visible. In the plates, a star indicates the visible or approximately assessed beginning of the body chamber, whenever possible. Therefore, absence of star either means that the specimens are fully chambered phragmocones or that the beginning of the body chamber was undeterminable.

All statistical analyses were implemented with R, version 4.1.0 (R Core Team 2021). Whether parameter distributions are unimodal or at least bimodal was tested with the Hartigans' dip test ('dip.test' function of the 'diptest' package; Hartigan and Hartigan 1985). A generalised linear model (GLM) with a Poisson family of errors was performed to analyse whether the number of tubercles in each row per whorl covaries with the maximum preserved whorl height in *Mariella*. The significance level was set to $P < 0.05$.

SYSTEMATIC PALAEONTOLOGY

Most of the species described below are frequently mentioned in the literature. Thus, we include

only the most recent citations in the synonymy lists along with the citation of the original description. Uncertain values in the measurements section of each species are in italics.

Order Ammonoidea Zittel, 1884
Suborder Phylloceratina Arkell, 1950
Superfamily Phylloceratoidea Zittel, 1884
Family Neophylloceratidae Joly, 1993
Subfamily Hyporbulitinae Joly, 1993
Genus *Hyporbulites* Breistroffer, 1947

TYPE SPECIES: *Phylloceras velledae* var. *seresitensis* Pervinquière, 1907 (p. 52), by the subsequent designation of Breistroffer (1947, p. 98).

Hyporbulites seresitensis (Pervinquière, 1907)
(Pl. 1, Figs 1–4)

1907. *Phylloceras velledae* var. *seresitensis* Pervinquière, p. 52.
2009. *Hyporbulites seresitensis seresitensis* (Pervinquière, 1907); Klein *et al*., pp. 90, 93 (with full synonymy).
2019. *Phylloceras* (*Hypophylloceras*) *seresitense seresitense* (Pervinquière, 1907); Kennedy in Gale *et al*., p. 189, pl. 1, figs 11–18; pl. 2, figs 13, 14, 21, 22; text-fig. 13B.
2020. *Phylloceras* (*Hypophylloceras*) *seresitense seresitense* (Pervinquière, 1907); Kennedy, p. 154, pl. 2, figs 14–18; pl. 3, figs 21, 22.
2021. *Hyporbulites seresitensis* (Pervinquière, 1907); Jattiot *et al*., p. 4, fig. 4I–V (with additional synonymy).

TYPE (after Kennedy 2020): Pervinquière (1907, p. 52) introduced *seresitensis* as a variety of *Phylloceras velledae* of Michelin (1834), but did not figure any of the 20 specimens he mentioned. See Kennedy in Gale *et al*. (2019, p. 190) and Kennedy (2020, p. 154) for further discussion.

MATERIAL: Two wholly septate specimens; UBGD 293051, 293052.

MEASUREMENTS:

	D	H	W	U	W/H
UBGD 293051 (Pl. 1, Figs 1–3)	*38.0 (100)*	21.4 (*56.3*)	13.4 (*35.3*)	1.9 (*5.0*)	0.63
UBGD 293052 (Pl. 1, Fig. 4)	~ 55	–	–	–	–

DESCRIPTION: The shell is very involute, compressed, with nearly flat, parallel flanks and a narrowly rounded venter; surface is smooth. The whorl section is elliptic on juvenile specimens to ogival on largest specimens (see Jattiot *et al*. 2021, fig. 4I–K); maximum breadth near mid-flank. The suture line is complex with typical characteristics of *Hyporbulites*: tetraphyllic S1 and S2 saddles with elongated terminal phyllites.

DISCUSSION: The reader is referred to Joly (2000) and Jattiot *et al*. (2021). The W/H ratio of specimen UBGD 293051 (= 0.63) is comparable to that of specimens from the *Mortoniceras* (*M.*) *fallax* Zone at Salazac (Jattiot *et al*. 2021). Better preserved specimens display fine phylloceratid striation (lirae; see Joly 2000, pl. 39, fig. 15b).

OCCURRENCE (after Kennedy 2020): Upper Aptian (Balearics) to Cenomanian. The geographic distribution extends from UK (southern England), through southern France, Switzerland, Hungary, Ukraine (Crimea), northern Spain, the Balaerics, Italy (Sardinia), northern Algeria, central Tunisia, Angola, South Africa (KwaZulu-Natal), Madagascar, south India (Tamil Nadu), Russia (Sakhalin), Japan (Hokkaido), to USA (Alaska and California).

Suborder Lytoceratina Hyatt, 1889
Superfamily Tetragonitoidea Hyatt, 1900
Family Tetragonitidae Hyatt, 1900
Subfamily Tetragonitinae Hyatt, 1900
Genus *Tetragonites* Kossmat, 1895

TYPE SPECIES: *Ammonites timotheanus* Pictet in Pictet and Roux, 1847 (p. 295, pl. 2, fig. 6; pl. 3, figs 1, 2), by the original designation of Kossmat (1895, p. 131 (35)).

Tetragonites timotheanus
(Pictet in Pictet and Roux, 1847)
(Pl. 1, Figs 5–9)

1847. *Ammonites timotheanus* Pictet in Pictet and Roux, p. 39, pl. 2, fig. 6; pl. 3, fig. 1.
2009. *Tetragonites timotheanus timotheanus* (Pictet, 1847); Klein *et al*., pp. 230, 245 (with full synonymy).
2017. *Tetragonites timotheanus timotheanus* (Pictet, 1847); Tajika *et al*., p. 45, fig. 11AJ, AK.
2018a. *Tetragonites timotheanus timotheanus* (Pictet, 1847); Tajika *et al*., p. 249, fig. 474.
?2019. *Tetragonites subtimotheanus* Wiedmann, 1962; Kennedy in Gale *et al*., p. 192, pl. 2, figs. 7–12; pl. 3, figs. 1–6; text-fig. 14D.

?2019. *Tetragonites subtimotheanus* Wiedmann, 1962; Gautam *et al*., p. 17, figs 5C–E.
2021. *Tetragonites timotheanus* (Pictet, 1847); Jattiot *et al*., p. 4, fig. 4W–AB (with additional synonymy).

TYPE: The lectotype, by the subsequent designation of Wiedmann (1962), is one of the original specimens of *Ammonites timotheanus* of Pictet (in Pictet and Roux 1847, p. 39, pl. 3, fig. 1), from the upper Albian of Saxonet (Savoie, France); it was refigured by Wiedmann (1973, pl. 7, fig. 6).

MATERIAL: Two wholly septate specimens; UBGD 293040, UBGD 293041.

MEASUREMENTS:

	D	H	W	U	W/H
UBGD 293040 (Pl. 1, Figs 5, 6)	12.0 (100)	4.7 (39.2)	–	3.7 (30.8)	–
UBGD 293041 (Pl. 1, Figs 7–9)	20.7 (100)	–	–	–	–

DESCRIPTION: The shell is moderately evolute and smooth. There are four constrictions per half whorl, strongly prorsiradiate on flanks and feebly convex on the venter. The whorl section is depressed trapezoidal, with a flat venter and slightly angular ventrolateral shoulders; maximum breadth near umbilicus.

DISCUSSION: See Jattiot *et al*. (2021).

OCCURRENCE: Lower Cretaceous (middle Albian to lower Cenomanian); UK (England), Spain, France, Germany, Hungary, Iran, India, Egypt, Madagascar.

Family Gaudryceratidae Spath, 1927
Genus *Anagaudryceras* Shimizu, 1934

TYPE SPECIES: *Ammonites sacya* Forbes, 1846 (p. 113, pl. 14, fig. 10), by the original designation of Shimizu (1934, p. 67).

Anagaudryceras sp.
(Pl. 1, Figs 10, 11)

MATERIAL: One specimen consisting of a small, incomplete nucleus; UBGD 293055.

MEASUREMENTS:

	D	H	W	U	W/H
UBGD 293055 (Pl. 1, Figs 10, 11)	~ 26	*7.5*	*11*	–	*1.47*

DESCRIPTION: The shell is very evolute (the umbilicus roughly estimated to comprise about 50% of the diameter) and low-whorled, the whorls slowly expanding. The umbilicus is relatively shallow, with a low umbilical wall that slopes outwards, merging with the inflated flanks. The whorl section is extremely depressed, reniform (W/H = 1.47), with a broad, somewhat flattened venter. The inner whorls display fine, dense lirae, as well as a barely perceptible constriction and a possible collar rib. The partly preserved external whorl exhibits rarely preserved lirae. They arise at the umbilical seam, pass slightly forward across the umbilical wall and shoulder, and are distinctly prorsiradiate on the flanks, on which they are feebly flexed (forward to mid-flank, backward across the ventrolateral shoulder). They do not appear to cross the venter. Additionally, there appear to be a few ribs, similar in shape to the lirae but slightly thicker. More conspicuously, the external whorl bears a deep, relatively broad constriction associated with a distinctive collar rib. The latter, which is parallel to the lirae, exhibits a gently rounded apical slope and a steep, abrupt apertural slope, thus producing a singular scale-like appearance.

DISCUSSION: Although it invites comparison with the type specimens of *A. pulchrum* (Crick, 1907) from the Upper Albian of Zululand (Kennedy and Klinger 1979, pl. 13, figs 1–3), this single specimen is too small and poorly preserved for identification to specific level.

Suborder Ammonitina Hyatt, 1889
Superfamily Desmoceratoidea Zittel, 1895
Family Desmoceratidae Zittel, 1895
Subfamily Desmoceratinae Zittel, 1895
Genus and subgenus *Desmoceras* Zittel, 1884

TYPE SPECIES: *Ammonites latidorsatus* Michelin, 1838, by the subsequent designation of Böhm (1895, p. 364).

Desmoceras (*Desmoceras*) *latidorsatum*
(Michelin, 1838)
(Pl. 1, Figs 12–25)

1838. *Ammonites latidorsatus* Michelin, p. 101, pl. 12, fig. 9.
2007. *Desmoceras* (*Desmoceras*) *latidorsatum* (Michelin, 1838); Kennedy and Latil, p. 458, pl. 2, fig. 1; pl. 6, figs 2, 3; text-fig. 4.
2011. *Desmoceras* (*Desmoceras*) *latidorsatum* (Michelin,

1838); Klein and Vašíček, pp. 141, 144 (with additional synonymy).

2013. *Desmoceras latidorsatum* (Michelin, 1838); Bermúdez *et al*., p. 2587, fig. 3B, C.

2018a. *Desmoceras* (*Desmoceras*) *latidorsatum* (Michelin, 1838); Tajika *et al*., p. 259, fig. 499.

2019. *Desmoceras* (*Desmoceras*) *latidorsatum* (Michelin, 1838); Kennedy in Gale *et al*., p. 206, pl. 4, figs 19–25; pl. 11, figs 7–14).

2019. *Desmoceras* (*Desmoceras*) *latidorsatum* (Michelin, 1838); Gautam *et al*., p. 20, fig. 6f, g (with additional synonymy).

2020. *Desmoceras* (*Desmoceras*) *latidorsatum* (Michelin, 1838); Kennedy, p. 168, pl. 7, figs 16–18; pl. 8, figs 14–19.

2021. *Desmoceras* (*Desmoceras*) *latidorsatum* (Michelin, 1838); Jattiot *et al*., p. 8, fig. 5A–Q (with additional synonymy).

2021. *Desmoceras* (*Desmoceras*) *latidorsatum* (Michelin, 1838); Latil *et al*., p. 9, fig. 8a, b.

TYPE (after Kennedy 2020): The holotype by monotypy, and now lost, is the original of Michelin (1838, p. 101, pl. 12, fig. 9), from the Albian Gault Clay of Aube, France. The neotype (Joly in Gauthier 2006, p. 97, pl. 3, fig. 1) is MNHN. F. B46095, *ex* d'Orbigny Collection 5773-B1. It is from the condensed Albian of Escragnolles, Var, France.

MATERIAL: Eight phragmocones; UBGD 293043-293050.

MEASUREMENTS:

	D	H	W	U	W/H
UBGD 293043 (Pl. 1, Figs 24, 25)	23.4 (100)	10.8 (46.2)	13.1 (56.0)	5.0 (21.4)	1.21
UBGD 293044	–	14.2	16.5	–	1.16
UBGD 293045 (Pl. 1, Figs 12–14)	30.3 (100)	14.0 (46.2)	16.8 (55.4)	6.8 (22.4)	1.20
UBGD 293046 (Pl. 1, Figs 15, 16)	37.0 (100)	18.9 (51.1)	17.2 (46.5)	5.6 (15.1)	0.91
UBGD 293047 (Pl. 1, Figs 17, 18)	47.6 (100)	23.3 (48.9)	23.1 (48.5)	9.0 (18.9)	0.99
UBGD 293048 (Pl. 1, Figs 19, 20)	55.1 (100)	27.6 (50.1)	30.3 (55.0)	*10.4 (18.9)*	1.10
UBGD 293049 (Pl. 1, Fig. 23)	*55.0 (100)*	24.8 (*45.1*)	29.8 (*54.2*)	–	1.20
UBGD 293050 (Pl. 1, Figs 21, 22)	19.7 (100)	9.6 (48.7)	8.7 (44.2)	3.4 (17.3)	0.91

DESCRIPTION: The shell is very involute to involute. The umbilicus is deep with high, feebly convex umbilical wall and rounded umbilical shoulders. The whorl section is highly variable, from slightly compressed (specimens UBGD 293046 and UBGD 293050; Pl. 1, Figs 15, 16, 21, 22) to inflated, even cadicone-like. Flanks are slightly convex and the venter very broadly rounded without ventrolateral shoulders; maximum breadth near umbilicus. Constrictions are absent in our material. The suture line is divided, with finely frilled elements. The saddles are more or less square and bifid; lobes are long and trifid with narrow necks and widely splayed ends. The present specimens, all preserved as internal moulds, bear a conspicuous siphonal line.

DISCUSSION: Nearly all specimens are inflated, which concurs with the assumption that late Albian populations may exhibit a preponderance of inflated forms (Cooper and Kennedy 1979; Wright and Kennedy 1984). In most localities (see e.g., Kennedy and Klinger 2013; Kennedy and Fatmi 2014; Jattiot *et al*. 2021), specimens with and without constrictions occur in variable proportions. The absence of constrictions in our entire sample (all specimens are preserved as internal moulds) is presumably not a preservational artefact, since some internal moulds of *D. latidorsatum* from the *Mortoniceras* (*M.*) *fallax* Zone at the neighbouring Salazac locality display conspicuous constrictions (Jattiot *et al*. 2021). For a thorough discussion of this species and its possible confusion with other taxa, see comprehensive accounts by Wiedmann and Dieni (1968), Cooper and Kennedy (1979), Kennedy and Klinger (2013) and Jattiot *et al*. (2021).

OCCURRENCE (after Kennedy 2020): Middle Albian to Upper Cenomanian; UK (southern England), southern France, Italy (Sardinia), northern Spain, southern Germany, Switzerland, Hungary, Romania, Serbia, Poland, Ukraine (Crimea), northern Algeria, central Tunisia, Egypt, Nigeria, Angola, South Africa (KwaZulu-Natal), Mozambique, Madagascar, south India (Tamil Nadu), Pakistan, Japan, New Zealand, Mexico and Venezuela.

Subfamily Puzosiinae Spath, 1922
Genus and subgenus *Puzosia* Bayle, 1878

TYPE SPECIES: *Ammonites planulatus* J. de C. Sowerby, 1827 (p. 136, pl. 570, fig. 5), *non* Schlotheim, 1820 (p. 59) = *Ammonites mayorianus* d'Orbigny, 1841 (p. 267, pl. 79, figs 1–3), by the subsequent designation of Douvillé (1879, p. 91).

Puzosia (*Puzosia*) *mayoriana* (d'Orbigny, 1841)
(Pl. 2; Pl. 3, Figs 1–8)

1841. *Ammonites mayorianus* d'Orbigny, p. 267, pl. 79, figs 1–3.
2007. *Puzosia* (*Puzosia*) *mayoriana* (d'Orbigny, 1841); Kennedy and Latil, p. 460, pl. 1, figs 1–6; pl. 3, fig. 1.
2011. *Puzosia* (*Puzosia*) *mayoriana* (d'Orbigny, 1841); Klein and Vašiček, pp. 67, 77 (with additional synonymy).
2017. *Puzosia* (*Puzosia*) *mayoriana* (d'Orbigny, 1841); Tajika *et al.*, p. 27, figs 6AJ, AK; 7E–H, L–O.
2018b. *Puzosia* (*Puzosia*) *mayoriana* (d'Orbigny, 1841); Tajika *et al*., fig. 2K, L.
2020. *Puzosia* (*Puzosia*) *mayoriana* (d'Orbigny, 1841); Kennedy, p. 165, pl. 6, figs 1–4, 7–10; pl. 7, figs 1, 2, 7–9, 15; text-fig. 9D (with additional synonymy).
2021. *Puzosia* (*Puzosia*) *mayoriana* (d'Orbigny, 1841); Jattiot *et al*., p. 8, figs 5R–AN, 6 (with additional synonymy).

TYPE (after Kennedy 2020): The lectotype, by the subsequent designation of Wright and Wright (1951, p. 35), is BMNH 9381, the original of J. de C. Sowerby (1827, pl. 570, fig. 5), from the Cenomanian Lower Chalk of Hamsey, near Lewes, Sussex.

MATERIAL: Fourteen specimens; UBGD 293001-293014, 293042.

MEASUREMENTS:

	D	H	W	U	W/H
UBGD 293001 (Pl. 2, Figs 1, 2)	~90	–	–	–	–
UBGD 293002	~90	–	–	–	–
UBGD 293003	~85	–	–	–	–
UBGD 293004	~80	–	–	–	–
UBGD 293005 (Pl. 2, Figs 4–6)	92.5 (100)	*30.6* (*33.1*)	*24.3* (*26.3*)	*35.8* (*38.7*)	0.79
UBGD 293006 (Pl. 2, Figs 3)	*95.0* (100)	33.7 (35.5)	–	*35.0* *(36.8)*	–
UBGD 293007 (Pl. 2, Figs 7–9)	95.0 (100)	30.5 (32.1)	*25.0* (*26.3*)	40.3 (42.4)	*0.82*
UBGD 293008 (Pl. 3, Figs 1–3)	58.4 (100)	20.7 (35.4)	21.5 (36.8)	21.4 (36.6)	1.04
UBGD 293009	–	21.4 (–)	22.9 (–)	–	1.07
UBGD 293010	–	*23.8* (–)	23.4 (–)	–	0.98
UBGD 293011	~62	22.3 (–)	22.6 (–)	–	1.01
UBGD 293012 (Pl. 3, Figs 4, 5)	22.3 (100)	8.7 (39.0)	8.5 (38.1)	7.4 (33.2)	0.98
UBGD 293013 (Pl. 3, Figs 6–8)	32.0 (100)	14.4 (45.0)	10.7 (33.4)	6.8 (21.3)	0.74
UBGD 293042	18.8 (100)	8.2 (43.6)	*8.4* (*44.7*)	4.6 (24.5)	*1.02*

DESCRIPTION: The shell coiling varies from involute to evolute; the whorl section is oval. The umbilicus is rather shallow with high, steep umbilical wall and gently rounded umbilical shoulders. Flanks are broad, slightly convex, converging towards an evenly rounded venter of variable width; maximum breadth near umbilicus. Present specimens have 3–4 constrictions per half whorl. The constrictions are straight and prorsiradiate on the inner flank, flexed back and convex at mid-flank, projected forward on the ventrolateral shoulder and form a chevron on venter. Fine, weak ribs, about as wide as the interspaces, typically arise on the outer third of the flanks (see Pl. 2, Figs 3–9). They are concave on the outer flank and pass uninterrupted across the venter, on which they form a linguoid peak. Suture line moderately indented with rather narrow asymmetrically bifid saddles and asymmetrically trifid lobes. No mature specimens (microconchs or macroconchs) were identified in our material. Most of the material from the lower part of the sampled level consists of wholly septate or incomplete juvenile macroconchs with a small portion of the body chamber preserved (e.g., specimen UBGD 293008, Pl. 3, Figs 1–3, with inner whorls not preserved), between 18.8 and about 62 mm in diameter. Specimen UBGD 293007 is the largest (95 mm in diameter; Pl. 2, Figs 7–9), best preserved specimen from the lower part of the sampled level. This specimen shows no evidence of onset of maturity, such as growth lines/ribs/suture lines approximation or lappet development, characteristic of microconchs (see Cooper and Kennedy 1987), even though 180º of its body chamber is preserved. Accordingly, this specimen is also regarded as a juvenile macroconch. Only specimen UBGD 293013 (Pl. 3, Figs 6–8) is interpreted as a juvenile microconch based on its whorl section and coiling (see discussion). All specimens from the upper part of the sampled level (Pl. 2, Figs 1–6) are poorly preserved internal moulds, between about 80 mm to about 95 mm in diameter. Their state of preservation precludes reliable measurements. Overall, they are indeed overall distorted by post-mortem crushing to varying degrees; inner whorls are always either badly crushed or not preserved. Given their size and the absence of indications of maturity, they are all regarded as juvenile macroconchs. A much larger wholly septate fragment, not identifiable at the species level, suggests that macroconch adult diameters reach at least 300 mm for the genus *Puzosia*.

DISCUSSION: We here interpret *P. sharpei* Spath, 1923 and *P. communis* Spath, 1923 as macroconchs and microconchs of *P.* (*P.*) *mayoriana*, respectively

(see also Wright and Kennedy 1984; Cooper and Kennedy 1987; Kennedy and Klinger 2014; Jattiot *et al*. 2021). Microconchs are fairly small, with adults ranging between 40–60 mm in diameter (Cooper and Kennedy 1987), whereas macroconchs are much larger. Macroconchs are also more inflated, with a somewhat wider umbilicus than microconchs, at comparable diameters (Cooper and Kennedy 1987; Jattiot *et al*. 2021). As stressed by Kennedy and Latil (2007), the co-occurrence of individuals with numerous (Pl. 2, Figs 1, 2) and fewer ribs (e.g., Pl. 2, Fig. 3) is not all that uncommon (see also Thomel 1992). The present specimens have 3–4 constrictions per half whorl; according to Cooper and Kennedy (1987), there are commonly 6–7 constrictions per whorl.

OCCURRENCE (after Kennedy 2020): Upper Albian to upper Cenomanian; UK (southern England), France, Spain, Switzerland, Germany, Poland, Romania, Bulgaria, Ukraine (Crimea), Georgia, Kazakhstan, northern Algeria, central Tunisia, Egypt, Madagascar and, possibly, Japan.

Superfamily Hoplitoidea Douvillé, 1890
Family Hoplitidae Douvillé, 1890
Subfamily Hoplitinae Douvillé, 1890
Genus *Callihoplites* Spath, 1925

TYPE SPECIES: *Ammonites catillus* J. de C. Sowerby, 1827 (p. 123, pl. 564), by the original designation of Spath (1925, p. 81).

Callihoplites cf. *cratus* (Seeley, 1865)
(Pl. 3, Figs 9–15)

1865. *Ammonites cratus* Seeley, p. 240, pl. 11, fig. 2.
2008. *Callihoplites cratus* (Seeley, 1865); Kennedy *et al*., p. 40, pl. 5, figs 18, 19.
2008. *Callihoplites leptus* (Seeley, 1865); Kennedy *et al*., p. 40, pl. 5, figs 20–22.
2014. *Callihoplites cratus* (Seeley, 1865); Klein, pp. 113, 116 (with additional synonymy).
pars 2014. *Callihoplites* cf. *tetragonus* (Seeley, 1865); Mosavinia *et al*., p. 77, fig. 4E only.
2020. *Callihoplites cratus* (Seeley, 1865); Wilmsen *et al*., p. 7, fig. 4C.
2021. *Callihoplites cratus* (Seeley, 1865); Jattiot *et al*., p. 17, figs 9, 10AE–AG (with additional synonymy).

TYPE: The lectotype, by the subsequent designation of Spath (1928), of *Callihoplites cratus* is SMC B1517, the original of Seeley (1865, p. 240, pl. 21, fig. 2) from the Cambridge Greensand; it was refigured by Kennedy *et al*. (2008, pl. 5, figs 18, 19).

MATERIAL: The available specimens (UBGD 293056-293060) are very poorly preserved, consisting mostly of small fragments. Although not fragmented, UBGD 293056 is heavily damaged and distorted by post-mortem crushing.

MEASUREMENTS:

	D	H	W	U	W/H
UBGD 293056 (Pl. 3, Figs 9–11)	~ 48	–	–	–	–

DESCRIPTION: Originally, the shell of the figured specimen (UBGD 293056; Pl. 3, Figs 9-11) was presumably moderately involute with relatively thick whorls. The preserved ornamentation of this specimen consists of strong umbilical tubercles, giving rise to up to three prorsiradiate concave ribs, with additional ribs intercalated. The ribs loop to relatively numerous ventrolateral clavi.

DISCUSSION: Upon comparison with well-preserved material of the two species *C. cratus* and *C. tetragonus* (Seeley, 1865) from Salazac (Jattiot *et al*. 2021, figs 9, 10), the present material appears to be attributable to the former species rather than the latter. Specimen UBGD 293056 (Pl. 3, Figs 9–11) peculiarly resembles representatives of the '*robustus*' *C. cratus* variant (e.g., Jattiot *et al*. 2021, fig. 9C, D). The present specimens probably belong to *C. cratus*, but their fragmentary nature combined with poor preservation and scarcity precludes a definitive assignment. The reader is referred to Jattiot *et al*. (2021) for a thorough description and discussion of *C. cratus*.

Callihoplites tetragonus (Seeley, 1865)
(Pl. 3, Figs 16–19)

1865. *Ammonites raulinianus* var. *tetragonus* Seeley, p. 243.
2008. *Callihoplites tetragonus* (Seeley, 1865); Kennedy *et al*., p. 38, pl. 1, figs 1–18; pl. 2, figs 1–26; pl. 3, figs 1–24; pl. 4, figs 1–5; pl. 5, figs 1–6, 10–17 (with additional synonymy).
2008. *Callihoplites tetragonus* (Seeley, 1865); Amédro, pl. 6, figs 1, 3.
2014. *Callihoplites tetragonus* (Seeley, 1865); Klein, pp. 113, 120 (with additional synonymy).
2017. *Callihoplites tetragonus* (Seeley, 1865); Tajika *et al*., p. 31, fig. 9Q, R.

2021. *Callihoplites tetragonus* (Seeley, 1865); Jattiot *et al*., p. 17, fig. 10AH–AD (with additional synonymy).

TYPE: The lectotype, by the subsequent designation of Spath (1928), is SMC B1581, the original of Seeley (1865, p. 243), from the remanié phosphatised late Albian fauna at the base of the Cenomanian Cambridge Greensand of Cambridgeshire. It was refigured by Kennedy *et al*. (2008, pl. 5, figs 13–15).

MATERIAL: One well-preserved 180º body chamber fragment; UBGD 293287.

MEASUREMENTS:

	D	H	W	U	W/H
UBGD 293287 (Pl. 3, Figs 16–19)	~ 34	–	–	11.1	–

DESCRIPTION: The coiling is presumed moderately evolute, with a depressed, reniform whorl section and a broad venter. The umbilicus appears relatively deep with a moderately high umbilical wall and gently rounded umbilical shoulders. Sharp, high and conical umbilical tubercles give rise to inconspicuous folds on flanks. On the adapical portion of the fragment, there are singularly strong ventrolateral clavi; these rapidly weaken on the final sector of shell, which suggests approaching maturity. Thus, the present individual is tentatively interpreted as an incomplete, near-mature microconch. On the venter, the ventrolateral clavi alternate and are linked by barely discernible folds in a zigzag fashion.

DISCUSSION: Although the material at hand consists only of a single fragment, the peculiar morphology and ornamentation of the specimen leaves no doubt as to its assignment to *C. tetragonus*. More specifically, this single specimen fully resembles the holotype of *C. gymnus* Spath, 1928 (refigured by Kennedy *et al*. 2008, pl. 5, figs 10–12) as well as the specimen assigned to *C.* aff. *gymnus* in Renz (1968, pl. 5, fig. 7), both of which are included in the synonymy list of *C. tetragonus* by Kennedy *et al*. (2008, p. 38). The reader is referred to Kennedy *et al*. (2008) and Jattiot *et al*. (2021) for thorough descriptions and discussions (including extensive comparisons with other species such as *C. cratus*).

OCCURRENCE: Lower Cretaceous (upper Albian, *Mortoniceras* (*M.*) *fallax* and *Mortoniceras* (*S.*) *rostratum* zones); UK (England), France, Belgium, Switzerland, China (Tibet).

Genus *Lepthoplites* Spath, 1925

TYPE SPECIES: *Lepthoplites falcoides* Spath, 1925 (p. 144), by the original designation of Spath (1925, p. 144).

Lepthoplites cf. *cantabrigiensis* Spath, 1925
(Pl. 3, Figs 20–24)

1925. *Lepthoplites cantabrigiensis* Spath, p. 144.
1926. *Lepthoplites cantabrigiensis* Spath, 1925; Spath, pl. 13, fig. 8.
1928. *Lepthoplites cantabrigiensis* Spath, 1925; Spath, p. 235, pl. 24, figs 1, 12.
2008. *Lepthoplites cantabrigiensis* Spath, 1925; Amédro, pl. 2, fig. 4; pl. 5, fig. 9.
2014. *Lepthoplites cantabrigiensis cantabrigiensis* Spath, 1925; Klein, pp. 136, 137 (with additional synonymy).
2021. *Lepthoplites cantabrigiensis* Spath, 1925; Jattiot *et al*., p. 25, fig. 11A–AF (with additional synonymy).

TYPE: The holotype by monotypy of *Lepthoplites cantabrigiensis* (B.M., no. C.4806c) is the original of Spath (1926, pl. 13, fig. 8) from the Cambridge Greensand.

MATERIAL: Two poorly-preserved specimens (UBGD 293061, 293062), of which one (UBGD 293061) is heavily distorted by post-mortem crushing.

MEASUREMENTS:

	D	H	W	U	W/H
UBGD 293061 (Pl. 3, Figs 20, 21)	~ 25	–	–	–	–
UBGD 293062 (Pl. 3, Figs 22, 23)	24.3 (100)	11.3 (46.5)	7.6 (31.3)	–	0.67

DESCRIPTION: The shell is moderately involute, with a compressed whorl section and a subtabulate venter. Inner flanks are flat and nearly parallel, whereas outer flanks converge towards the venter; maximum breadth slightly above mid-flank. The umbilical wall is steep with gently rounded shoulders. The parts of shell with preserved ornamentation suggest dense and sinuous ribs that arise in groups of 2 or 3 from elongated, prorsiradiate umbilical bullae. Each of these ribs terminates in tiny crenulations at ventrolateral shoulder.

DISCUSSION: The assignment of these two poorly-preserved specimens to *Lepthoplites* is based on their

ornamentation (i.e., each sinuous rib on flank terminates in tiny crenulations on ventrolateral shoulders; see Jattiot *et al*. 2021 for a thorough comparison with the related genus *Callihoplites*). More specifically, ornamentation on both specimens as well as the shell ratios of specimen 63 strongly invite comparison with those of the well-preserved *L. cantabrigiensis* representatives from Salazac (see Jattiot *et al*. 2021). The present specimens probably belong to *L. cantabrigiensis*, but their fragmentary nature combined with poor preservation and scarcity precludes a definitive assignment.

Genus *Discohoplites* Spath, 1925

TYPE SPECIES: *Ammonites coelonotus* Seeley, 1865 (p. 237, pl. 10, fig. 2), by the original designation of Spath (1925, p. 83).

Discohoplites cf. *valbonnensis* (Hébert and Munier-Chalmas, 1875)
(Pl. 3, Figs 25–28)

1875. *Ammonites valbonnensis* Hébert and Munier-Chalmas, p. 114, pl. 4, fig. 3.
2011. *Discohoplites valbonnensis valbonnensis* (Hébert and Munier-Chalmas, 1875); Gale *et al*., p. 75.
2011. *Savelievella varicosa* (Spath, 1928); Cooper and Owen, p. 344, fig. 5I, J.
2014. *Savelievella valbonnensis valbonnensis* (Hébert and Munier-Chalmas, 1875); Klein, p. 77 (with additional synonymy).
2021. *Discohoplites valbonnensis* (Hébert and Munier-Chalmas, 1875); Jattiot *et al*., p. 27, fig. 11AG–BS (with additional synonymy).

TYPE (after Kennedy *et al*. 2008): The holotype of *Discohoplites valbonnensis*, by monotypy, is the original of Hébert and Munier-Chalmas (1875, p. 114, pl. 4, fig. 3), from the Upper Albian of Salazac (Gard, France).

MATERIAL: One specimen; UBGD 293063.

MEASUREMENTS:

	D	H	W	U	W/H
UBGD 293063 (Pl. 3, Figs 25–28)	*25.6* (100)	9.9 (*38.7*)	9.1 (*35.5*)	9.7 (*37.9*)	0.92

DESCRIPTION: The shell of this specimen is moderately evolute (U/D ~ 38%) with a subquadratic (very slightly compressed) whorl section. The umbilicus is shallow, with a low, inclined wall and narrowly rounded umbilical shoulders. The venter is flattened with a narrow, deep, mid-ventral groove. The ornamentation consists of forward-projected umbilical bullae that give rise to two falcate ribs strongly projecting forward across the ventrolateral shoulders. Additional single ribs are rarely intercalated. Noteworthy, the ribs are so distinctively falcate (due to the singularly forward-projected umbilical bullae) on the final sector of shell that it produces a lateral pseudo-groove.

DISCUSSION: It is not excluded that the somewhat singular ornamentation (i.e., distinctively falcate ribs and lateral pseudo-groove) of the specimen could originate from a slight, inconspicuous pathology. Apart from this, as well as from slightly more evolute coiling, the overall shape and ornamentation of this single specimen agree well with those of *D. valbonnensis* representatives from Salazac (see e.g., Jattiot *et al*. 2021, fig. 11BK–BM). The species was comprehensively reviewed by Jattiot *et al*. (2021), who discussed in detail how it differs from other species.

Genus and subgenus *Arrhaphoceras* Whitehouse, 1927

TYPE SPECIES: *Ammonites woodwardi* Seeley, 1865 (p. 236, pl. 11, fig. 3), by the original designation of Whitehouse (1927 p. 109).

Arrhaphoceras (*Arrhaphoceras*) *substuderi* Spath, 1928
(Pl. 3, Figs 29–32)

1928. *Arrhaphoceras substuderi* Spath, p. 254, pl. 24, fig. 19; text-fig. 84a–d.
1968. *Arrhaphoceras substuderi* Spath, 1928; Renz, p. 31, pl. 2, figs. 20–22 (with full synonymy).
2014. *Arrhaphoceras substuderi* Spath, 1928; Klein, pp. 123, 125 (with additional synonymy).
?2015. *Arrhaphoceras* cf. *substuderi* Spath, 1928; Kennedy and Machalski, p. 549, text-fig. 2C, D, Q).

TYPES: The paratype and the holotype are the original of Spath (1928, text-fig. 84b, c, respectively) from the Cambridge Greensand.

MATERIAL: Two small phragmocones; UBGD 293053, 293054.

MEASUREMENTS:

	D	H	W	U	W/H
UBGD 293053 (Pl. 3, Fig. 29)	22.5 (100)	9.3 (41.3)	10.6 (47.1)	6.2 (27.6)	1.14
UBGD 293054 (Pl. 3, Figs 30–32)	25.9 (100)	10.4 (40.2)	11.2 (43.2)	8.3 (32.0)	1.08

DESCRIPTION: The shell is moderately involute (U/D ~ 28% for specimen UBGD 293053, 32% for specimen UBGD 293054). The flanks markedly converge towards a broad venter, producing a trapezoidal whorl section; maximum whorl width near umbilical shoulders. The umbilicus is deep with a relatively high umbilical wall and well-rounded umbilical shoulders. Based mainly on specimen 55, the ornamentation is characterised by high, sharp, conical umbilical tubercles that give rise to two or three feebly concave, relatively fine but wiry ribs, as well as additional intercalated ribs. Each of these lateral ribs ends on ventrolateral shoulders in a very faint node that is difficult to differentiate from the low, blunt, prorsiradiate rib that sweeps forward on the venter (see Pl. 3, Fig. 32). The ribs extend to the mid-line of the venter, where they alternate in position, rather than meeting in a symmetrical chevron.

DISCUSSION: The two specimens at hand are identical in all respects (size, shell shape and ornamentation) to the types and other specimens illustrated by Spath (1928, pl. 24, fig. 19; text-fig. 84a–d), as well as to the *A. substuderi* individuals figured by Renz (1968, pl. 2, figs 20–22; two of which were originally figured by Pictet and Campiche 1860). *Arrhaphoceras* (*Arrhaphoceras*) *studeri* (Pictet and Campiche, 1860) presumably differs by its larger size, more depressed whorl section (reniform) and its more distant ribbing (Spath 1928, p. 255), while *A.* (*A.*) *woodwardi* (Seeley, 1865) is supposedly distinguished by a wider umbilicus and more regularly tripartite ribbing (Spath 1928, p. 255).

OCCURRENCE: *Mortoniceras* (*M.*) *fallax* Zone of the UK (southern and eastern England) and Switzerland, *M.* (*S.*) *rostratum* Zone at Clansayes, France, and *M.* (*S.*) *perinflatum* Zone of the UK (southern England) and south-eastern France.

Superfamily Acanthoceratoidea de Grossouvre, 1894
Family Lyelliceratidae Spath, 1921
Subfamily Stolickzaiinae Breistroffer, 1953
Genus and subgenus *Stoliczkaia* Neumayr, 1875

TYPE SPECIES: *Ammonites dispar* d'Orbigny, 1841 (p. 142, pl. 45, figs 1, 2), by the subsequent designation of Diener (1925, p. 179).

Stoliczkaia (*Stoliczkaia*) *dispar* (d'Orbigny, 1841)
(Pls 4, 5)

1841. *Ammonites dispar* d'Orbigny, p. 142, pl. 45, figs 1, 2.
2007. *Stoliczkaia* (*Stoliczkaia*) *dispar* (d'Orbigny, 1841); Kennedy and Latil, p. 465, pl. 6, figs 4–6.
2015. *Stoliczkaiella* (*Stoliczkaiella*) *dispar* (d'Orbigny, 1841); Kennedy and Gale, p. 258, pl. 3, fig. 4; pl. 4, fig. 1 (with additional synonymy).
2018. *Stoliczkaiella* (*Stoliczkaiella*) *dispar* (d'Orbigny, 1841); Klein, pp. 222, 225 (with additional synonymy).
non 2019. *Stoliczkaia* (*Stoliczkaia*) *dispar* (d'Orbigny, 1841); Gautam *et al*., p. 22, figs 7G, H [*Stoliczkaia*? (*Lamnayella*) sp.].

TYPE (after Kennedy and Latil 2007): The holotype, by monotypy, is the original of d'Orbigny (1841, pl. 45, figs 1, 2), from Bédouin, south of Mont Ventoux, Vaucluse, France. It is in the Renaux collection, housed in the Faculté des Sciences, Montpellier, France, and was refigured by Wright and Kennedy (1994, fig. 4).

MATERIAL: Twenty-five specimens; UBGD 293014, 293016-293039.

MEASUREMENTS:

	D	H	W	U	W/H
UBGD 293014	~ 85	–	–	–	–
UBGD 293016	91.5	–	–	–	–
UBGD 293017 (Pl. 4, Figs 5–7)	*89.0* (100)	47.8 (*53.7*)	23.9 (*26.9*)	*10.5* (*11.8*)	*0.50*
UBGD 293018 (Pl. 4, Figs 8, 9)	71.5	–	–	–	–
UBGD 293019 (Pl. 4, Figs 10–12)	*91.7* (100)	46.6 (*50.8*)	20 (*21.8*)	*13.5* (*14.7*)	0.43
UBGD 293020 (Pl. 4, Figs 3, 4)	97.5 (100)	40.3 (41.3)	21.1 (21.6)	25.8 (26.5)	0.52
UBGD 293021 (Pl. 4, Figs 1, 2)	120.0 (100)	*55.6* (*46.3*)	*24.2* (*20.2*)	*22.3* (*18.6*)	*0.44*
UBGD 293022 (Pl. 5, Figs 7–9)	27.6 (100)	13.9 (50.4)	9.8 (35.5)	4.7 (17.0)	0.71
UBGD 293023 (Pl. 5, Figs 4–6)	*30.4* (100)	16.2 (*53.3*)	11.9 (*39.1*)	4.3 (*14.1*)	0.73
UBGD 293024 (Pl. 5, Figs 1–3)	35.1 (100)	19.1 (54.4)	11.7 (33.3)	4.4 (12.5)	0.61
UBGD 293025 (Pl. 5, Figs 10–12)	59.6 (100)	*30.8* (*51.7*)	17.9 (30.0)	–	0.58
UBGD 293026	37.3 (100)	–	–	–	–

UBGD 293027	40.2 (100)	21.2 (52.7)	13.5 (33.6)	5.6 (13.9)	0.64
UBGD 293028	33.1 (100)	16.3 (49.2)	12.3 (37.2)	–	0.75
UBGD 293029	32.5 (100)	16.6 (51.1)	12.0 (36.9)	6.3 (19.4)	0.72
UBGD 293030	*34.5* (100)	*18.2* (*52.8*)	11.0 (*31.9*)	*4.5* (*13.0*)	0.60
UBGD 293031	33.1 (100)	17.4 (52.6)	–	5.5 (16.6)	–
UBGD 293032	~ 28	13.4	9.1	–	0.68
UBGD 293033	~ 48	22.1	14.5	–	0.66
UBGD 293034 (Pl. 5, Figs 13–15)	~ 55	25.8	16.8	–	0.65
UBGD 293035 (Pl. 5, Figs 18–20)	*51.0* (100)	23.2 (*45.5*)	14.8 (*29.0*)	–	0.64
UBGD 293036 (Pl. 5, Figs 21–23)	~ 55	22.9	15.1	–	0.66
UBGD 293037 (Pl. 5, Figs 16, 17)	~ 38	17.3	11.8	–	0.68

DESCRIPTION: The material from the lower part of the sampled level consists of rather small, variably damaged specimens (from 27.6 to 59.6 mm in diameter; Pl. 5, Figs 1–23), of which specimens UBGD 293022, UBGD 293023 and UBGD 293024 are the best preserved (Pl. 5, Figs 1–9). Conversely, material from the upper part of the sampled level mostly consists of relatively large (from 71.5 to 120 mm in diameter) specimens that are preserved as significantly worn, orangish-yellowish internal moulds (Pl. 4, Figs 1–12). As a general rule, their external whorl is distorted and/or crushed to various degrees, whereas the inner whorls are badly crushed or not preserved.

The coiling is very involute to involute, the umbilicus comprising 12–26% of the diameter (16% on average). On the phragmocone, the umbilical wall is low and convex, but it becomes distinctly concave on the adult body chamber. The whorl section is compressed, with a whorl width to height ratio (W/H) of 0.62 on average (although likely accentuated by crushing, with regard to the large specimens from the upper part of the sampled level). Inner flanks are feebly convex, while outer flanks are flattened and convergent. The venter is obtusely fastigiate with rather angular ventrolateral shoulders at earliest growth stages, gradually becoming rounded with rounded ventrolateral shoulders. At juvenile stages (see e.g., Pl. 5, Figs 1–9), ornamentation consists of primary ribs arising at the umbilical seam, which strengthen into long bullae on umbilical shoulders and inner flanks. Both long and short intercalated ribs are present and the primary ribs occasionally bifurcate. All ribs strengthen and coarsen on ventrolateral shoulders and produce sharp ventrolateral tubercles only at earliest juvenile stages (see e.g., Pl. 5, Figs 8, 9). Indeed, these ventrolateral tubercles rapidly fade away as size increases (see e.g., Pl. 5, Fig. 3). The ribs are strong, coarse and nearly straight on the venter. On the body chamber of larger specimens (Pl. 5, Figs 1–12), the preserved ornamentation consists of very thick, coarse ribs on the venter, of which some occasionally extend to the flanks (especially on specimen UBGD 293020; Pl. 4, Fig. 3). These ribs progressively fade away on two specimens (21 and 22, Pl. 4, Figs 1–4). Therefore, their final sector of shell appears completely smooth, which is interpreted as a sign of maturity. Accordingly, specimens UBGD 293020 and UBGD 293021 are viewed as typical, near-complete mature adult *S. dispar* macroconchs. The markedly egressive coiling of specimen UBGD 293020 (i.e., coiling becomes increasingly more evolute on the outer whorl, where the U/D ratio reaches a maximum value of about 27%) further reinforces this interpretation. Four relatively small individuals (specimens UBGD 293034, UBGD 293035, UBGD 293038 and UBGD 293039; Pl. 5, Figs 13–23), each of which is represented mainly by a portion of body chamber, exhibit a distinctively coarse and distant ribbing (especially on venter). With regard to specimen UBGD 293038 (Pl. 5, Figs 21–23), the final sector of preserved body chamber conspicuously smoothens and somewhat constricts, which strongly suggests maturity. Accordingly, specimen UBGD 293038 is interpreted as a near-adult microconch. Regarding specimens UBGD 293034, UBGD 293035 and UBGD 293039 (Pl. 5, Figs 13–20), the preserved sector of shell does not allow for assessing whether they are incomplete, near-adult microconchs similar to specimen UBGD 293038, or coarsely ornamented juvenile macroconchs with preserved portions of body chamber (see also discussion).

DISCUSSION: According to Wright and Kennedy (1994) and Kennedy and Latil (2007), *S. clavigera* (Neumayr, 1875) differs from co-occurring *S. dispar* by its less compressed whorl section, persistent coarse ribs on adults (whereas *S. dispar* becomes near-smooth at maturity), as well by its more robust, parallel flanks on the early and middle growth stages (in contrast with convergent flanks in *S. dispar*).

All non-distorted phragmocones from the lower part of the sampled level (and presumably the earliest preserved growth stages in specimens 19 and 20 from the upper part of the sampled level) are significantly compressed (W/H ranging from 0.58 to 0.75), similar to previously published representatives

of *S. dispar* (compare e.g., specimens UBGD 293022, UBGD 293023, UBGD 293024, Pl. 5, Figs 1–9 with Wright and Kennedy 1994, figs 11n–p, 12a, b). Specimens UBGD 293023 and UBGD 293024 also closely resemble two specimens from Switzerland (Sainte-Croix) figured by Renz (1968, pl. 7, fig. 4 and pl. 6, fig. 2, respectively). Finally, specimen UBGD 293025 (59.6 mm in diameter and wholly septate) is identical in ornamentation and shape to the largest phragmocone (76 mm in diameter) figured by Wright and Kennedy (1994, fig. 12o–p), as well as to specimen L39895 in Renz (1968, pl. 6, fig. 1).

Compared to specimens UBGD 293022, UBGD 293023 and UBGD 293024, similar-sized specimens of *S. clavigera* (e.g., Wright and Kennedy 1994, figs 11k–m, q–r) exhibit thicker whorls. Furthermore, the W/H ratio of the largest *S. clavigera* phragmocone (65 mm in diameter) figured by Wright and Kennedy (1994, fig. 12m, n) is 0.9 (Wright and Kennedy 1994, p. 577), which is much higher than the W/H ratio of comparably sized Clansayes specimens (e.g., 0.58 in specimen UBGD 293025, Pl. 5, Figs 10–12). The assignment of our sample to *S. dispar* is further reinforced by the near-mature specimens from the upper part of the sampled level, which exhibit a smooth final sector of shell (Pl. 4, Figs 1–3). Among these, specimen UBGD 293020 compares particularly well with the adult *S. dispar* specimen figured by Kennedy and Latil (2007, pl. 6, figs 4–6).

The relatively small specimens UBGD 293034, UBGD 293035, UBGD 293038 and UBGD 293039 (Pl. 5, Figs 13–23), each of which is represented mainly by a portion of body chamber, exhibit a remarkably coarse and distant ribbing (especially on the venter) that is reminiscent of that observed on the external whorl of *S. dispar* macroconchs (e.g., Pl. 4, Figs 1–7). Regarding specimen UBGD 293038 (Pl. 5, Figs 21–23), the final sector of preserved body chamber conspicuously smoothens and somewhat constricts, therefore strongly suggesting maturity. Accordingly, specimen UBGD 293038 is interpreted as a near-adult *S. dispar* microconch. Regarding specimens UBGD 293034, UBGD 293035 and UBGD 293039 (Pl. 5, Figs 13–20), the preserved sector of shell does not allow for assessing whether they are incomplete, near-adult *S. dispar* microconchs akin to specimen UBGD 293038, or coarsely ornamented juvenile *S. dispar* macroconchs with preserved portions of body chamber. These four specimens (especially specimen UBGD 293038) might alternatively suggest the occurrence at Clansayes of a distinct, small *Stoliczkaia* species, but this hypothesis must remain uncorroborated awaiting the discovery of additional similar material. Noteworthy, these four specimens are also somewhat reminiscent of *Stoliczkaia* (*Shumarinaia*) *africana* Pervinquière, 1907, whose lectotype (a 180º wholly septate fragment with a maximum preserved diameter of 29 mm, refigured by Kennedy 2020, pl. 15, figs 26–28) similarly exhibits strong, distant and rectiradiate ventral ribs. However, the latter is distinguished by its strong ventral clavi, its incipient siphonal tubercle at the adapical end of the fragment, and more secondarily by its presumed slightly larger adult size. Moreover, *S.* (*S.*) *africana* has never been recorded from France (so far recorded from Central Tunisia, Spain, Nigeria and Brazil; Kennedy 2020). Although smaller, specimen UBGD 293038 also shows some similarities with the original specimen of *S. notha* var. *ultima* Spath, 1931 refigured by Wright and Kennedy (1994, fig. 10e–g). According to Wright and Kennedy (1994), the early growth stage with a trituberculate venter, and the middle growth stage with a rounded venter and numerous crowded ribs, plus an evolute body chamber with coarse adapical and much weakened adapertural ornament distinguish *S. notha* from the younger species *S. dispar* (*S. notha* occurs in the *Mortoniceras fallax* Zone; see e.g., Wright and Kennedy 1994, Jattiot *et al*. 2021).

Cooper and Kennedy (1979) thoroughly described *S. tenuis* Renz, 1968 and discussed in detail how it differs from other species, including *S. dispar*.

OCCURRENCE (after Kennedy and Gale 2015): Upper upper Albian, *Mortoniceras* (*S.*) *rostratum* and *Mortoniceras* (*S.*) *perinflatum* Zones; UK (southern England), south-eastern France, Switzerland, Germany (?), Hungary, Bulgaria, Turkmenistan, and central Tunisia.

Family Brancoceratidae Spath, 1934
Subfamily Mortoniceratinae Douvillé, 1912
Genus *Mortoniceras* Meek, 1876

DISCUSSION: It is common practice to either synonymise *Pervinquieria* Böhm, 1910 with *Mortoniceras* Meek, 1876 or to regard the first as a subgenus of the latter (e.g., Kennedy *et al.* 1998). Recently, Kennedy in Gale *et al*. (2019) and Kennedy (2020) changed this traditional approach by treating *Pervinquieria* as a separate genus rather than a synonym of *Mortoniceras*. Kennedy in Gale *et al.* (2019, p. 213) refers to the ontogenetic development

of the type species of *Mortoniceras* (i.e., *Ammonites vespertinus* Morton, 1834) and its ventrolateral tuberculation to argue for separation from *Pervinquieria*. However, we do not see any difference in the ornamentation of both taxa, except for the spiral ridges that are supposedly characteristic of *Pervinquieria*. *Mortoniceras vespertinus* is very poorly known, thus hindering any thorough approach. Therefore, we here still treat *Pervinquieria* as a synonym of *Mortoniceras*.

TYPE SPECIES: *Ammonites vespertinus* Morton, 1834 (p. 40, pl. 17, fig. 1), by the original designation of Meek (1876, p. 448).

Subgenus *Subschloenbachia* Spath, 1921
(= *Durnovarites* Spath, 1932, p. 380)

TYPE SPECIES: *Ammonites rostratus* J. Sowerby, 1816 (p. 163, pl. 173), by the original designation of Spath (1921, p. 284).

Mortoniceras (*Subschloenbachia*) *rostratum*
(J. Sowerby, 1817)
(Pls 6–13)

1817. *Ammonites rostratus* J. Sowerby, p. 163, pl. 173.
2007. *Mortoniceras* (*Subschloenbachia*) *rostratum* (J. Sowerby, 1817); Kennedy and Latil, p. 463, pl. 3, fig. 2; pl. 3, figs 3, 6–9; pl. 4, figs 7, 8.
2017. *Mortoniceras rostratum* (J. Sowerby, 1817); Tajika *et al*., p. 34, fig. 8G, H.
2018. *Mortoniceras* (*Mortoniceras*) *rostratum* (J. Sowerby, 1817); Klein, pp. 101, 122 (with additional synonymy).
2019. *Pervinquieria* (*Subschloenbachia*) *rostrata* (J. Sowerby, 1817); Kennedy in Gale *et al*., p. 214, pl. 13; pl. 14, figs 1, 2.
2020. *Mortoniceras* (*Subschloenbachia*) *rostratum* (J. Sowerby, 1817); Wilmsen *et al*., p. 7, figs 4D, 5A.
2021. *Mortoniceras* (*Subschloenbachia*) *rostratum* (J. Sowerby, 1817); Latil *et al*., p. 15, fig. 12a–i.

TYPE (after Kennedy and Latil 2007): The holotype, by monotypy, is OUM K835, the original of J. Sowerby (1817, p. 163, pl. 173), from the upper Albian Upper Greensand of Roke, near Benson, Oxfordshire, England, UK, refigured by Kennedy *et al*. (1998, figs 9–11).

MATERIAL: Twenty-one specimens; UBGD 293099-293119.

MEASUREMENTS:

	D	H	W	U	W/H
UBGD 293099	~ 22	–	–	–	–
UBGD 293100 (Pl. 13, Figs 7–9)	19.0 (100)	6.1 (32.1)	6.4 (33.7)	8.0 (42.1)	1.05
UBGD 293101	~ 31	–	–	–	–
UBGD 293102	26.9 (100)	9.3 (34.6)	9.6 (35.7)	11.0 (40.9)	1.03
UBGD 293103 (Pl. 13, Figs 4–6)	32.6 (100)	11.3 (34.7)	11.3 (34.7)	13.7 (42.0)	1.00
UBGD 293104 (Pl. 13, Figs 1–3)	28.4 (100)	11.2 (39.4)	–	10.3 (36.3)	–
UBGD 293105	26.6 (100)	10.6 (39.8)	–	9.3 (35.0)	–
UBGD 293106 (Pl. 11, Figs 7, 8)	41.0 (100)	14.0 (34.1)	13.2 (32.2)	16.8 (41.0)	0.94
UBGD 293107 (Pl. 11, Figs 4–6)	~ 38	15.2	21.1	–	1.39
UBGD 293108 (Pl. 13, Figs 13–15)	69.7 (100)	28.0 (40.2)	38.0 (54.5)	*23.3* (*33.4*)	1.36
UBGD 293109 (Pl. 13, Figs 10–12)	77.5 (100)	31.4 (40.5)	37.3 (48.1)	*24.0* (*31.0*)	1.19
UBGD 293110 (Pl. 12, Figs 3, 4)	*107.4* (100)	*47.0* (*43.8*)	*49.0* (*45.6*)	–	*1.04*
UBGD 293111	~ 105	–	–	–	–
UBGD 293112	118.0 (100)	49.0 (41.5)	*40.5* (*34.3*)	–	0.83
UBGD 293113 (Pl. 12, Figs 1, 2)	~ 160	–	–	–	–
UBGD 293114 (Pl. 11, Figs 1–3)	~ 160	–	–	–	–
UBGD 293115	~ 160	–	–	–	–
UBGD 293116	~ 130	–	–	–	–
UBGD 293118 (Pl. 6, Fig. 1; Pl. 7, Figs 1, 2; Pl. 9, Figs 1, 2)	~ 170	–	–	–	–
UBGD 293119 (Pl. 10, Figs 1–3)	~ 180	–	–	–	–

DESCRIPTION: All specimens retrieved from the lower part of the sampled level depict the earliest or intermediate growth stages (from 19 mm to 77.5 mm in maximum preserved diameter). Among the smallest (< 35 mm in diameter), specimens UBGD 293100, UBGD 293103 and UBGD 293104 are the best preserved (Pl. 13, Figs 1–9). At this size, coiling is evolute (U/D ratio from 35 to 42%). The umbilicus is deep, with a moderately high wall and broadly rounded shoulders. The whorl section is quadratic (W/H ratio approximately equal to 1), with subparallel flanks. The ventrolateral shoulders are broadly rounded; the venter is broad, bearing a strong siphonal keel. Prominent umbilical tubercles give rise to one or two (predominantly one) ribs, with regular intercalated ribs. Each rib bears a pair of strong, well-individualised inner and outer ventrolateral tu-

bercles. Lateral tubercles are absent (Pl. 13, Figs 4–9) or only barely discernible (on final sector of shell on specimen UBGD 293104; Pl. 13, Fig. 3) at these earliest ontogenetic stages.

The slightly larger juvenile specimens UBGD 293106 and UBGD 293107 (about 52.5 and 38 mm in maximum preserved diameter, respectively; Pl. 11, Figs 4–8) strongly suggest a very wide juvenile intraspecific variation in shell shape, as specimen UBGD 293106 is somewhat compressed (W/H = 0.94), whereas specimen UBGD 293107 is remarkably depressed (W/H = 1.39). Their ribs bear coarse umbilical, and inner and outer ventrolateral tubercles; the outer ones progressively transition to broad, low clavi on specimen UBGD 293107. A fourth (lateral) tubercle is present on the final sector of shell on both specimens, although this is barely conspicuous in specimen UBGD 293107, partly due to a poor preservation.

Specimens UBGD 293108 and UBGD 293109 (Pl. 13, Figs 10–15), consisting of phragmocones 69.7 and 77.5 mm in diameter respectively, represent a later, intermediate ontogenetic stage. Their coiling is moderately involute (U/D = 33% and 31%, respectively). The umbilicus is very deep, with a very high wall and broadly rounded shoulders. These two specimens demonstrate an unusually wide intraspecific variation in whorl shape and ornamentation at this growth stage, as specimen UBGD 293108 shows a remarkably depressed, reniform whorl section (W/H = 1.36; Pl. 13, Fig. 14) and very coarse ornamentation, whereas specimen UBGD 293109 exhibits a less depressed, rectangular whorl section (W/H = 1.18; Pl. 13, Fig. 11) and significantly weaker ornamentation. This intraspecific variation might partly follow Buckman's first law of covariation (e.g., Westermann 1966; Guex *et al.* 2003; Hammer and Bucher 2005; Monnet *et al*. 2015), although in a contradicting manner this observation does not seem to apply to specimens UBGD 293106 and UBGD 293107 (Pl. 11, Figs 4–8). Noteworthy, even though the typical quadrituberculation (i.e., umbilical, lateral, inner and outer ventrolateral tubercles) is overall particularly well-expressed on specimen UBGD 293108, the outer ventrolateral tubercles rapidly transform into broad, low, poorly-differentiated clavi on the final sector of shell. Compared to specimen UBGD 293108, this typical quadrituberculation is much less obvious on specimen UBGD 293109, with only the umbilical tubercles being well-developed. Its shell is otherwise ornamented with barely conspicuous, bullate mid-lateral tubercles and only slightly stronger inner ventrolateral tubercles. The latter give rise to low, blunt, prorsiradiate ribs that sweep forward across the ventrolateral shoulder to barely discernible outer ventrolateral clavi.

The largest specimens (> 100 mm in maximum preserved diameter) were mostly retrieved from the upper part of the sampled level. Specimen UBGD 293110 (Pl. 12, Figs 3, 4) is interpreted as a near-complete phragmocone, most likely only lacking the adult body chamber. The beginning of its outer whorl further confirms (see specimens UBGD 293108 and UBGD 293109, Pl. 13, Figs 10–15) that there is a transitory growth stage (tentatively estimated between 40–50 and 90–100 mm in diameter, although assumed significantly variable) in which the outer ventrolateral tubercle – and thus the characteristic quadrituberculation – is elusive. Indeed, although the umbilical and inner ventrolateral, and to a lesser extent the lateral tubercles appear to have been rather well-defined (taking the deceptive preservation into account) at the beginning of the outer whorl of specimen UBGD 293110, the outer ventrolateral clavi were undoubtedly hardly differentiated from the low, blunt, prorsiradiate ribs that sweep forward across the ventrolateral shoulder.

However, at a diameter greater than about 90–100 mm (i.e., usually on the final section of phragmocones), all tubercles rapidly and markedly coarsen until the adapical end of the adult body chamber is reached; this is well illustrated by specimen UBGD 293110 and by the largest individuals in the collection. These largest individuals comprise near-mature specimens (Pl. 10, Figs 1–3; Pl. 11, Figs 1–3; Pl. 12, Figs 1, 2), an adult body chamber with preserved rostrum (Pl. 8, Figs 1–4; Pl. 9, Figs 3, 4), as well as a complete mature specimen with preserved rostrum (Pl. 6, Fig. 1; Pl. 7, Figs 1, 2; Pl. 9, Figs 1, 2). All are preserved as significantly worn, orangish-yellowish internal moulds. As a general rule, their external whorl (including a ~ 180º adult body chamber) is distorted and/or crushed to various degrees; inner whorls are badly crushed or not preserved. Coiling varies from moderately involute to moderately evolute on these larger specimens. The final section of the phragmocone and the first half of the adult body chamber bear wide umbilical bullae, coarse lateral and inner ventrolateral tubercles, and high, pinched outer ventrolateral clavi. The second half of the adult body chamber exhibits inner ventrolateral tubercles and outer ventrolateral clavi coalescing into massive, pinched clavi on the 5–7 ribs adapical of the rostrum, which are thus trituberculate. The final two ribs are markedly prorsiradiate. The adapical of the pair has effacing lateral and ventrolateral bullae as seen on

specimen UBGD 293117 (Pl. 8, Figs 1, 2; Pl. 9, Fig. 3); that of specimen UBGD 293118 (Pl. 6, Fig. 1; Pl. 9, Fig. 1) bears no actual bullae but is remarkably elevated at the earlier location of the lateral tubercle as well as at the base of the rostrum. The final rib is still somewhat coarse near the umbilicus, but lacks bullae. These final two ribs sweep back on the outer flank (accompanied by numerous growth lines), become markedly convex, and fuse together to produce the spiral rostrum. The adapically coiled rostrum extends back in a 180º arc on specimen UBGD 293118, and the preserved termination is nearly in contact with the ventral keel. On specimen UBGD 293117, the rostrum extends back in a 240º arc and its preserved termination shifts onto the right flank and keeps curving upwards. A short section of shell bearing strong growth lines immediately precedes the aperture. None of the Clansayes specimens exhibits spiral strigations as documented by Kennedy and Latil (2007, pl. 2, fig. 2); this is probably due to an imperfect preservation.

DISCUSSION: According to Kennedy and Latil (2007, p. 456), this species is "always quadrituberculate on the phragmocone and on the beginning of the body chamber and trituberculate on the terminal part of the body chamber". However, our extensive material from Clansayes demonstrates a more intricate ontogenetic variation regarding this feature. In the earliest stages, the lateral tubercles are absent or only barely discernible (Pl. 13, Figs 1–9). At slightly larger sizes, they become more apparent (Pl. 11, Figs 4–8). There is then a transitory stage (beginning remarkably early in specimen UBGD 293107; Pl. 11, Figs 4–6) in which the outer ventrolateral tubercle is elusive (as it turns into a clavus barely differentiated from the low, blunt, prorsiradiate ribs that sweep forward across the ventrolateral shoulder), whereas the umbilical, lateral and inner ventrolateral tubercles are very obvious (Pl. 13, Figs 10–15). Once a certain diameter is reached (generally on the final section of phragmocone), all tubercles rapidly and distinctively strengthen; at the beginning of the body chamber the characteristic quadrituberculation is most fully expressed. Finally, the quadrituberculation is permanently lost on the terminal part of the body chamber, as the inner ventrolateral tubercles and outer ventrolateral clavi coalesce into massive, pinched clavi on the 5–7 ribs adapical of the rostrum, which are thus trituberculate.

Among the near-adult and adult specimens (Pl. 6, Fig. 1; Pl. 7, Figs 1, 2; Pl. 8, Figs 1–4; Pl. 9, Figs 1–4; Pl. 10, Figs 1–3; Pl. 11, Figs 1–3; Pl. 12, Figs 1, 2), specimen UBGD 293113 (Pl. 12, Figs 1, 2) probably represents an end-member depressed variant. Its remarkably thick whorls are associated with singularly dense ribbing on the outer whorl (compare with, e.g., the similarly-sized specimen UBGD 293114; Pl. 11, Figs 1–3). It is unclear whether specimen UBGD 293108 or specimen UBGD 293109 (both also significantly depressed; Pl. 13, Figs 10–15), best corresponds to the juvenile stages of specimen UBGD 293113. Noteworthy, specimen UBGD 293109 is strikingly identical both in shape and ornamentation to the phragmocone fragment USNM 486594 figured by Kennedy *et al.* (1998, fig. 14F, G).

Some of the small specimens (e.g., Pl. 11, Figs 7, 8; Pl. 13, Figs 1–9) are somewhat similar to specimens tentatively interpreted as immature representatives of *M. nanum* Spath, 1933 by Jattiot *et al*. (2021, fig. 15AM–BC). However, the latter are consistently more evolute (U/D ratio from 44 to 50%). We agree with Kennedy and Latil (2007) that the slightly older *M.* (*Mortoniceras*) *fallax* (Breistroffer, 1940a), characterizing the eponymous zone, differs from *M.* (*S.*) *rostratum* by the appearance of a definitive trituberculation at an earlier stage (i.e., before the body chamber) and its larger adult size. According to Kennedy and Latil (2007), the upper Albian ammonite succession in the Montlaux section (Hautes-Alpes, France) provides unequivocal evidence for a *M.* (*S.*) *rostratum* Zone succeeded by a *Mortoniceras* (*S.*) *perinflatum* Zone. Kennedy *et al*. (1998) thoroughly compared the type specimens of *M.* (*S.*) *rostratum* and *M.* (*S.*) *perinflatum* and stressed that characters of the phragmocones of the two holotypes are identical. They also emphasised that no adult body chambers of *M.* (*S.*) *perinflatum* have been illustrated, which to our knowledge is still the case, except for what may be part of an adult body chamber of *M.* (*S.*) *perinflatum* in Scholz (1979, pl. 28, fig. 3) according to Kennedy *et al*. (2005). Nevertheless, as stated by Kennedy *et al.* (1998), Kennedy *et al.* (2005) and Kennedy and Latil (2007), *M.* (*S.*) *rostratum* can be separated from *M.* (*S.*) *perinflatum* on the basis of its consistently less depressed whorl section. This hypothesis however is not supported by a statistical analysis based on extensive material of both species. Furthermore, as already noted by Kennedy *et al.* (1998), there are remarkably depressed *M.* (*S.*) *rostratum* individuals (e.g., Pl. 11, Figs 4–6; Pl. 13, Figs 10–15; see also Kennedy *et al*. 1998, fig. 14F, G). Unfortunately, the study by Kennedy and Latil (2007) adds nothing to the debate, since the whorl thickness of the alleged *M.* (*S.*) *perinflatum* specimens figured in this work is

unavailable. This observation implies that the assignment of specimens from the Montlaux section to *M.* (*S.*) *perinflatum* is highly doubtful. Finally, Latil *et al*. (2021) recently figured three specimens that they assigned to *M.* (*S.*) *perinflatum* without argumenting their identification. The whorl section of these figured specimens is variable, from slightly compressed to strongly depressed (W/H ratio between 0.90 and 1.40; Latil *et al*. 2021, p. 17). Noteworthy, Latil *et al*. (2021, p. 17) acknowledge that their material "shows a high morphological variability, the more compressed being very similar to *Mortoniceras* (*S.*) *rostratum* when only phragmocones are preserved [which is the case in the three figured specimens]."

In sum, in our opinion it is clear that firm evidence for the separation of *M.* (*S.*) *rostratum* and *M.* (*S.*) *perinflatum* as two distinct species is still lacking in the literature. Accordingly, the existence of a *Mortoniceras* (*S.*) *perinflatum* Zone above the *M.* (*S.*) *rostratum* Zone remains speculative (see also general discussion).

OCCURRENCE (after Latil *et al*. 2021): The species is widespread in the upper upper Albian of Bulgaria, Caucasus, Ukraine (Crimea), France, UK (England), Germany, Hungary, Poland, Romania (?), Spain, Switzerland, central Tunisia, Angola, Madagascar, Iran, USA (Texas), India and Japan.

Superfamily Scaphitoidea Gill, 1871
Family Scaphitidae Gill, 1871
Subfamily Scaphitinae Gill, 1871
Genus *Scaphites* Parkinson, 1811

TYPE SPECIES: *Scaphites equalis* J. Sowerby, 1813 (p. 53, pl. 18, figs 1–3), by the subsequent designation of Meek (1876, p. 413).

Scaphites hugardianus d'Orbigny, 1842
(Pl. 14, Figs 1–13)

1842. *Scaphites hugardianus* d'Orbigny, pp. 521, 525.
2016a. *Scaphites hugardianus* d'Orbigny, 1842; Klein, pp. 54, 77 (with additional synonymy).
2017. *Scaphites hugardianus* d'Orbigny, 1842; Tajika *et al*., p. 44, fig. 11N.
2021. *Scaphites hugardianus* d'Orbigny, 1842; Jattiot *et al*., p. 34, fig. 19A–X (with additional synonymy).

MATERIAL: Three singularly small individuals represented only by their adult body chamber; UBGD 293064-293066.

MEASUREMENTS:

	D	H	W	U	W/H
UBGD 293064 (Pl. 14, Figs 1–3)	NA	5.8	7.7	NA	1.33
UBGD 293065 (Pl. 14, Figs 4, 5)	NA	5.5	7.8	NA	1.42
UBGD 293066 (Pl. 14, Figs 6, 7)	NA	4.9	6.7	NA	1.37

DESCRIPTION: The whorl section is strongly depressed, reniform with a broadly rounded venter. The preserved ornamentation comprises fine prorsiradiate ribs, some of them polyfurcating (usually bifurcating) across the venter. Tubercles occur at the point of bifurcation and arise in alternating order across the venter; they are variable in strength and number, bullate or nodate (Cooper 1990; Jattiot *et al*. 2021). A very poorly-preserved, inconspicuous apertural constriction indicating maturity is present in specimen UBGD 293065 (Pl. 14, Fig. 4). The mid-ventral structures observed on the body chamber of specimens UBGD 293064 and UBGD 293065 (Pl. 14, Figs 3, 5) are presumably associated with the soft tissues in life (Kennedy 2004; Jattiot *et al*. 2021).

DISCUSSION: Except for their smaller adult size, these specimens are identical in all respects to typical *S. hugardianus* from the *Mortoniceras* (*M.*) *fallax* Zone at Salazac (Jattiot *et al*. 2021); two of the smallest Salazac specimens are here refigured for comparison (Pl. 14, Figs 8, 9, 12, 13). The observed smaller adult size at Clansayes might suggest a miniaturization process through time, from the *Mortoniceras* (*M.*) *fallax* Zone to the overlying *Mortoniceras* (*S.*) *rostratum* Zone (at least in the shallow peripheral domains of the south-eastern France sedimentary basin). Alternatively, this difference in *S. hugardianus* adult size observed between Clansayes and Salazac localities might be correlated with differences in the corresponding local environments (see geological settings).

The reader is referred to Cooper (1990), Wright and Kennedy (1996) and Jattiot *et al*. (2021) for more detailed descriptions and discussions including comparisons with other species. Although *S. hugardianus* might be a *nomen dubium* (Wright and Kennedy 1996), we here strictly follow the long-recognised limits of the species.

OCCURRENCE: Lower Cretaceous (upper Albian-?lower Cenomanian); UK (England), Spain, France, Switzerland, Italy (Sardinia), Hungary, Algeria, Madagascar.

Scaphites meriani Pictet and Campiche, 1861
(Pl. 14, Figs 14–30)

pars 1861. *Scaphites meriani* Pictet and Campiche, p. 16, pl. 40, figs 1–4, 8 only.
1965. *Scaphites* (*Scaphites*) *meriani* Pictet and Campiche, 1861; Wiedmann, p. 426, pl. 54, fig. 6; pl. 57, figs 3, 4; text-figs 5a–c (with synonymy).
1968. *Scaphites* (*Scaphites*) *meriani* Pictet and Campiche, 1861; Renz, p. 94, text-fig. 33a.
1968. *Scaphites* (*Scaphites*) sp. indet.; Renz, p. 94, pl. 18, fig. 19.
1979. *Scaphites* (*Scaphites*) *meriani* Pictet and Campiche, 1861; Scholz, p. 44, pl. 1, figs 26–28.
1996. *Scaphites* (*Scaphites*) *meriani* Pictet and Campiche, 1861; Kennedy in Gale *et al*., p. 590, fig. 30p.
2007. *Scaphites* (*Scaphites*) sp. Kennedy and Latil, p. 474, pl. 12, figs 5, 6.
2011. *Scaphites meriani* Pictet and Campiche, 1861; Gale *et al*., p. 99, fig. 40B, E.
2016a. *Scaphites meriani meriani* Pictet and Campiche, 1861; Klein, pp. 55, 84 (with additional synonymy).
?2021. *Scaphites* aff. *meriani* Pictet and Campiche, 1861; Latil *et al*., p. 28, fig. 17g, h.

TYPE (after Latil *et al*. 2021): The lectotype is the adult specimen figured by Pictet and Campiche (1861, pl. 44, fig. 1), designated and refigured by Wiedmann (1965, p. 426, pl. 54, fig. 6).

MATERIAL: One phragmocone (UBGD 293067; Pl. 14, Figs 14, 15), four body chamber fragments (UBGD 293068-293071), and three complete, adult body chambers (UBGD 293072-293074; Pl. 14, Figs 16-30).

MEASUREMENTS:

	D	H	W	U	W/H
UBGD 293068	NA	–	*24*	NA	NA
UBGD 293070 (Pl. 14, Figs 20–22)	NA	18.7	34.6	NA	1.85
UBGD 293072 (Pl. 14, Figs 16–19)	NA	11.5	21.2	NA	1.84
UBGD 293073 (Pl. 14, Figs 23–26)	NA	16.3	29.9	NA	1.83
UBGD 293074 (Pl. 14, Figs 27–30)	NA	17.5	31.8	NA	1.82

DESCRIPTION: Based on specimen UBGD 293067 (Pl. 14, Figs 14, 15), the early stages of *S. meriani* can be described as inflated, very involute, with an excessively depressed and thus, extremely reniform whorl section; the venter is exceptionally wide and very low (Pl. 14, Fig. 15). The presence of a bulge, as commonly observed on the inner edge of the beginning of the shaft in *S. hugardianus*, cannot be determined. Although very poorly preserved, there were presumably no tubercles on the original shell.

As shown by specimens UBGD 293070, UBGD 293072, UBGD 293073, and UBGD 293074 (Pl. 14, Figs 16–30), the adult body chamber of *S. meriani* is also excessively depressed, producing an extreme reniform whorl section (W/H ratio about 1.84 on average), with an extremely large, very low venter. The body chamber ornamentation comprises fine but wiry prorsiradiate ribs on the flanks. These ribs regularly unify in pairs at a coarse ventrolateral tubercle; only in very rare instances a single lateral rib produces a ventrolateral tubercle. The number of intercalated nontuberculate ribs varies between one and three. The tubercles arise in alternating order across the venter. An estimation of the tubercle number is hampered by the imperfect preservation. There appear to be about 6–8 tubercles (8 in specimens UBGD 293072 and UBGD 293073; Pl. 14, Figs 16–19, 23–26) on the adult body chamber of our specimens, although this appears to be subject to an even greater variation (9–10 body chamber tubercles are mentioned in Scholz 1979). Ornamentation on the venter consists of very fine but still somewhat wiry ribs; their number is considerable due to branching and intercalation on the ventrolateral shoulders.

The shell is likely dimorphic, with specimen UBGD 293072 (Pl. 14, Figs 16–19) interpreted as a fully grown microconch, and specimens UBGD 293073 and UBGD 293074 (Pl. 14, Figs 23–30) as fully grown macroconchs (see discussion below). Noteworthy, specimen UBGD 293073 displays scars and slight ribbing disruptions on the venter (Pl. 14, Fig. 26).

DISCUSSION: In macroconchs approaching maturity, the whorl becomes markedly constricted (i.e., the whorl thickness significantly decreases) and the ornamentation fades away (ventrolateral tubercles are lost). However, a narrow but deep apertural constriction as seen on mature *S. hugardianus* (see e.g., Cooper 1990; Jattiot *et al*. 2021) is not present on our specimens. The whorl becomes constricted at near-maturity in microconchs as well (Pl. 14, Figs 16–18), but the ornamentation does not conspicuously fade away, with ventrolateral tubercles still present immediately prior to the aperture. In all cases, full maturity is characterised by a strong apertural collar-lappet (e.g., Pl. 14, Figs 16–18, 27–29).

We concur with Kennedy in Gale *et al*. (1996) in regarding *S. meriani* as a distinct, valid species (as opposed to Cooper 1990). In our opinion, *S. meriani* is distinguished from *S. hugardianus* by the combination of its much larger adult size (through a much longer body chamber), coarse tubercles, and extreme

reniform whorl section (W/H ratio about 1.84 on average versus about 1.37 on average in the Clansayes *S. hugardianus* material). Although we acknowledge that the *S. meriani* adult microconch individual identified at Clansayes (Pl. 14, Figs 16–19) is comparable in size to an exceptionally large *S. hugardianus* specimen from Salazac (Jattiot *et al*. 2021, refigured here for comparison in Pl. 14, Figs 10, 11), its extreme reniform whorl section and very low venter immediately separates both specimens. More secondarily, maturity in *S. hugardianus* is not characterised by a marked decrease in whorl thickness and loss of ornamentation.

Scaphites meriani was documented from the *Mortoniceras* (*S.*) *perinflatum* Zone (but see general discussion) by Gale *et al*. (1996, fig. 30p). We suggest that it also occurs within the *M.* (*S.*) *rostratum* and *M.* (*S.*) *perinflatum* Zones in the Montlaux section (based on specimens described as *Scaphites* sp.; Kennedy and Latil 2007, pl. 12, figs 5, 6). Noteworthy, the occurrence of *S. meriani* appears to not extend down to the *Mortoniceras* (*M.*) *fallax* Zone, since it is undoubtedly absent in the recently described extensive material from Salazac (Jattiot *et al*. 2021). Conversely, the occurrence of *S. hugardianus*, abundant in the *Mortoniceras* (*M.*) *fallax* Zone at Salazac (Jattiot *et al*. 2021), indisputably extends up to the *Mortoniceras* (*S.*) *rostratum* (this work) and *perinflatum* Zones (Gale *et al*. 1996, fig. 17a–c, g).

OCCURRENCE: *M.* (*S.*) *rostratum* and *M.* (*S.*) *perinflatum* Zones; Hungary, Romania, Italy (Sardinia), Switzerland, central Tunisia, and Madagascar (?).

Suborder Ancyloceratina Wiedmann, 1966
Superfamily Turrilitoidea Gill, 1871
Family Turrilitidae Gill, 1871
Genus and subgenus *Mariella* Nowak, 1916

TYPE SPECIES: *Turrilites bergeri* Brongniart, 1822 (p. 395, pl. 7, fig. 3), by the original designation of Nowak (1916, p. 10).

DISCUSSION: *Mariella* (*M.*) *bergeri* (Brongniart, 1822), *M.* (*M.*) *miliaris* (Pictet and Campiche, 1861), *M.* (*M.*) *crassituberculata crassituberculata* Spath, 1937 and *M.* (*M.*) *crassituberculata extrema* Renz, 1968 represent a contemporaneous group of very closely allied taxa. According to Klinger and Kennedy (1978, p. 28), "various morphological variants of *M.* (*M.*) *bergeri* have been named and described, and all are linked by transitional passage forms". Wiedmann and Dieni (1968) synonymised *M.* (*M.*) *crassituberculata crassituberculata* with *M.* (*M.*) *bergeri*, and even suggested the inclusion of *M.* (*M.*) *miliaris*. Following Wiedmann and Dieni's (1968) view, as Klinger and Kennedy (1978, p. 28) underlined, the following sequence could be proposed for a *M.* (*M.*) *bergeri* group, based on an increasing coarseness of ornamentation: *M.* (*M.*) *miliaris* - *M.* (*M.*) *bergeri* - *M.* (*M.*) *crassituberculata crassituberculata* - *M.* (*M.*) *crassituberculata extrema* (see also Cooper 1998). In this work, we focused on the question whether these four taxa could be firmly discriminated on the basis of an extensive collection.

Mariella (*Mariella*) *bergeri* (Brongniart, 1822)
(Pl. 15, Figs 9–40; Pls 16, 17; Pl. 18, Figs 1–6)

1822. *Turrilites bergeri* Brongniart, p. 395, pl. 7, fig. 3.
?1968. *Mariella* (*Mariella*) *bergeri* aff. *conduciensis* Breistroffer, 1940; Renz, p. 86, pl. 17, fig. 27.
?1968. *Mariella* (*Mariella*) n. sp. Renz, p. 87, pl. 18, fig. 7.
1968. *Mariella* (*Mariella*) *bergeri bergeri* (Brongniart, 1822); Renz, p. 85, pl. 17, figs 37, 41; pl. 18, figs 3, 4, 8, text-fig. 31f, k.
1968. *Mariella* (*Mariella*) *bergeri* ssp.? Renz, p. 86, pl. 18, fig. 16.
1968. *Mariella* (*Mariella*) *crassituberculata crassituberculata* Spath, 1937; Renz, p. 86, pl. 18, figs 5, 6.
1968. *Mariella* (*Mariella*) *crassituberculata extrema* Renz, p. 87, pl. 18, fig. 9.
1978. *Mariella* (*Mariella*) *bergeri* (Brongniart, 1822); Klinger and Kennedy, p. 28, pl. 1, fig. H, text-fig. 6E.
2007. *Mariella* (*Mariella*) *bergeri* (Brongniart, 1822); Kennedy and Latil, p. 472, pl. 10, figs 1, 2, 13 (with additional synonymy).
2015. *Mariella bergeri bergeri* (Brongniart, 1822); Klein, pp. 131, 133 (with additional synonymy).
2017. *Mariella bergeri* (Brongniart, 1822); Tajika *et al*., p. 42, fig. 11D, I, K.
2018a. *Mariella bergeri* (Brongniart, 1822); Tajika *et al*., p. 277, fig. 551.
?2019. *Mariella* (*Mariella*) *bergeri* (Brongniart, 1822); Gautam *et al*., p. 25, figs 7D–F.
2020. *Mariella* (*Mariella*) *bergeri* (Brongniart, 1822); Kennedy, p. 237, pl. 36, figs 19, 21, 23.
2021. *Mariella* (*Mariella*) *bergeri* (Brongniart, 1822); Latil *et al*., p. 26, fig. 17c–e.

TYPE (after Kennedy and Latil 2007): The holotype, by monotypy, is the original of Brongniart (1822, pl. 7, fig. 3), from the Montagne de Fiz, Savoie, France. The specimen has not been traced.

MATERIAL AND MEASUREMENTS: See Supplementary Appendix; N = 98.

DESCRIPTION: Turriliticones, dextral (7%) or sinistral (93%), with considerable intraspecific variation in whorl shape (more or less rounded flanks) and ornamentation. Apical angle variable, related to whorl shape. The ornamentation typically consists of four rows of conical tubercles (although they may tend towards slight transversal elongation in some instances), highly variable in strength. The number of tubercles in each row per whorl is remarkably variable (see discussion below). As a general rule, the tubercles of the upper row are placed some way above mid-flank and each is connected to the inter-whorl suture by a more or less pronounced rib, while the lower two rows are slightly closer together than the rest. The tubercles of the fourth, lowest row are partially concealed in the inter-whorl suture. In rare instances, exceptionally well-preserved (i.e., when the external shell layer is preserved) tubercles of the lowest row give rise to short spines (Pl. 16, Figs 6–8, 10–12). When exposed, the base of the whorl shows that the tubercles of the lowest row are linked to radial ribs progressively weakening towards the umbilicus.

Specimens UBGD 293215 and UBGD 293255 (Pl. 16, Figs 5–12) are interpreted as adult microconchs, with maturity being indicated by an exceptionally well-preserved peristome and a loosely coiled final sector of body chamber. Specimen UBGD 293246 (Pl. 15, Figs 32, 33) is similarly seen as an adult microconch with partly preserved and/or incipient peristome. Specimen UBGD 293270 (Pl. 16, Figs 13, 14) is presumably a body-chamber fragment of an adult macroconch with incipient peristome.

Specimen UBGD 293235 (Pl. 15, Figs 23–25) is strongly pathological, as it shows a deformed, slightly inflated shell with a chaotic sculpture. It can be referred to the chaotica forma-type pathology *sensu* Keupp (1977). The last whorl of specimen UBGD 293266 (Pl. 17, Fig. 11) exhibits uppermost tubercles that give rise to two ribs; these are linked at the inter-whorl suture in a zigzag fashion. This singular ornamentation is likely due to a minute pathology on the upper flank. Finally, very minor disruptions in the arrangement of the tubercles can sometimes be observed (see e.g., Pl. 15, Figs 18, 39).

DISCUSSION: *Mariella* (*M.*) *bergeri* is typically interpreted as having a total of about 25 tubercles per whorl in each row (e.g., Spath 1937; Klinger and Kennedy 1978). According to Klinger and Kennedy (1978), the ornamentation of *M.* (*M.*) *miliaris* is in the same style as that of *M.* (*M.*) *bergeri*, but more delicate, with up to 54 tubercles per whorl in each row. Renz (1968, p. 88) indeed estimated the number of 'ribs' per whorl (i.e., the number of tubercles per whorl in each row) to be 54 on the holotype of *M.* (*M.*) *miliaris*. Considering that the holotype only comprises about half a whorl, which makes difficult an accurate assessment of the total number of tubercles per whorl in each row, we assume that this number is largely overestimated. Klinger and Kennedy (1978) also implicitly suggest that *M.* (*M.*) *bergeri* has a higher whorl section. According to Wright and Kennedy (1996), *M.* (*M.*) *miliaris* is distinguished by its large apical angle and dense ornamentation in which the tubercles are elongated and rib-like, whereas the tubercles of *M.* (*M.*) *bergeri* are much coarser and rounded. The sole *M.* (*M.*) *miliaris* specimen documented by Wright and Kennedy (1996), supposedly from the lower Cenomanian based on its preservation, has 34 tubercles per whorl in each row with a maximum preserved whorl height of 21.5 mm. Finally, according to Tajika *et al*. (2017), the tubercles of *M.* (*M.*) *miliaris* are finer and denser than those of *M.* (*M.*) *bergeri*; these authors counted 34 tubercles per whorl in each row on one of their figured specimens (with a maximum preserved whorl height of 29 mm; Tajika *et al*. 2017, Fig. 11O).

In order to revise the taxonomic status of these two species, the accurate assessment of the range of variation in the number of tubercles per whorl in each row within the large *Mariella* collection from Clansayes is needed. First, the distribution of the number of tubercles per whorl in each row within our sample (N = 76) appears to be graphically bimodal (Text-fig. 5). This visual observation is confirmed by a statistical inspection (Hartigan's dip test, D = 0.064935, p = 0.01408), which allows for the discrimination of two groups. In the first group, the number of tubercles per whorl in each row ranges from 19 to 30, the mean value being around 25 (i.e., 25.3). This conforms very well to the definition of *M.* (*M.*) *bergeri* by Spath (1937) and Klinger and Kennedy (1978) as having a total of about 25 tubercles per whorl in each row. In the second group, the number of tubercles per whorl in each row ranges from 33 to 40; these values are comparable to those expected on *M. miliaris* individuals based on the description of this species by Klinger and Kennedy (1978), Wright and Kennedy (1996) and Tajika *et al*. (2017). There are no specimens with intermediate values of 31 or 32 tubercles in each row per whorl, further supporting the existence of two distinct species, namely *M.* (*M.*) *bergeri* and *M.* (*M.*) *miliaris*. However, analysing the number of tubercles per whorl

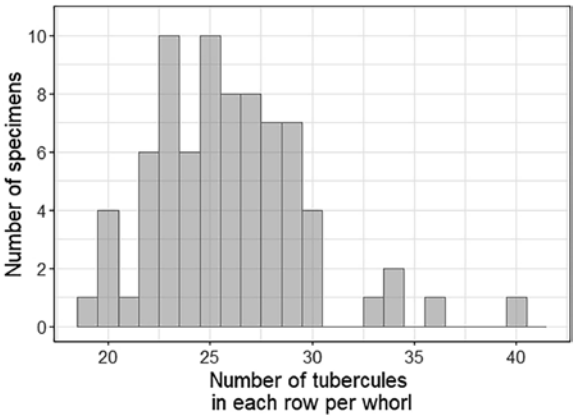

Text-fig. 5. Distribution of the number of tubercles in each row per whorl among *Mariella* spp. specimens from Clansayes, France.

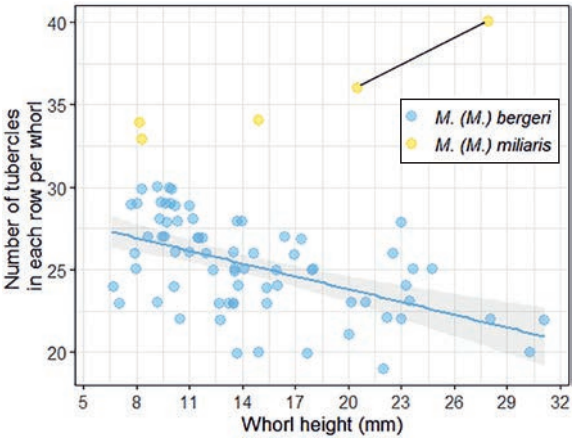

Text-fig. 6. Observed number of tubercles in each row per whorl among specimens of *Mariella* (*M.*) *bergeri* (Brongniart, 1822) and *Mariella* (*M.*) *miliaris* (Pictet and Campiche, 1861) according to their whorl height, with regression line and confidence interval for the *M.* (*M.*) *bergeri* sample. The black line connects values taken at two different ontogenetic stages of a *M.* (*M.*) *miliaris* individual (specimen UBGD 293280; Pl. 18, Figs 7–9).

in each row alone ignores the role that ontogeny might play on this morphological character (as recently shown by Jattiot *et al.* 2021, based on an extensive *Mariella* collection from the upper Albian at Salazac). Nevertheless, a visual inspection of the number of tubercles per whorl in each row according to maximum preserved whorl height (we here use the maximum preserved whorl height as a proxy for growth) within each group (Text-fig. 6) suggests again that there are two separate species. Indeed, specimens assigned to *M.* (*M.*) *miliaris* based on Text-fig. 5 consistently have more tubercles per whorl in each row than *M.* (*M.*) *bergeri* individuals, regardless of the specimen size. Consequently, *M.* (*M.*) *miliaris* is here considered as a valid, distinct species, being mainly distinguished from *M.* (*M.*) *bergeri* by its higher number of tubercles per whorl in each row [between 33 and 40 versus around 25 in *M.* (*M.*) *bergeri*]. As mentioned above, the number of 54 tubercles per whorl in each row given by Renz (1968, p. 88) based on the holotype, which comprises only less than half a whorl, is most certainly largely overestimated.

Two different ontogenetic patterns can even be identified within *M.* (*M.*) *bergeri* and *M.* (*M.*) *miliaris* as discriminated in the Clansayes sample. Indeed, a graphical inspection (Text-fig. 6) strongly suggests that the number of tubercles per whorl in each row decreases with growth in *M.* (*M.*) *bergeri*, whereas it appears to increase with growth in *M.* (*M.*) *miliaris*. The assessment of the number of tubercles per whorl in each row at two different ontogenetic stages on some specimens of *M.* (*M.*) *bergeri* supports this pattern of decreasing number of tubercles throughout ontogeny. For example, specimen UBGD 293259 (Pl. 17, Figs 1–3) bears 30 tubercles per whorl in each row at a conceptual maximum preserved whorl height of about 12 mm, and 25 at the actual maximum preserved whorl height of 16 mm; while specimen UBGD 293249 (Pl. 17, Figs 4–6) shows 29 tubercles per whorl in each row at a conceptual maximum preserved whorl height of 13.6 mm, and 26 at the actual maximum preserved whorl height of 17 mm. Regarding *M.* (*M.*) *miliaris*, specimen UBGD 293280 (Pl. 18, Figs 7–9) similarly allows us to count the number of tubercles per whorl in each row at two different ontogenetic stages. This specimen well supports the hypothesis of an increasing number of tubercles during ontogeny, as it bears 36 tubercles per whorl in each row at a conceptual maximum preserved whorl height of 20.4 mm, and 40 at the actual maximum preserved whorl height of 27.9 mm (note that these measurements are considered independently in Text-figs 5, 6).

Based on the values of model residuals (i.e., deviance of individual data points from the average relationship; see Supplementary Appendix) from the *M.* (*M.*) *bergeri* sample, it can be shown that specimens UBGD 293223, UBGD 293243, UBGD 293245, UBGD 293253, UBGD 293262 and UBGD 293267 (Pl. 15, Figs 21, 26–28; Pl. 17, Figs 7–9, 12) exhibit a lower number of tubercles per whorl in each row than expected for their size, whereas specimens UBGD 293212, UBGD 293213, UBGD 293248, UBGD 293261 and UBGD 293271 (Pl. 15, Figs 14, 20, 29–31; Pl. 16, Figs 1–3; Pl. 17, Figs 14–16) exhibit a higher number of tubercles per whorl in each row than ex-

pected for their size. This should typically be interpreted as intraspecific variability for this morphological parameter. Consequently, we acknowledge that the smallest *M.* (*M.*) *bergeri* specimens with higher number of tubercles per whorl in each row than expected for their size (e.g., Pl. 15, Figs 14, 20) may somewhat resemble similarly-sized *M.* (*M.*) *miliaris* individuals (e.g., Pl. 15, Figs 3–5). Nevertheless, the number of tubercles per whorl in each row never exceeds 30 among these *M.* (*M.*) *bergeri* specimens; therefore, they remain separated from *M.* (*M.*) *miliaris* specimens (Text-fig. 6).

Based on these extreme variants, it appears that the number of tubercles per whorl in each row and the strength of tubercles are negatively correlated. Indeed, the *M.* (*M.*) *bergeri* specimens with a low number of tubercles (among both small and large specimens) all display very coarse, strong tubercles (Pl. 15, Figs 21, 26–28; Pl. 17, Figs 7–9, 12). Conversely, most *M. bergeri* specimens with a high number of tubercles (among both small and large specimens) display relatively fine tubercles (e.g., Pl. 15, Figs 14, 20, 29–31; Pl. 17, Figs 14–16). This correlation can be further extended to *M.* (*M.*) *miliaris*: all available specimens have a high number of tubercles; therefore, these latter are particularly fine (see Pl. 15, Figs 1–8; Pl. 18, Figs 7–9).

Mariella (*M.*) *crassituberculata crassituberculata* Spath, 1937 and *M.* (*M.*) *crassituberculata extrema* Renz, 1968 supposedly differ from *M.* (*M.*) *bergeri* specimens by their coarser tubercles. Despite the fact that the holotype of *M.* (*M.*) *crassituberculata crassituberculata* (Renz, 1968, pl. 18, fig. 6) preserves less than half a whorl, Renz (1968) roughly estimated its number of tubercles per whorl in each row to be around 21. Renz (1968) also tentatively estimated the number of tubercles per whorl in each row to be around 15 for the holotype of *M.* (*M.*) *crassituberculata extrema* (Renz 1968, pl. 18, fig. 9), even though the latter preserves only half a whorl. As discussed above, the number of tubercles per whorl in each row and the strength of tubercles appears to be negatively correlated in *M.* (*M.*) *bergeri*. Thus, the Clansayes material comprises coarsely ornamented *M.* (*M.*) *bergeri* variants with a singularly low number of tubercles according to their size (i.e., 19 or 20; e.g., Pl. 15, Figs 26, 27, Pl. 17, Figs 8, 9), among which specimen UBGD 293262 (Pl. 17, Figs 8, 9) fully resembles the holotype of *M.* (*M.*) *crassituberculata crassituberculata* (Renz, 1968, pl. 18, fig. 6). In turn, we here interpret *M.* (*M.*) *crassituberculata crassituberculata* and *M.* (*M.*) *crassituberculata extrema* as end-member variants of *M.* (*M.*) *bergeri*.

More secondarily, although methodology issues preclude comparisons of published apical angle estimates and thus impede its use as a diagnostic character [*M.* (*M.*) *miliaris* is distinguished by its large apical angle according to Wright and Kennedy 1996], we strongly suggest that the apical angle and the whorl shape are partly correlated. Indeed, low-whorled *Mariella* specimens appear to consistently show a large apical angle. Based on this, it can also be tentatively hypothesised that, as a general rule, *M.* (*M.*) *miliaris* individuals have lower whorls than typical *M.* (*M.*) *bergeri* representatives at comparable size (compare, e.g., Pl. 18, Figs 7–9 with Pl. 18, Figs 1–3). Finally, we do not concur with Wright and Kennedy (1996) in distinguishing *M.* (*M.*) *miliaris* by tubercles that are elongated and rib-like [*versus* rounded in *M.* (*M.*) *bergeri*]. Indeed, although it is true that specimen UBGD 293280 exhibits slightly transversally elongated tubercles (Pl. 18, Figs 1–3), tubercles of other, well-preserved *M.* (*M.*) *miliaris* specimen (see e.g., specimen UBGD 293205, Pl. 15, Figs 3–5) do not significantly differ in shape from those of typical *M.* (*M.*) *bergeri* specimens (compare with e.g., the similarly-sized specimen UBGD 293195, Pl. 15, Fig. 12). We here strongly suggest that the shape of the tubercles (along with their strength) is highly dependent on preservation (different wearing degree of the internal mould, as well as potential preservation of external shell layers) and to a lesser extent ontogeny. Specimen UBGD 293211 (Pl. 15, Figs 15, 16) well illustrates this statement, as it exhibits slightly longitudinally elongated tubercles on the upper row, which become well-rounded on the lower row. Thus, in our opinion the shape of the tubercles bears no diagnostic value.

OCCURRENCE (after Latil *et al*. 2021): Widespread in the upper upper Albian *Mortoniceras* (*S.*) *rostratum*, *Mortoniceras* (*S.*) *perinflatum* and *Arrhaphoceras* (*P.*) *briacensis* Zones; UK (southern England), France, Switzerland, Germany, Spain, Italy, Hungary, Romania, Ukraine (Crimea), Caucasus, Turkmenistan, Iran, Morocco, Algeria, Tunisia, India, South Africa, Venezuela and USA (California).

Mariella (*Mariella*) *miliaris*
(Pictet and Campiche, 1861)
(Pl. 15, Figs 1–8; Pl. 18, Figs 7–9)

1861. *Turrilites bergeri* Brongniart var. *miliaris* Pictet and Campiche, p. 136, pl. 58, fig. 5.
1968. *Mariella* (*Mariella*) *miliaris* (Pictet and Campiche, 1861); Renz, p. 88, pl. 18, fig. 10; text-figs 31m, 32h.
1996. *Mariella* (*Mariella*) *miliaris* (Pictet and Campiche,

1861); Wright and Kennedy, p. 333, pl. 100, fig. 28 (with additional synonymy).

?1996. *Mariella* (*Mariella*) cf. *miliaris* (Pictet and Campiche, 1861); Kennedy in Gale *et al*., p. 583, figs 28c, h, k, m, n; 29a–d, j, k.

?1999. *Mariella* (*Mariella*) cf. *miliaris* (Pictet and Campiche, 1861); López-Horgue *et al*., p. 387, fig. 16j, k.

2015. *Mariella miliaris* (Pictet and Campiche, 1861); Klein, pp. 132, 146 (with additional synonymy).

2017. *Mariella miliaris* (Pictet and Campiche, 1861); Tajika *et al*., p. 42, fig. 11J, O, S–U.

2018. *Mariella miliaris* (Brongniart, 1822); Tajika *et al*., p. 278, fig. 553.

TYPE (after Wright and Kennedy 1996): The holotype, by monotypy, is no. 40041 in the collections of the Musée Géologique de Lausanne, Switzerland, the original of Pictet and Campiche (1861, p. 136, pl. 58, fig. 5), from the upper upper Albian of La Vraconne, near Saint Croix, Vaud, Switzerland. It was refigured by Renz (1968, pl. 18, fig. 10).

MATERIAL: Four specimens; UBGD 293186, 293205, 293241, 293280.

MEASUREMENTS: See Supplementary Appendix; N = 4.

DESCRIPTION: Turriliticones with relatively low-whorls (and associated rather large apical angle. The four available specimens are sinistral. The ornamentation consists of four rows of tubercles that are to some extent variable in shape (e.g., slightly elongated transversally on specimen UBGD 293280, Pl. 18, Figs 7–9; rounded, conical on specimen UBGD 293205, Pl. 15, Figs 3–5). The number of tubercles per whorl in each row varies from 33 to 40 within our material (Text-fig. 6). As a general rule, the tubercles of the upper row are placed some way above mid-flank and each is connected to the inter-whorl suture by a relatively weak rib, while the lower two rows are slightly closer together than the rest. The tubercles of the fourth, lowest row are partially concealed in the inter-whorl suture. When exposed, the base of the whorl shows that the tubercles of the lowest row are linked to radial ribs progressively weakening towards the umbilicus.

DISCUSSION: The number of available specimens (i.e., 4, which are all sinistral) is too low to determine whether or not dextral individuals occur in comparable proportions than what is observed in *Mariella bergeri* (see above). Specimen UBGD 293280 (Pl. 18, Figs 7–9) is remarkably similar in shell shape and ornamentation to the holotype (Pictet and Campiche 1861, pl. 58, fig. 5; refigured by Renz 1968, pl. 18, fig. 10). The sole specimen documented by Wright and Kennedy (1996), supposedly from the lower Cenomanian based on its preservation, has 34 tubercles in each row per whorl at a maximum preserved whorl height of 21.5 mm, which fits well with our material (Text-fig. 6). The reader is referred to the *M. bergeri* discussion (see above) for a thorough comparison of the two species.

OCCURRENCE: Lower to Upper Cretaceous (upper Albian to lower Cenomanian, *M. mantelli* Zone); UK (England), France, Switzerland, Italy (Sardinia), Hungary, Romania, Turkmenistan, Madagascar, South Africa (KwaZulu-Natal).

Mariella sp. 1
(Pl. 18, Fig. 12)

MATERIAL: One specimen; UBGD 293192.

MEASUREMENTS: See Supplementary Appendix; N = 1.

DESCRIPTION: The single specimen is a fragment of a sinistral turriliticone, comprising a very small portion of a whorl. The ornamentation consists of only two rows of tubercles that are rather close to each other, of which the upper one is place around mid-flank. Each tubercle of the upper row is connected to the equivalent tubercle of the lower row by a conspicuous rib. This rib extends both upwards and downward on the upper and lower flank to the umbilicus.

DISCUSSION: At first sight, the ornamentation of this specimen appears somewhat intermediate between *Mariella* and *Turrilitoides* (see typical representatives of *Turrilitoides* in Jattiot *et al*. 2021). However, this fragment likely belonged to a pathological *Mariella bergeri* individual that suffered a minor, non-lethal injury and represents somehow a case of ornamental compensation (see e.g., Guex 1967, 1968).

Mariella sp. 2
(Pl. 18, Figs 10, 11)

MATERIAL: One specimen; UBGD 293294.

MEASUREMENTS: See Supplementary Appendix; N = 1.

DESCRIPTION: The single specimen is a small fragment of a sinistral turriliticone, comprising one whorl. The ornamentation consists of only three rows of tubercles, which are equally distant. The tubercles (25 per whorl in each row) are rather sharp and slightly elongated transversally. The tubercles of the upper row are placed around mid-flank and each is connected to the inter-whorl suture by a relatively long rib. The tubercles of the fourth, lowest row are linked to radial ribs progressively weakening towards the umbilicus.

DISCUSSION: The holotype of *M.* (*M.*) *taeniata* (Pictet and Campiche, 1862), from the upper upper Albian of La Vraconne, Sainte-Croix (see revision in Renz 1968, p. 91, pl. 18, fig. 1, text-fig. 32g), similarly exhibits only three rows of tubercles. However, it differs from the present specimen by a slightly different arrangement of the rows of tubercles on the whorl (the first, uppermost row and the second being singularly distant) as well as in having 36 tubercles per whorl in each row (versus 25 in the present specimen). Since *M.* (*M.*) *taeniata* is poorly represented (see Avram *et al*. 1993, fig. 141; López-Horgue *et al*. 1999, fig. 16a–d; Tajika *et al*. 2018a, fig. 554), its validity is actually questionable. Alternatively, the holotype of *M.* (*M.*) *taeniata* might be interpreted as a pathological *M.* (*M.*) *miliaris* individual [based on its 36 tubercles per whorl in each row; see discussion for *M.* (*M.*) *bergeri*], with the usual, uppermost row of tubercles missing, rather than a representative of a distinct, separate species. By extension, according to its number of tubercles per whorl in each row (i.e., 25), the present specimen may be seen as a similarly pathological *M.* (*M.*) *bergeri* specimen (supposedly also with the usual, uppermost row of tubercles missing). Noteworthy, the holotype of *M.* (*M.*) *canaliculata* (Breistroffer 1947), which is the only figured specimen for the species according to Klein (2015; refigured by Renz 1968, pl. 18, fig. 2), might just as well actually be a pathological *Mariella bergeri* specimen exhibiting a longitudinal scar.

Family Anisoceratidae Hyatt, 1900
Genus *Anisoceras* Pictet, 1854

TYPE SPECIES: *Hamites saussureanus* Pictet in Pictet and Roux, 1847 (p. 374, pl. 13, figs 1–4), by the original designation of Pictet (1854, p. 705).

Anisoceras armatum (J. Sowerby, 1817)
(Pl. 19)

1817. *Hamites armatus* J. Sowerby, p. 153, pl. 168.
2007. *Anisoceras armatum* (J. Sowerby, 1817); Kennedy and Latil, p. 467, pl. 7, fig. 7; pl. 10, figs 11, 14 (with full synonymy).
2008. *Anisoceras armatum* (J. Sowerby, 1817); Kennedy *et al*., p. 45, pl. 8, figs 23–29; pl. 9, figs 18–21, 31, 32; pl. 10, figs 14, 15 (with additional synonymy).
2015. *Anisoceras armatum* (J. Sowerby, 1817); Klein, pp. 25, 27 (with additional synonymy).
2017. *Anisoceras armatum* (J. Sowerby, 1817); Tajika *et al*., p. 39, figs 9AI, 10F, K, L.
2018b. *Anisoceras armatum* (J. Sowerby, 1817); Tajika *et al*., fig. 2S, T.
2018b. *Anisoceras perarmatum* Pictet and Campiche, 1861; Tajika *et al*., fig. 2AI.
2021. *Anisoceras armatum* (J. Sowerby, 1817); Latil *et al*., p. 26, fig. 17a, b.

TYPE (after Kennedy and Latil 2007): The holotype, by monotypy, is the original of J. Sowerby (1817, pl. 168), no. K673a, b in the collections of the Oxford University Museum of Natural History, from the upper Albian Upper Greensand of Roke, 1.5 km (1 mile) NNE of Benson, Oxfordshire, UK. It was refigured by Kennedy *et al*. (1998, fig. 30).

MATERIAL: Nine specimens; UBGD 293084, 293087-293093, 293097.

MEASUREMENTS:

	D	H	W	U	W/H
UBGD 293084	NA	18.6	18.8	NA	1.08
UBGD 293087	NA	9.1	9.3	NA	1.02
UBGD 293088 (Pl. 19, Figs 7, 8)	NA	10.7	11	NA	1.03
UBGD 293089	NA	12.8	12.8	NA	1.00
UBGD 293090 (Pl. 19, Figs 1, 2)	NA	~ 19	–	NA	–
UBGD 293091 (Pl. 19, Figs 5, 6)	NA	13.6	13.4	NA	0.99
UBGD 293093 (Pl. 19, Figs 9, 10)	NA	~ 29	–	NA	–
UBGD 293097	NA	~ 38	–	NA	–

DESCRIPTION: Short, curved, and slightly helicoid fragments have whorl heights of up to an estimated 19 mm (Pl. 19, Figs 1, 2, 5–8). The intercostal whorl section is subcircular to circular (the oval whorl section of specimen UBGD 293090 very likely results from post-mortem crushing). As a general rule, the dorsum bears weak, even, transverse, feebly convex ribs that regularly link in pairs at strong, flat-topped lower flank tubercles. A pair of coarse, nearly straight ribs link to larger ventrolateral tubercles (according to Kennedy *et al*. 2008, dorso- and ventrolateral tubercles are the bases of septate spines). The ventrolateral tubercles are connected across the venter by a pair of broad, barely differentiated ribs, producing a weak

swelling. The pairs of tuberculate ribs are very regularly separated by one or two intercalated, nontuberculate, single ribs. The remainder of the material consists of a very short, but well-preserved portion of a much larger phragmocone (specimen UBGD 293092; Pl. 19, Figs 3, 4), as well as a large, fairly well-preserved phragmocone section (specimen UBGD 293093; Pl. 19, Figs 9, 10). Noteworthy, specimen UBGD 293094 preserves clavi-like ventrolateral tubercles parallel to direction of growth, and high, conical and sharp lower flank tubercles. Specimen UBGD 293093 comprises curved earliest growth stages and a nearly straight shaft approximately 110 mm long, with a maximum preserved whorl height of about 29 mm. This specimen was retrieved from the upper part of the sampled level and was most certainly subjected to post-mortem crushing, which prevents the determination of its initial whorl width. Overall, its ornamentation follows the same pattern as that of smaller specimens described above. Noteworthy, it displays a very regular alternation of single, nontuberculate ribs and tuberculate pairs of ribs, except on the adapertural sector of shell where there are no nontuberculate ribs between three consecutive tuberculate pairs of ribs.

DISCUSSION: *Anisoceras armatum* and *A. perarmatum* Pictet and Campiche, 1861 commonly occur together (e.g., Cooper and Kennedy 1979; Kennedy *et al.* 1998; Kennedy and Latil 2007; this work), which led some authors (e.g., Scholz 1979) to regard them as conspecific. According to Kennedy *et al.* (1998, p. 42), the "absence of intercalated non-tuberculate ribs on the phragmocone and penultimate shaft characterises the lectotype of *Anisoceras perarmatum*, and serves to separate it from the holotype of *A. armatum*". Kennedy and Latil (2007, p. 468) later stated that *A. perarmatum* "lacks nontuberculate ribs throughout most of its ontogeny, although they develop on the final shaft of the adult body chamber". However, as noted by Kennedy *et al.* (1998, p. 42) and Kennedy and Latil (2007, p. 469), "there are specimens referred to *A. perarmatum* that may have a few intercalated ribs at these growth stages [on the phragmocone and penultimate shaft], and are thus intermediate between the two species". Such intermediate specimens were figured by Cooper and Kennedy (1979, fig. 18) and Kennedy and Latil (2007, pl. 7, figs 4, 5), and they are also present in the Clansayes collection (Pl. 22, Figs 1–5). In our opinion, it is not appropriate to unjustifiably assign these puzzling specimens to one of the two species; instead, they are here kept in open nomenclature (see below). In our work, only specimens with very few or no intercalated nontuberculate ribs on the phragmocone and penultimate shaft were assigned to *A. perarmatum* (see below). Conversely, only specimens exhibiting very regular-non tuberculate ribs were assigned to *A. armatum*. In order to thoroughly investigate whether all specimens of *A. armatum* and *A. perarmatum* belong to the same taxon, it is critically important to accurately determine (based on well-preserved and most complete adult specimens) the morphological changes occurring throughout ontogeny, as well as assess the potential ornamental variability with respect to whorl shape.

According to Cooper and Kennedy (1979, p. 207), *A. armatum* and *A. saussureanum* (Pictet in Pictet and Roux, 1847), contemporary in the latest Albian, "probably do not bear specific separation. However, until the type and topotype material of *A. saussureanum* are restudied with regard to their intraspecific variation, it seems preferable to retain these two well-known species separate". The *Anisoceras* material from Clansayes adds nothing to the debate.

Although *A. armatum* is recorded from the *Mortoniceras* (*M.*) *fallax* Zone at Strépy-Thieu (Belgium, Kennedy *et al.* 2008), it apparently does not occur in the *Mortoniceras* (*M.*) *fallax* Zone at Salazac (Jattiot *et al.* 2021).

OCCURRENCE (after Latil *et al.* 2021): Upper upper Albian; Belgium, UK (southern England), France, Germany, Switzerland, Hungary, Serbia, Spain, central Tunisia, South Africa, Mozambique, Angola, USA (Texas), Georgia and India.

Anisoceras perarmatum Pictet and Campiche, 1861
(Pls 20, 21)

pars 1861. *Anisoceras perarmatum* Pictet and Campiche, p. 65, pl. 49, figs 1–5, non fig. 6.
2015. *Anisoceras perarmatum dorsocostatum* Chiriac, 1981; Klein, pp. 26, 36 (with full synonymy).
2015. *Anisoceras perarmatum perarmatum* Pictet and Campiche, 1861; Klein, pp. 26, 37 (with full synonymy).
2015. *Anisoceras perarmatum renzi* Kotetishvili, 1977; Klein, pp. 26, 39 (with full synonymy).
2015. *Anisoceras perarmatum simplex* Renz, 1968; Klein, pp. 26, 39 (with full synonymy).
2017. *Anisoceras perarmatum* Pictet and Campiche, 1861; Tajika *et al*., p. 40, text-fig. 10g.
2019. *Anisoceras perarmatum* Pictet and Campiche, 1861; Gautam *et al*., p. 22, figs. 7A–C.
2019. *Anisoceras perarmatum* Pictet and Campiche, 1861; Kennedy in Gale *et al*., p. 276, pl. 50, figs 2–4, 7; pl. 51, figs 9–12.

TYPE (after Kennedy in Gale *et al*. 2019): The lectotype, by the subsequent designation of Renz (1968, p. 74) is the original of Pictet and Campiche (1861, pl. 49, fig. 1), no. 21280 in the collections of the Musée Géologique de Lausanne, Switzerland. It was refigured by Renz (1968, pl. 13, fig. 5; text-figs 27a, 28g), and is from the upper upper Albian south of La Vraconne, Vaud, Switzerland.

MATERIAL: Seven specimens; UBGD 293075, 293076, 293079-293082.

MEASUREMENTS:

	D	H	W	U	W/H
UBGD 293080 (Pl. 21, Figs 7, 8)	NA	19.5	18.9	NA	0.97
UBGD 293081	NA	18.5	17.2	NA	0.93
UBGD 293082 (Pl. 21, Fig. 4)	NA	*23.9*	*24.5*	NA	*1.03*

DESCRIPTION: Three specimens retrieved from the lower part of the sampled level illustrate the phragmocone of intermediate growth stages. Poorly-preserved but ostensibly not distorted, they are short sections of a nearly straight shaft (e.g., Pl. 21, Figs 4, 7, 8). The intercostal whorl section is circular. Pairs of dorsolateral ribs are linked at conical lower flank tubercles, the latter being joined to conical ventrolateral tubercles by a pair of looped lateral ribs. The ventrolateral tubercles are linked across the venter by a pair of ribs. On the dorsum, traces of weak ribs are visible between the paired ribs. There appear to be no nontuberculate ribs in specimen UBGD 293082 (Pl. 21, Fig. 4), while there is a single one on the adapertural sector of specimen UBGD 293080 (although barely discernable on flank; Pl. 21, Figs 7, 8).

The present material also includes three more complete specimens (specimens UBGD 293075, UBGD 293076 and UBGD 293079; Pl. 20, Figs 1–3; Pl. 21, Figs 1–3, 5, 6), retrieved from the upper part of the sampled level. Although greatly distorted by post-mortem crushing, which precludes an assessment of the original shell shape, their preservation still allows for description of the ornamentation. Specimens UBGD 293076 and UBGD 293079 (Pl. 21, Figs 1–3, 5, 6), interpreted as near-mature microconchs (maximum preserved length of about 100 mm), preserve two subparallel shafts and the linking curved section. Overall, they bear the same ornamental pattern that is observed on specimens UBGD 293080 and UBGD 293082 described above. There are no nontuberculate ribs until the middle of the curved section, which supposedly corresponds to the beginning of the adult body chamber. As regards ornamentation on the entire preserved section of body chamber, nontuberculate ribs consistently intercalate between the pairs of tuberculate ribs. Specimen UBGD 293075 (Pl. 20, Figs 1–3) also preserves two subparallel shafts and the linking curved section, but is much larger (maximum preserved length of about 160 mm) and accordingly, is regarded as a near-mature macroconch. Ornamentation on the phragmocone shaft is identical to that of specimens UBGD 293076 and UBGD 293079, except for the presence of a single nontuberculate rib. As seen on specimens UBGD 293076 and UBGD 293079, nontuberculate ribs begin to occur regularly at the presumed beginning of the adult body chamber (i.e., on the middle of the curved section). However, ornamentation of the final sector of body chamber significantly diverges, with the paired tuberculate ribs being replaced by single tuberculate ribs and one or two nontuberculate ribs in between. The ventrolateral tubercles are stronger than those on the lower flank. Ornamentation on the dorsum of both specimens is not preserved.

DISCUSSION: See *A. armatum*.

OCCURRENCE (after Kennedy in Gale *et al*. 2019): Upper upper Albian, and possibly occurring in the lower Cenomanian. The geographic distribution extends from Switzerland to UK (southern England), France, Italy (Sardinia), Spain, Germany, Hungary, Romania, Ukraine (Crimea), Georgia, north Africa, Nigeria, Angola, South Africa (KwaZulu-Natal), Mozambique, India, and USA (Texas).

Anisoceras pseudoelegans Pictet and Campiche, 1861
(Pl. 23, Figs 1–4)

1861. *Anisoceras pseudo-elegans* Pictet and Campiche, p. 69, pl. 48, fig. 5; pl. 50, figs 4, 5.
2008. *Anisoceras pseudoelegans* Pictet and Campiche, 1861; Amédro, pl. 5, fig. 10; pl. 6, fig. 7.
2011. *Anisoceras pseudoelegans* Pictet and Campiche, 1861; Gale *et al*., p. 87, fig. 31E.
2015. *Anisoceras pseudoelegans* Pictet and Campiche, 1861; Klein, pp. 26, 41 (with additional synonymy).
2017. *Anisoceras pseudoelegans* Pictet and Campiche, 1861; Tajika *et al*., p. 40, fig. 10I, J.
2021. *Anisoceras pseudoelegans* Pictet and Campiche, 1861; Jattiot *et al*., p. 38, fig. 24I–T (with additional synonymy).

TYPE: The lectotype is the original of Pictet and Campiche (1861, pl. 48, fig. 5) from the upper upper

Albian of Saint Croix, Vaud, Switzerland. It was designated and refigured by Spath (1939, p. 557, text-fig. 196a, b).

MATERIAL: Three phragmocone fragments; UBGD 293088, 293094, 293095.

MEASUREMENTS:

	D	H	W	U	W/H
UBGD 293094 (Pl. 23, Figs 1, 2)	NA	38.4	28.2	NA	0.73
UBGD 293095 (Pl. 23, Figs 3, 4)	NA	30.4	22	NA	0.72

DESCRIPTION: The figured specimens are two short, slightly curved (barely discernible in specimen UBGD 293094) phragmocone fragments (Pl. 23, Figs 1–4) of large, thus probably macroconch individuals (maximum preserved whorl height of 38.4 mm for specimen UBGD 293094 and 30.4 mm for specimen UBGD 293095). The whorl section is fairly compressed and oval (W/H = 0.73 for specimen UBGD 293094, 0.72 for specimen UBGD 293095). Although mostly effaced in the present material due to poor preservation, fine and dense ribs usually arise from the dorsal region in this species (see e.g., Tajika *et al*. 2017; Jattiot *et al*. 2021). Specimen UBGD 293094 preserves one worn, elongated bullae on the dorsal part of the illustrated flank, linked to a partly preserved ventrolateral bullae by a group of three ribs. Dorsolateral bullae (not visible in specimen UBGD 293095 due to poor preservation) on specimens of *Anisoceras pseudoelegans* from Salazac (Jattiot *et al*. 2021) are typically linked to bullate ventrolateral tubercles (as observed in specimen UBGD 293095) by groups of three (rarely two) ribs, with generally one or two (sometimes three) nontuberculate ribs between. Ribs are straight and fade away across the venter (see better examples in Jattiot *et al*. 2021).

DISCUSSION: This species mainly differs from other *Anisoceras* species (e.g., *A. armatum* and *A. perarmatum*, see above) by its finer and denser ribbing (Spath 1939; Kennedy in Gale *et al*. 1996; Szives 2007; Tajika *et al*. 2017; Jattiot *et al*. 2021). Furthermore, the present material as well as specimens from the *Mortoniceras* (*M.*) *fallax* Zone at Salazac (Jattiot *et al*. 2021) suggest that phragmocones of *A. pseudoelegans* are consistently more compressed than those of *A. armatum* and *A. perarmatum*, resulting in a typically oval whorl section (*versus* circular in uncrushed *A. armatum* and *A. perarmatum* phragmocone shafts; see W/H ratios in Supplementary Appendix). The strength and density of ornamentation are known to sometimes covary with whorl shape among planispiral and heteromorphic ammonites, following Buckman's first law of covariation (see e.g., Westermann 1966; Guex *et al.* 2003; Hammer and Bucher 2005; Monnet *et al*. 2015; as well as Jattiot *et al*. 2021 for a recent example in the heteromorph genus *Mariella*). Therefore, *A. pseudoelegans* might alternatively represent a compressed, weakly and densely ornamented variant of a morphologically highly variable, broader species including *A. armatum* and/or *A. perarmatum*. An assessment of the range of intraspecific variation within *Anisoceras* species based on extensive, contemporary assemblages from expanded successions is critically needed to decipher the taxonomy of this genus.

OCCURRENCE: Lower Cretaceous (upper Albian); UK (England), France, Italy (Sardinia), Switzerland, Hungary, South Africa (KwaZulu-Natal), Japan.

Anisoceras sp.
(Pl. 22)

MATERIAL: Five specimens; UBGD 293077, 293078, 293085, 293086, 293098.

MEASUREMENTS:

	D	H	W	U	W/H
UBGD 293077 (Pl. 22, Figs 1–3)	NA	21.3	22.7	NA	1.07
UBGD 293078 (Pl. 22, Figs 4, 5)	NA	19.8	20	NA	1.01
UBGD 293085 (Pl. 22, Fig. 6)	NA	*18.6*	*18.8*	NA	*1.01*
UBGD 293086	NA	*25.5*	*24*	NA	0.94
UBGD 293098 (Pl. 22, Fig. 7 *pars*)	NA	–	–	NA	–

DESCRIPTION: Among the material at hand, two specimens are short sections of phragmocones of intermediate growth stages, of which one is figured here (specimen UBGD 293085, Pl. 22, Fig. 6). It consists of a fragment of slightly curved shaft, 19.5 mm in maximum preserved whorl height; with a circular whorl section. Ornamentation on the dorsum is not preserved. On the dorsolateral shoulders, there are barely differentiated (most likely due to a poor preservation) pairs of ribs that join at strong, flat-topped, worn, lower flank tubercles. From these tubercles, a pair of coarse, nearly straight ribs reunite on larger and worn ventrolateral tubercles. The latter are linked across the venter by a pair of broad, barely differentiated ribs, producing a low swelling. In between the three adapical pairs of tuberculate ribs, although barely detectable, are single, fine, nontuberculate ribs

similar to those of *A. armatum*. In contrast, there are no intercalated nontuberculate ribs between the three adapertural pairs of tuberculate ribs, which instead suggests *A. perarmatum*.

A larger, more complete, well-preserved specimen (Pl. 22, Figs 1–3) is interpreted as a microconch (approximately 100 mm long, with a maximum preserved whorl height of 22 mm). It comprises part of the presumed phragmocone shaft (even though the last visible suture line is on the most adapical sector of shell) and the curved section, as well as part of the adult body chamber shaft. The whorl section is circular on the nearly straight shaft and very slightly thicker on the curved section. Ornamentation is particularly distinctive on the adapertural sector of shell, which exhibits elongated, clavi-like ventrolateral tubercles parallel to direction of growth and conical dorsolateral tubercles. Ornamentation on the shaft is intermediate between that of *A. armatum* and *A. perarmatum*, consisting of a very regular alternation of two pairs of tuberculate ribs with one single nontuberculate rib in between, and two pairs of tuberculate ribs with no intercalated ribs. This ornamental pattern is observed until the beginning of the curved section. At this point, one or two nontuberculate ribs systematically intercalate between the pairs of tuberculate ribs.

Another specimen (Pl. 22, Fig. 7 *pars*) consists of a massive, very poorly preserved fragment of adult body chamber and an approximately 130 mm long, nearly straight shaft section. Undoubtedly, both fragments belonged to the same individual, most likely a very large macroconch. Due to significant taphonomic processes, the segment of shell connecting the two fragments (i.e., the curved section) is not preserved, and both fragments were shifted from their initial anatomical location. Although the original whorl shape cannot be accurately determined due to post-mortem distortion, the shell was most likely subcircular or circular on the phragmocone shaft and remarkably depressed on the adult body chamber. As observed on specimen UBGD 293077, the ornamental pattern of this specimen is unquestionably intermediate to that of *A. armatum* and *A. perarmatum*. Beginning at the preserved adapical end of the nearly straight shaft fragment, two pairs of tuberculate ribs with no intercalated ribs are followed by two pairs of tuberculate ribs with a single nontuberculate rib, and so on until the adapertural end of the fragment. On the adult body chamber fragment, single nontuberculate ribs intercalate between pairs of tuberculate ribs, except for the ultimate adapertural sector of shell, on which there are two single nontuberculate ribs.

DISCUSSION: See *A. armatum*. Similar intermediate specimens were described by Cooper and Kennedy (1979, fig. 18) and Kennedy and Latil (2007, pl. 7, figs 4, 5).

OCCURRENCE: Upper upper Albian; south-eastern France and Angola.

Genus *Idiohamites* Spath, 1925

TYPE SPECIES: *Hamites tuberculatus* J. Sowerby, 1818 (p. 30, pl. 215, fig. 5), by the original designation of Spath (1925, p. 189).

Idiohamites elegantulus Spath, 1939
(Pl. 23, Figs 5–7)

1939. *Idiohamites elegantulus* Spath, p. 599, text-fig. 216a–g.
1968. *Idiohamites elegantulus laticostatus* Renz, p. 73, pl. 11, figs 38, 41, 42; pl. 12, figs 1, 2; text-figs 25m, 26i–m.
1968. *Idiohamites recticostatus* Renz, p. 71, pl. 13, figs 1, 2.
1994. *Idiohamites dorsetensis* Spath, 1939; Latil, p. 9, fig. 1.
2007. *Idiohamites elegantulus* Spath, 1939; Kennedy and Latil, p. 470, pl. 8, figs 1–7; pl. 9, figs. 1–3, 5–8.
2015. *Idiohamites elegantulus elegantulus* Spath, 1939; Klein, pp. 48, 54 (with additional synonymy).
2015. *Idiohamites elegantulus laticostatus* Renz, 1968; Klein, pp. 48, 54 (with additional synonymy).

TYPE (after Kennedy and Latil 2007): The holotype, by original designation, is the original of Spath (1939, text-fig. 216a–c), BMNH C31542, from the upper upper Albian *dispar* Zone ammonite bed in the Upper Greensand of Ringstead, Dorset, UK.

MATERIAL: Two large fragments retrieved from the upper part of the sampled level; UBGD 293149, 293150.

MEASUREMENTS:

	D	H	W	U	W/H
UBGD 293149 (Pl. 23, Figs 6, 7)	NA	*41*	*29.9*	NA	*0.73*
UBGD 293150 (Pl. 23, Fig. 5)	NA	*29.2*	*20.7*	NA	*0.71*

DESCRIPTION: Specimen UBGD 293150 (Pl. 23, Fig. 5) comprises of a nearly straight shaft approximately 70 mm long, linked by a curved sector to the adapertural shaft. The early phragomocone stages are not preserved. This specimen is interpreted as a

microconch; the maximum preserved whorl height is estimated to be 29.2 mm. Specimen UBGD 293149 (Pl. 23, Figs 6, 7) most likely represents a body chamber fragment of a near-mature macroconch; its maximum preserved whorl height is estimated to be 41 mm. The whorl section of both specimens is compressed, with a whorl width to height ratio (W/H) of 0.73 for specimen UBGD 293149 and 0.71 for specimen UBGD 293150, although this observation is most certainly accentuated by post-mortem crushing. The ornamentation of the dorsum is too poorly preserved to be properly described. On the phragmocone shaft of specimen UBGD 293150, coarse ribs arise from the dorsolateral shoulders. These are straight, feebly prorsiradiate and distant on the flanks. The preservation of specimen UBGD 293150 is very poor for most of its outer shell (i.e., ventrolateral region and venter). Hints of small ventral clavi exist on the outer shell, but it is very equivocal whether these ventral clavi unite a pair of flank ribs (possibly merged on lower flanks) or are associated with a single rib. On the curved sector and terminal shaft of specimen UBGD 293150 as well as on specimen UBGD 293149, the ribs are relatively dense, changing from prorsiradiate to markedly rursiradiate. On specimen UBGD 293149, pairs of lateral ribs (possibly merged on dorsolateral shoulders) appear to regularly link to a well-developed ventral clavi, with two nontuberculate ribs in between (a slight disruption in ribbing is noticeable in the middle of the fragment, two nontuberculate ribs merging into one on the flank; see arrow in Pl. 23, Fig. 6). All ribs cross the venter; tuberculate ribs are linked over the venter by a coarse rib that may be feebly divided into a pair of riblets.

DISCUSSION: Specimen UBGD 293149 is similar in size, shape and overall ornamentation to the corresponding adapertural shaft of specimen UJF-ID.10680 figured by Kennedy and Latil (2007, pl. 8, figs 5–7), while specimen UBGD 293150 resembles the microconch specimen UJF-ID.10681 figured by Kennedy and Latil (2007, pl. 9, figs 1, 2). According to Kennedy and Latil (2007), adult microconch body chambers differ from macroconch body chambers in size only.

The reader is referred to Kennedy and Latil (2007) for a more detailed discussion.

OCCURRENCE (after Kennedy and Latil 2007): *Mortoniceras* (*S.*) *rostratum* and *Mortoniceras* (*S.*) *perinflatum* Zones; UK (southern England), Switzerland, south-eastern France.

Family Hamitidae Gill, 1871
Genus *Hamites* Parkinson, 1811

TYPE SPECIES: *Hamites attenuatus* J. Sowerby, 1814 (p. 137, pl. 61, figs 4, 5), by the subsequent designation of Diener (1925, p. 65).

Hamites virgulatus Brongniart, 1822
(Pl. 24, Figs 1–23)

1822. *Hamites virgulatus* Brongniart, p. 395, pl. 7, fig. 6.
2015. *Hamites* (*Hamites*) *virgulatus interruptus* Renz, 1968; Klein, pp. 75, 99 (with additional synonymy).
2015. *Hamites* (*Hamites*) *virgulatus virgulatus* Brongniart, 1822; Klein, pp. 75, 100 (with additional synonymy).
2017. *Hamites virgulatus* Brongniart, 1822; Tajika *et al*., p. 41, fig. 10S.
2018b. *Hamites subvirgulatus* Spath, 1941; Tajika *et al*., fig. 2AA, AB.
2019. *Hamites* cf. *subvirgulatus* Spath, 1941; Kennedy in Gale *et al*., p. 279, pl. 53, figs 2, 3.
2020. *Hamites virgulatus* Brongniart, 1822; Kennedy, p. 227, pl. 32, figs 18–21, 23, 24.
2021. *Hamites virgulatus* Brongniart, 1822; Jattiot *et al*., p. 38, fig. 24U–AR (with additional synonymy).

TYPE (after Kennedy 2020): The neotype, designated by Renz (1968, p. 65), is the original of Pictet and Campiche (1861, pl. 54, fig. 6), from the upper upper Albian of Saint Croix, Vaud, Switzerland. It was refigured by Renz (1968, pl. 11, fig. 11; text-fig. 23d), and is no. L39952 in the collections of the Musée Geologique de Lausanne, Switzerland.

MATERIAL AND MEASUREMENTS: See Supplementary Appendix; N = 23.

DESCRIPTION: This species is represented at Clansayes by numerous curved fragments of various sizes, of which the longest and best-preserved are figured here (Pl. 24, Figs 1–23). The coiling appears variable in our sample, specimen UBGD 293180 (and to a lesser extent specimen UBGD 293172) exhibiting a markedly curved, hook-like portion (Pl. 24, Figs 17, 18, 23). The whorl section is circular or slightly compressed, oval. The ribs are slightly variable in strength, variably oriented on the flanks (from slightly rursiradiate to slightly prorsiradiate) and transverse on the venter. They are effaced on the dorsum, strengthening across the dorsolateral margin. For the material at hand, the rib index (number of ribs in a distance equal to maximum preserved whorl height) is most frequently 5 or 6; no specimens

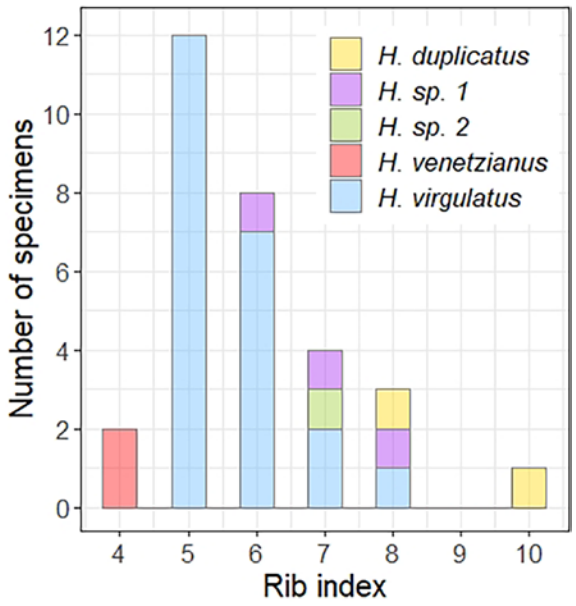

Text-fig. 7. Distribution of the rib index among *Hamites* spp. taxa.

have a rib index of 4 (Text-fig. 7). The rib density is stable throughout ontogeny on most specimens (see e.g., specimen UBGD 293158; Pl. 24, Figs 9–11, with a consistent rib index of 6; and specimen UBGD 293159; Pl. 24, Figs 12–14, with a consistent rib index of 5). Nevertheless, on the two presumably immature specimens (specimens UBGD 293155 and UBGD 293157; Pl. 24, Figs 1–3, 6–8, respectively), the rib density very slowly increases throughout ontogeny (rib index increases to 6 on the adapertural sector of shell) and they become slightly finer. More importantly, one mature specimen with partly-preserved aperture (specimen UBGD 293156; Pl. 24, Figs 4, 5) exhibits a marked change in rib density throughout ontogeny. Indeed, although the rib index is 6 on the adapical sector, there are fine and distinctly approximated ribs on the adapertural sector, with the rib index consequently increasing to 8 in this area. Based on this feature, which signifies approaching maturity, specimens displaying a distinct change in rib density throughout ontogeny with a similar adapertural rib approximation (with a rib index of 7 on the adapertural sector) are interpreted as near mature individuals (specimens UBGD 293178 and UBGD 293180; Pl. 24, Figs 19, 20, 23). Maturity in this species is characterised by an aperture with two collars separated by a deep constriction (see well-preserved examples in Jattiot *et al*. 2021).

DISCUSSION: A variation in rib density has been previously recognised within this species (see Spath 1941; Wiedmann and Dieni 1968; Cooper and Kennedy 1979; Scholz 1979; Jattiot *et al*. 2021). As demonstrated by Jattiot *et al*. (2021), the rib index in *H. virgulatus* representatives from the *Mortoniceras* (*M.*) *fallax* Zone at Salazac varies from 4 to 6 (these values are evenly distributed among them). In the Clansayes material, there are no specimens with a rib index of 4, and 5 is the most common value; the rib index increases to 7 or 8 due to a distinct rib approximation in mature specimens or specimens approaching maturity (specimens UBGD 293156, UBGD 293178, UBGD 293180; Pl. 24, Figs 4, 5, 19, 20, 23; Text-fig. 7). In turn, differentiation between specimen UBGD 293156 (rib index of 8 immediately before the aperture; Pl. 24, Figs 4, 5) and *H. duplicatus* individuals (see below) appears peculiarly difficult. However, the early growth stages of these near-mature or mature specimens show a rib index of 6, strongly indicating a *H. virgulatus* affiliation. In contrast, even though mature specimen UBGD 293181 (with partly preserved aperture; Pl. 24, Figs 24–26) also has a rib index of 8 on the adapertural sector of shell, it is assigned to *H. duplicatus* based on its consistent rib density throughout ontogeny (rib index remains 8 on the adapical sector of shell).

Noteworthy, mature representatives of *H. virgulatus* from the *Mortoniceras* (*M.*) *fallax* Zone at Salazac (Jattiot *et al*. 2021, fig. 24U–AR) do not exhibit approximated ribs before the aperture and the rib index never exceeds 6. Thus, *H. virgulatus* and *H. duplicatus* representatives are much more easily differentiated at this locality (see Jattiot *et al*. 2021).

Of secondary importance, a single poorly-preserved, presumed immature specimen with an intermediate rib index of 7 (specimen UBGD 293170, '*H.* sp. 2' in Text-fig. 7) was not assigned to either of the two species (see also Jattiot *et al*., 2021, fig. 26O).

See Jattiot *et al*. (2021) for thorough discussions on *Hamites* taxonomy.

OCCURRENCE (after Kennedy 2020): Upper Albian; UK (southern England), France, Switzerland, Spain, Italy (Sardinia), Hungary, Poland, Romania, Ukraine (Crimea), north-eastern Algeria, Angola, South Africa (northern KwaZulu-Natal), southern Mozambique, Madagascar, United States (Texas), Mexico, Australia (Western Territories), and possibly Venezuela.

Hamites duplicatus Pictet and Campiche, 1861
(Pl. 24, Figs 24–31)

1861. *Hamites duplicatus* Pictet and Campiche, p. 98.

2015. *Hamites* (*Hamites*) *duplicatus* Pictet and Campiche, 1861; Klein, pp. 74, 82 (with full synonymy).
2017. *Hamites duplicatus* Pictet and Campiche, 1861; Tajika *et al*., p. 40, fig. 10T.
2018. *Hamites duplicatus* Pictet and Campiche, 1861; Kennedy and Morris, p. 96, text-figs 9f–i, 10a.
2019. *Hamites* (*Hamites*) *duplicatus* Pictet and Campiche, 1861; Kennedy in Gale *et al*., p. 279, pl. 52, figs 4–6, 8–10, 15 (*pars*); pl. 53, fig. 1.
2020. *Hamites duplicatus* Pictet and Campiche, 1861; Kennedy, p. 226, pl. 32, figs 25–28.
2021. *Hamites duplicatus* Pictet and Campiche, 1861; Jattiot *et al*., p. 39, fig. 26A–N (with additional synonymy).

TYPE (after Kennedy 2020): The lectotype, by the subsequent designation of Spath (1941, p. 641), is the original of Pictet in Pictet and Roux (1847, pl. 14, fig. 7), from the upper Albian of Mont Saxonnet, Savoie, France.

MATERIAL: Three small fragments; UBGD 293181-293183.

MEASUREMENTS: See Supplementary Appendix; N = 3.

DESCRIPTION: This species is represented at Clansayes by three very short, slightly curved fragments (Pl. 24, Figs 24–31). The whorl section is slightly compressed, oval. The ribs are fine and dense, gently rursiradiate on the flanks, transverse on the venter. They are effaced on the dorsum, strengthening across the dorsolateral margin. The rib index for this species was recently shown by Jattiot *et al*. (2021) to range from 8 to 12, based on specimens from the *Mortoniceras* (*M.*) *fallax* Zone at Salazac. With regard to the available Clansayes material, the rib index is 8 for specimen UBGD 293181 and 10 for specimen UBGD 293182 (Pl. 24, Figs 24–26, 27–29, respectively). The rib density does not increase when approaching maturity in specimen UBGD 293181 (Pl. 24, Figs 24–26), similarly to mature *H. duplicatus* representatives from Salazac (Jattiot *et al*. 2021, fig. 26F–N). As in *H. virgulatus*, maturity (as far as microconchs are concerned) is characterised by an aperture with two collars separated by a deep constriction (partly preserved in specimen UBGD 293181; see Jattiot *et al*. 2021 for better examples).

DISCUSSION: The reader is referred to Jattiot *et al*. (2021) as well as to the discussion on *H. virgulatus*.

OCCURRENCE (after Kennedy 2020): Upper upper Albian to lower upper Cenomanian. The distribution extends from UK (southern and eastern England) to France, Italy (Sardinia), Switzerland, Germany, Poland, Hungary, Dagestan, Kazakhstan, Iran, north-eastern Algeria, central Tunisia, Angola, Tanzania, Madagascar, and India (Tamil Nadu).

Hamites venetzianus Pictet in Pictet and Roux, 1847
(Pl. 24, Figs 32–35)

1847. *Hamites venetzianus* Pictet in Pictet and Roux, p. 390, pl. 14, fig. 6.
2004. *Hamites venetzianus* Pictet, 1847; Kennedy, p. 892, text-figs 27b, 29g–j, l, m.
?2007. *Hamites venetzianus* Pictet, 1847; Kennedy and Latil, p. 471, pl. 9, fig. 4 (with additional synonymy).
2015. *Hamites* (*Hamites*) *venetzianus sulcatus* Renz, 1968; Klein, pp. 75, 98 (with additional synonymy).
2015. *Hamites* (*Hamites*) *venetzianus venetzianus* Pictet, 1847; Klein, pp. 75, 99 (with additional synonymy).
2020. *Hamites venetzianus* Pictet, 1847; Kennedy, p. 227, pl. 33, figs 7, 8.

TYPE (after Kennedy 2020): The holotype, by monotypy, is the original of Pictet in Pictet and Roux (1847, pl. 14, fig. 6), from the upper Albian of Perte-du-Rhône, Ain, France.

MATERIAL: Two specimens; UBGD 293160, 293161.

MEASUREMENTS: See Supplementary Appendix; N = 2.

DESCRIPTION: Specimen UBGD 293160 (Pl. 24, Figs 32, 33) preserves part of a slightly diverging, nearly straight, and slightly compressed (oval) phragmocone shaft, as well as most of its presumed adult body chamber comprising the last part of the adapical shaft, a curved sector (slightly compressed, oval) and an incomplete, subcircular adapertural shaft. Based on specimen UBGD 293160, specimen UBGD 293161 (Pl. 24, Figs 34, 35) can be interpreted as a fragment of adult body chamber, more specifically of the subcircular adapertural shaft. The ribs are singularly coarse and thick, distinctly rursiradiate on the adapertural shaft, more or less rectiradiate on the curved sector, slightly prorsiradiate on the adapical shaft (see specimen UBGD 293160; Pl. 24, Figs 32, 33), and transverse on the venter. They are effaced on the dorsum, strengthening across the dorsolateral margin. For these two specimens, the rib index is slightly variable, from 3 to 4 (3 on the adapical shaft and curved sector, 4

on the adapertural shaft). Both specimens are interpreted as microconchs.

DISCUSSION: Kennedy (2004) documented fragments of coarsely ribbed *Hamites* individuals from an upper Albian expanded sequence (Pawpaw Shale, Texas), which match the types of *H. venetzianus* and *H. tenawa* (the latter synonymised with *H. venetzianus* by Kennedy 2004). The rib index of these specimens is 3 (Kennedy 2004, p. 892). Furthermore, according to Kennedy (2004, p. 893), "the coarse, thick ribs of these fragments are highly distinctive, and correspond to those of the holotype, Swiss, and English specimens". Following these taxonomic interpretations, we assigned the two present *Hamites* specimens from Clansayes to *H. venetzianus*, based on the combination of their low rib index and coarse, thick ribs. Of secondary importance, their coiling differs from that of *H. virgulatus* and *H. duplicatus* most complete Clansayes representatives (compare e.g., with *H. virgulatus* specimen UBGD 293159; Pl. 24, Figs 12–14). The Cenomanian *H. simplex* d'Orbigny, 1842 is mainly characterised by annular ribs that are barely weakened on the dorsum (Wright and Kennedy 1995). The reader is also referred to Jattiot *et al*. (2021) for thorough discussions on *Hamites* taxonomy.

Hamites venetzianus was also documented from the *Mortoniceras* (*S.*) *rostratum* Zone [and *Mortoniceras* (*S.*) *perinflatum* Zone] by Kennedy and Latil (2007). However, the attribution of the single figured specimen (Kennedy and Latil 2007, pl. 9, fig. 4) is somewhat doubtful since it is described as having a rib index of 5, which tends to indicate *H. virgulatus*. *Hamites venetzianus* was not identified within the extensive material from the *Mortoniceras* (*M.*) *fallax* Zone at Salazac (Jattiot *et al*. 2021).

OCCURRENCE (after Kennedy 2020): Upper upper Albian; south-eastern France, UK (southern England), Switzerland, Poland, central Tunisia, USA (Texas), and, possibly, Angola.

Hamites sp.
(Pl. 24, Figs 36–41)

MATERIAL: Four specimens; UBGD 293151-293154.

MEASUREMENTS: See Supplementary Appendix; N = 4.

DESCRIPTION: The present material comprises four fragments of relatively large whorls (from 18.3 to 19.9 mm in maximum preserved whorl height), of which three are figured here (Pl. 24, Figs 36–41). The shell is gently curved, with a compressed, oval whorl section. The rib index appears variable among specimens: 6 on specimen UBGD 293154 (Pl. 24, Figs 39–41), 7 on specimen UBGD 293153 (Pl. 24, Fig. 38) and 8 on specimen UBGD 293152 (Pl. 24, Figs 36, 37; rib index is 7 on the venter). The ribs are effaced on the dorsum and strengthen across the dorsolateral margin; they are straight, slightly rursiradiate on the flanks and transverse on the venter. On the flanks, the ribs are strong, narrow and sharp, and are of comparable strength on the venter, only slightly broader. Given their notably large size, these specimens are interpreted as sections of macroconchs.

DISCUSSION: The range of rib density for these specimens (Text-fig. 7) includes rib index values observed in *H. virgulatus* (6) and *H. duplicatus* (8). This intermediate, variable rib density, as well as the scarcity and incomplete preservation of the material (e.g., lack of earlier ontogenetic stages) preclude and identification at the specific level. Moreover, these presumed macroconch individuals are roughly twice as large as other *Hamites* representatives occurring at Clansayes.

Noteworthy, no similar-sized specimens were retrieved by Jattiot *et al*. (2021) from the *Mortoniceras* (*M.*) *fallax* Zone at Salazac, where *Hamites virgulatus* is common; in turn, only *Hamites* microconchs were identified at this locality. More generally, to our knowledge no comparably large-sized *Hamites* specimens have been previously described from the *M.* (*M.*) *fallax* or *M.* (*S.*) *rostratum* Zones in south-eastern France. Comparably sized *Hamites* specimens are described in Spath (1941), among which the final portion of the holotype of *H. gardneri* Spath, 1941 (Spath 1941, text-fig. 225a–c) is the most similar. However, all of the large specimens described by Spath (1941) are older (Lower Gault, Folkestone, England). This observation might indicate that large *Hamites* fragments from Clansayes alternatively represent another, undescribed species occurring in the *M.* (*S.*) *rostratum* Zone. Extensive material from Clansayes is critically needed for further discussion.

Family Baculitidae Gill 1871
Genus and subgenus *Lechites* Nowak, 1908

TYPE SPECIES: *Baculites Gaudini* Pictet and Campiche, 1861 (p. 112, pl. 55, figs 5–9), by the original designation of Nowak (1908, p. 350).

Lechites (*Lechites*) *gaudini*
(Pictet and Campiche, 1861)
(Pl. 23, Figs 8–16)

1861. *Baculites gaudini* Pictet and Campiche, p. 112, pl. 55, figs 5–9.
2016b. *Lechites* (*Lechites*) *gaudini* (Pictet and Campiche, 1861); Klein, pp. 2, 4 (with full synonymy).
2017. *Lechites gaudini* (Pictet and Campiche, 1861); Tajika *et al*., p. 43, fig. 9S, T, AF.
2019. *Lechites* (*Lechites*) *gaudini* (Pictet and Campiche, 1861); Kennedy in Gale *et al*., p. 291, pl. 58, fig. 5.
2020. *Lechites* (*Lechites*) *gaudini* (Pictet and Campiche, 1861); Kennedy, p. 229, pl. 34, figs 1–5, 19, 20 (with additional synonymy).
2021. *Lechites* (*Lechites*) *gaudini* (Pictet and Campiche, 1861); Jattiot *et al*., p. 40, fig. 26P–AH.
2021. *Lechites gaudini* (Pictet and Campiche, 1861); Latil *et al*., p. 28, fig. 17f.

TYPE (after Kennedy 2020): The lectotype, by the subsequent designation of Spath (1941, p. 663) is the original of Pictet and Campiche (1861, p. 112, pl. 55, fig. 5), refigured by Renz (1968, pl. 17, fig. 3). It is no. L40012 in the collections of the Musée Geologique de Lausanne, Switzerland, and from the upper upper Albian of Sainte-Croix, Vaud, Switzerland.

MATERIAL AND MEASUREMENTS: See Supplementary Appendix; N = 28.

DESCRIPTION: The shell is straight, very slowly expanding, typically with a slightly compressed, oval whorl section. The ornamentation consists of simple ribs that arise at the dorsolateral margin, and recurve slightly to become feebly convex and prorsiradiate across the flanks. The ribs broaden slightly ventrally and may pass across the venter or efface at the siphonal line; they efface across much of the dorsum. The rib density (covarying with the strength of ornamentation) is highly variable, with between 2 and 8 ribs in a distance equal to maximum preserved whorl height (Cooper and Kennedy 1977; compare specimen UBGD 293146; Pl. 23, Figs 11–13, exhibiting closely spaced and relatively weak ribs, with similar-sized specimen UBGD 293147; Pl. 23, Figs 8–10; displaying widely spaced and relatively coarse ribs). No mature individuals are present in our material (see Jattiot *et al*. 2021 for specimens with preserved aperture).

DISCUSSION: Reference is made to Cooper and Kennedy (1977) for a comprehensive review of this species, including a discussion of how it differs from other species referred to the genus. Following this work, we here interpret *L. gaudini* broadly, whose range of ornamental intraspecific variation is well illustrated by specimens UBGD 293146 and UBGD 293147 (Pl. 23, Figs 8–13). The ornamentation consisting of widely to closely spaced, even ribs distinguishes *L. gaudini* from the smooth to near-smooth shell of *L. moreti* Breistroffer, 1936 (see below), which exhibits widely spaced constrictions.

OCCURRENCE (after Latil *et al*. 2021): Upper Albian; UK (southern England), France, Switzerland, Hungary, Romania, Italy (Sardinia), Iran, Algeria, central Tunisia, Madagascar, South Africa, south India, Japan, Mexico, Australia and Antarctica (Alexander Island).

Lechites (*Lechites*) *moreti* Breistroffer, 1936
(Pl. 23, Figs 17–19)

pars 1861. *Baculites gaudini* Pictet and Campiche, p. 112, pl. 55, figs 10, 11 only.
1936. *Lechites moreti* Breistroffer, p. 66.
2016b. *Lechites* (*Lechites*) *moreti* Breistroffer, 1936; Klein, pp. 2, 6 (with full synonymy).
2020. *Lechites* (*Lechites*) *moreti* Breistroffer, 1936; Kennedy, p. 229, pl. 34, figs 9–12, 16–18, 21–25.
?2021. *Lechites* (*Lechites*) cf. *moreti* Breistroffer, 1936; Jattiot *et al*., p. 40, fig. 26AI–AK.

TYPES (after Kennedy 2020): The lectotype, by the subsequent designation of Spath (1941, p. 605), is specimen no. L40016 in the collections of the Musée Geologique de Lausanne, Switzerland, the original of Pictet and Campiche (1861, pl. 55, fig. 10), refigured by Renz (1968, pl. 16, fig. 10; text-fig. 29a). The paralectotype is specimen no. L40015, the original of Pictet and Campiche (1861, pl. 55, fig. 11), refigured by Renz (1968, pl. 16, fig. 12). Both are from the upper upper Albian of La Vraconne, near Saint Croix, Vaud, Switzerland.

MATERIAL: One small fragment; UBGD 293148.

MEASUREMENTS:

	D	H	W	U	W/H
UBGD 293148 (Pl. 23, Figs 17–19)	NA	8.9	8.0	NA	0.90

DESCRIPTION: The material comprises a single short, straight fragment, with a very low whorl ex-

pansion rate. It exhibits prominent constrictions, 2 in a distance equal to maximum preserved whorl height. These are effaced on the dorsum, strongly prorsiradiate and straight on the inner flanks, flexing backward, deepening and convex on the outer flanks and passing straight across the venter, where they are deepest and most prominent.

DISCUSSION: *Lechites* (*L.*) *moreti* is easily distinguished from other, ribbed *Lechites* species by its widely spaced constrictions, with broad swollen areas in between. The reader is referred to Renz (1968), Wiedmann and Dieni (1968), Cooper and Kennedy (1977), Scholz (1979), Kennedy and Latil (2007) and Kennedy (2020).

OCCURRENCE (after Kennedy 2020): Upper upper Albian; UK (southern England), south-eastern France, Spain, Italy (Sardinia), Switzerland, Germany, Hungary, Romania, Ukraine (Crimea), and Tunisia.

Order Nautilida Agassiz, 1847
Superfamily Nautiloidea de Blainville, 1825
Family Nautilidae de Blainville, 1825
Genus *Eutrephoceras* Hyatt, 1894

TYPE SPECIES: *Nautilus dekayi* Morton, 1834 (p. 33, pl. 8, fig. 4; pl. 13, fig. 4), by the original designation of Hyatt (1894, p. 555).

Eutrephoceras sublaevigatum (d'Orbigny, 1850)
(Pl. 25, Figs 1–8)

1840. *Nautilus laevigatus* d'Orbigny, p. 84, pl. 17, figs 1–4.
1850. *Nautilus sublaevigatus* d'Orbigny, Prodrome II, p. 184.
2017. *Eutrephoceras sublaevigatum* (d'Orbigny, 1850); Tajika *et al*., p. 25, fig. 5C, D, K, L.
2021. *Eutrephoceras sublaevigatum* (d'Orbigny, 1850); Jattiot *et al*., p. 41, fig. 27D–P.
2021. *Eutrephoceras sublaevigatum* (d'Orbigny, 1850); Sharifi *et al*., p. 8, fig. 6 (with additional synonymy).

TYPES: The lectotype, designated by Tintant in Gauthier (2006, p. 22), is no. LPMP-R4257 (d'Orbigny Collection no. 6773A-1) from Rochefort (Charente-Maritime, France, Cenomanian); it was refigured by Tintant in Gauthier (2006, pl. 5, figs 1, 2).

MATERIAL: Five phragmocones; UBGD 293289-293293.

MEASUREMENTS:

	D	H	W	U	W/H
UBGD 293289	*35.6* (100)	*21.3* (*59.8*)	27.8 (*78.1*)	*2.9* (*8.1*)	*1.31*
UBGD 293290 (Pl. 25, Figs 1, 2)	33.4 (100)	20.0 (59.9)	27.3 (81.7)	*2.3* (*6.9*)	1.37
UBGD 293291 (Pl. 25, Figs 3–5)	*30.5* (100)	17.8 (*58.4*)	*22.5* (*73.8*)	3 (*9.8*)	*1.26*
UBGD 293292 (Pl. 25, Figs 6, 7)	26.7 (100)	15.5 (58.1)	19.3 (72.3)	3.0 (11.2)	1.25
UBGD 293293 (Pl. 25, Fig. 8)	38.9 (100)	23.8 (61.2)	24.5 (63.0)	*4.3* (*11.1*)	1.03

DESCRIPTION: The shell is extremely involute, with a depressed, reniform whorl section and a very broadly rounded venter. The umbilicus is nearly closed with a high, feebly convex wall and broadly rounded shoulders. The suture line is slightly curved, with a broadly rounded median and dorsal saddles.

DISCUSSION: The reader is referred to Sharifi *et al*. (2021).

OCCURRENCE: Lower-Upper Cretaceous (Albian to Santonian); UK (England), Germany, Italy, Czech Republic, Poland, Bulgaria, Libya, India.

DISCUSSION

Ammonite species richness, distribution and palaeoecology

A total of 24 species (17 genera) of ammonites and one species of nautiloid are described from the *Mortoniceras* (*S.*) *rostratum* Zone at Clansayes (Table 1; Text-fig. 8). Among ammonites, only *M.* (*S.*) *rostratum* and *A. perarmatum* were previously documented from this level (Sornay 1950; Debelmas *et al*. 2004). Debelmas *et al*. (2004) also reported *Mortoniceras* (*M.*) *inflatum*, which was not identified in our substantial sample. This probably results from a misidentification, since it is commonly accepted that *M.* (*M.*) *inflatum* characterises an earlier level (i.e., the eponymous upper Albian zone; Text-fig. 2). Despite the scarcity of fossils within the sampled level, an unexpectedly high taxonomic richness is documented. This is particularly significant when compared to coeval assemblages found in different facies from the same area, such as the Marnes Bleues facies at the Col de Palluel section (Gale *et al*. 2011) which is interpreted as hemipelagic deposits (e.g., Amédro 2008). For example, 12 taxa were

Taxon		First reference	N	Stratigraphic range	Illustrated in
Hyporbulites	*seresitensis*	(Pervinquière, 1907)	2	Albian–middle Cenomanian	Pl. 1, Figs 1–4
Tetragonites	*timotheanus*	(Pictet, 1847)	2	middle Albian–lower Cenomanian	Pl. 1, Figs 5–9
Anagaudryceras	sp.		1	upper upper Albian (*Mortoniceras* (*S.*) *rostratum* Zone)	Pl. 1, Figs 10, 11
Desmoceras (*Desmoceras*)	*latidorsatum*	(Michelin, 1838)	8	middle Albian–upper Cenomanian	Pl. 1, Figs 12–25
Puzosia (*Puzosia*)	*mayoriana*	(d'Orbigny, 1841)	14	middle Albian–upper Cenomanian	Pl. 2; Pl. 3, Figs 1–8
Callihoplites	cf. *cratus*	(Seeley, 1865)	5	upper upper Albian	Pl. 3, Figs 9–15
Callihoplites	*tetragonus*	(Seeley, 1865)	1	upper upper Albian	Pl. 3, Figs 16–19
Lepthoplites	cf. *cantabrigiensis*	Spath, 1926	2	upper upper Albian	Pl. 3, Figs 20–24
Discohoplites	cf. *valbonnensis*	(Hébert and Munier-Chalmas, 1875)	1	upper upper Albian	Pl. 3, Figs 25–28
Arrhaphoceras (Arrhaphoceras)	*substuderi*	Spath, 1928	2	upper upper Albian	Pl. 3, Figs 29–32
Stoliczkaia (*Stoliczkaia*)	*dispar*	(d'Orbigny, 1841)	25	upper upper Albian	Pls 4, 5
Mortoniceras (Subschloenbachia)	*rostratum*	(Sowerby, 1817)	21	upper upper Albian (*Mortoniceras* (*S.*) *rostratum* Zone)	Pls 6–13
Scaphites	*hugardianus*	d'Orbigny, 1842	3	upper upper Albian–?lower Cenomanian	Pl. 14, Figs 1–13
Scaphites	*meriani*	Pictet and Campiche, 1861	8	upper upper Albian	Pl. 14, Figs 14–30
Mariella (Mariella)	*bergeri*	(Brongniart, 1822)	98	upper upper Albian	Pl. 15, Figs 9–40; Pls 16, 17; Pl. 18, Figs 1–6
Mariella (Mariella)	*miliaris*	(Pictet and Campiche, 1861)	4	upper upper Albian–?lower Cenomanian	Pl. 15, Figs 1–8; Pl. 18, Figs 7–9
Mariella (Mariella)	sp. 1		1	pper upper Albian (*Mortoniceras* (*S.*) *rostratum* Zone)	Pl. 18, Fig. 12
Mariella (Mariella)	sp. 2		1	upper upper Albian (*Mortoniceras* (*S.*) *rostratum* Zone)	Pl. 18, Figs 10, 11
Anisoceras	*armatum*	(Sowerby, 1817)	9	upper upper Albian	Pl. 19
Anisoceras	*perarmatum*	Pictet and Campiche, 1861	8	upper upper Albian	Pls 20, 21
Anisoceras	*pseudoelegans*	Pictet and Campiche, 1861	3	upper upper Albian	Pl. 23, Figs 1–4
Anisoceras	sp.		5	upper upper Albian (*Mortoniceras* (*S.*) *rostratum* Zone)	Pl. 22
Idiohamites	*elegantulus*	Spath, 1939	2	upper upper Albian	Pl. 23, Figs 5–7
Hamites	*virgulatus*	Brongniart, 1822	23	upper upper Albian	Pl. 24, Figs 1–23
Hamites	*duplicatus*	Pictet and Campiche, 1861	3	upper upper Albian	Pl. 24, Figs 24–31
Hamites	*venetzianus*	Pictet, 1847	2	upper upper Albian	Pl. 24, Figs 32–35
Hamites	sp.		4	upper upper Albian (*Mortoniceras* (*S.*) *rostratum* Zone)	Pl. 24, Figs 36–41
Lechites (*Lechites*)	*gaudini*	(Pictet and Campiche, 1861)	28	upper Albian–lower Cenomanian	Pl. 23, Figs 8–16
Lechites (*Lechites*)	*moreti*	Breistroffer, 1936	1	upper upper Albian	Pl. 23, Figs 17–19
Eutrephoceras	*sublaevigatum*	(d'Orbigny, 1850)	5	Albian–Campanian?	Pl. 25, Figs 1–8

Table 1. Cephalopod taxa identified in the studied material from Clansayes. N – number of studied specimens.

described by Kennedy and Latil (2007) and 14 taxa were reported by Gale *et al*. (2011) for correlative beds of the Clansayes *M.* (*S.*) *rostratum* level. Many of the ammonite taxa identified in the present work were also reported by Kennedy and Latil (2007) and Gale *et al*. (2011) from the *M.* (*S.*) *rostratum* Zone at the Montlaux and Col de Palluel sections, respectively. Nevertheless, the absence of *Mariella bergeri* within the defined *M.* (*S.*) *rostratum* Zone both at the Montlaux and Col de Palluel sections is remarkable, considering its abundance at Clansayes within the same zone. Conversely, *Stoliczkaia* (*S.*) *clavigera* apparently does not occur at Clansayes, whereas it is common in the *M.* (*S.*) *rostratum* Zone of the Montlaux section (Kennedy and Latil 2007). Noteworthy, the turriliticone species *Ostlingoceras puzosianum* (d'Orbigny, 1842) was also not retrieved from Clansayes, whereas it is common at Montlaux within the *M.* (*S.*) *perinflatum* Zone as interpreted by Kennedy and Latil (2007). Moreover, Gale *et al*.

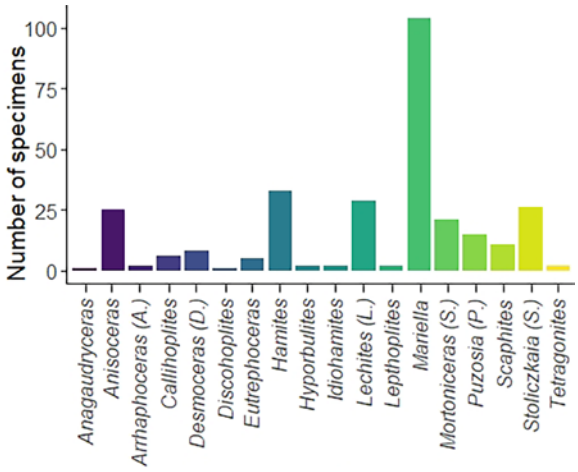

Text-fig. 8. Bar plot of the abundance of each cephalopod genus found at Clansayes (based on the corresponding number of studied specimens).

(2011) reported *Turrilitoides hugardianus* (d'Orbigny, 1842), *Cantabrigites helveticum* Renz, 1968 and several species of the genus *Kossmatella* Jacob, 1907 from the *M.* (*S.*) *rostratum* Zone at the Col de Palluel section, whereas these three genera were not found at Clansayes. Such absences at Clansayes are unlikely to be due to a sampling issue given the decade-long, intensive fieldwork conducted at this locality. Furthermore, the two modes of preservation observed at Clansayes (see geological settings) do not appear to have erased the original faunal signal. In turn, the marked differences in ammonite composition are likely to be related to differences in environmental conditions. Indeed, the Montlaux and Col de Palluel sections represent deeper palaeoenvironments compared to Clansayes, as shown by their calcareous clay- and marlstone deposits (Kennedy and Latil 2007; Gale *et al*. 2011).

In terms of abundance, the Clansayes assemblage is dominated by the genus *Mariella* (104 out of 295 specimens; Text-fig. 8). However, turriliticones likely produced more fossil fragments than most other taxa as their shell apparently gets fragmented easily under mechanical stress (based on observation of all collected specimens from Clansayes and Salazac localities; Jattiot *et al*. 2021). This is particularly well-illustrated by specimen UBGD 293277, which consists of two fragments barely connected together (Text-fig. 9). Frequent fragmentation of *Mariella* shells indicates that the minimum number of individuals is much lower than the number of sampled specimens (many of which are shell fragments). Nevertheless, this high abundance of *Mariella* at Clansayes echoes the work by Reboulet *et al*. (2005) who interpreted *Mariella* as an inhabitant of a neritic palaeoenvironment. Conversely, *Hamites* and *Lechites* are commonly seen as elements of the oceanic domain (Reboulet *et al*. 2005). The paradoxical high abundance of *Hamites* and *Lechites* at Clansayes (Text-fig. 8) suggests that their shells were transported from the oceanic domain to the Clansayes depositional environment (the basal fossiliferous layer that yielded these specimens being interpreted as transgressive deposits on top of a shelf margin wedge; see Geological Setting). In addition, given their remarkably elongated and thus fragile shell, the minimum number of *Hamites* and *Lechites* individuals is much lower than the number of sampled specimens (many of which are shell fragments). Overall, the Clansayes ammonite assemblage is characterised by the rarity or absence of taxa recognised as typical of the open ocean, including the lytoceratids *Kossmatella* (absent) and *Tetragonites* (only two sampled *T. timotheanus* specimens), as well as the phylloceratids (only two sampled *Hyporbulites seresitensis* specimens). Therefore, based on ammonites, Clansayes is interpreted as a near-shore environment, as confirmed by sedimentological evidence (see Geological Setting).

Ammonite zonation of the upper upper Albian

Kennedy and Latil (2007) reviewed the historical development of the European upper upper Albian ammonite zonation. According to these authors, a re-examination of the ammonites from the Montlaux section described by Latil (1994) and additional material from this locality show that *Mortoniceras* (*Subschloenbachia*) *perinflatum* succeeds *M.* (*S.*) *rostratum*, with no temporal overlap. Consequently, they proposed a sequence, from oldest to youngest, consisting of the *M.* (*Mortoniceras*) *fallax*, *M.* (*S.*) *rostratum* and *M.* (*S.*) *perinflatum* and *Arrhaphoceras* (*Praeschloenbachia*) *briacensis* Zones. All together, they are equivalent to the classic *Stoliczkaia dispar* Zone (see e.g., Latil 1994; Owen 1999). This biostratigraphic scheme for the upper upper Albian (Text-fig. 2) was subsequently widely used (e.g., Kennedy *et al*. 2008; Amédro and Matrion 2014; Reboulet *et al*. 2018). However, the statement by Kennedy and Latil (2007, p. 1) that the ammonites from the Montlaux section "provide unequivocal evidence for a *Mortoniceras* (*Subschloenbachia*) *rostratum* ammonite Zone succeeded by a *Mortoniceras* (*Subschloenbachia*) *perinflatum* ammonite Zone" is questionable. Indeed, as mentioned in the discussion of *M.* (*S.*) *rostratum* (see Systematic Palaeontology), the characters of the

Text-fig. 9. Taphonomic alteration of a *Mariella* (*M.*) *bergeri* (Brongniart, 1822) specimen from Clansayes (specimen UBGD 293277), consisting in the loss of nearly an entire whorl at specimen mid-height. Scale bar is 10 mm.

phragmocones of the *M.* (*S.*) *rostratum* and *M.* (*S.*) *perinflatum* holotypes are identical. In addition, to our knowledge, no adult body chambers of *M.* (*S.*) *perinflatum* have been illustrated so far. According to Kennedy *et al.* (1998, 2005) and Kennedy and Latil (2007), *M.* (*S.*) *rostratum* can supposedly be separated from *M.* (*S.*) *perinflatum* on the basis of its consistently less depressed whorl section (quantitatively expressed by a lower W/H ratio). However, this claim was not supported by any statistical analysis. The identification of a *M.* (*S.*) *perinflatum* Zone in the Montlaux section (Kennedy and Latil 2007) is indeed based on four specimens only, of which the three figured ones are too distorted for assessing whorl thickness. Thus, based on the criteria mentioned by Kennedy and Latil (2007), these three figured specimens cannot be identified at the species level, which strongly questions their proposed biostratigraphical scheme.

The same sequence [*M.* (*S.*) *rostratum* succeeded by *M.* (*S.*) *perinflatum*] has been established in Texas (Kennedy *et al*. 1998, 2005). However, no *M.* (*S.*) *perinflatum* specimens were figured by Kennedy *et al*. (1998), except for the holotype. Furthermore, among the four *M.* (*S.*) *perinflatum* specimens documented by Kennedy *et al*. (2005), in only two is a W/H ratio available. It is noteworthy that the first specimen (USNM 520206; Kennedy *et al*. 2005, fig. 11A–C) has a W/H ratio of 1.28, which is almost exactly the same as that of a specimen from the same locality assigned to *M.* (*S.*) *rostratum* (i.e., 1.26; specimen USNM 520232; Kennedy *et al*. 2005, fig. 10J, K). Given that it was suggested by Kennedy and Latil (2007) that *M.* (*S.*) *rostratum* can only be separated from *M.* (*S.*) *perinflatum* on the basis of its consistently less depressed whorl section (and thus lower W/H ratio), the assignment of specimen USNM 520206 to *M.* (*S.*) *perinflatum* rather than *M.* (*S.*) *rostratum* is contestable. The second specimen (USNM 520207; Kennedy *et al*. 2005, fig. 11D–F) has a W/H ratio of 1.63, which is higher than any of the W/H ratios obtained from the Clansayes specimens assigned to *M.* (*S.*) *rostratum* (1.39 being the highest value among them). However, as Kennedy *et al*. (2005, p. 365) stated, this specimen is distorted, making its H/W ratio questionable. Overall, evidence for the separation of *M.* (*S.*) *rostratum* and *M.* (*S.*) *perinflatum* as two distinct species is lacking in the literature. Accordingly, the existence of a *M.* (*S.*) *perinflatum* Zone above the *M.* (*S.*) *rostratum* Zone is speculative.

In turn, the presumed and surprising absence of *Mariella bergeri* in the Montlaux section within the *M.* (*S.*) *rostratum* Zone [but supposedly occurring within the *M.* (*S.*) *perinflatum* Zone; Kennedy and Latil 2007] may result from the misidentification of the studied *Mortoniceras* specimens. If these specimens were interpreted as representatives of the species *M.* (*S.*) *rostratum*, the whole ammonite fauna described from the Montlaux section by Kennedy and Latil (2007) would correspond to the *M.* (*S.*) *rostratum* Zone only. This would be consistent with our results, especially considering that *Mariella bergeri* commonly occurs at Clansayes within the *M.* (*S.*) *rostratum* Zone.

Shell chirality patterns through time in the genus *Mariella* and comparison with some extant gastropods

Based on a binomial test on an extensive material, Jattiot *et al*. (2021) showed that the distribution of sinistral and dextral *Mariella* specimens within the *Mortoniceras* (*M.*) *fallax* Zone at the Salazac locality is statistically biased towards sinistral coiling (62% *vs*. 38%, N = 150, $p = 0.004$), regardless of the species. We performed the same test on 158 specimens from Clansayes (including 55 from a private collection) that represent a nearly monospecific sample, as 153 of them were assigned to *Mariella bergeri*. This test reveals that the distribution of sinistral and dextral *Mariella* specimens from Clansayes is even more statistically biased towards sinistral coiling (93 % *vs*. 7 %, $p < 0.001$). This suggests the existence of a shell chirality pattern in *Mariella* characterised by an increase in the proportion of sinistral specimens from the *M.* (*M.*) *fallax* Zone to the overlying *M.* (*S.*) *rostratum* Zone, at least in south-eastern France. Although a potential palaeoecology-related effect on the observed differences cannot be totally ruled out since the Salazac and Clansayes localities correspond to slightly different palaeoenvironmental settings, this increase in sinistral *Mariella* specimen frequency may hypothetically be part of a global evolutionary pattern. Indeed, *Mariella* survived into the early Cenomanian and, to our knowledge, nearly all worldwide documented Cenomanian *Mariella* (and more generally Cenomanian turrilitids) appear to be sinistral, although this assumption requires further investigation. Klinger and Kennedy (1978, p. 38) stated that "all Cenomanian [*Mariella*] forms (and indeed all Cenomanian Turrilitidae) are sinistral". However, we know one Cenomanian *Mariella* species that comprises dextral specimens, namely *Mariella numida* (Pervinquière, 1910) (see Kennedy 2020, pl. 37, fig. 12).

Regarding extant mollusk species, most gastropod species show a uniform chirality, and reversal of this asymmetry is rare (Wandelt and Nagy 2004). More precisely, most snail species are dextral (Wandelt and Nagy 2004; Davison *et al*. 2020). Exceptions include, e.g., the common pond snail *Physa* Draparnaud, 1805, which is an entirely sinistral species, or another common pond snail, *Lymnaea* Lamarck, 1799, in which both dextral and sinistral forms are found (sinistral individuals representing up to 2% of the population; Wandelt and Nagy 2004). This strongly biased shell chirality distribution in extant gastropods (in which dextral coiling is overwhelmingly dominant) recalls that observed within the *Mariella* population from the *M.* (*S.*) *rostratum* Zone at Clansayes and the Cenomanian *Mariella* populations (in which sinistral coiling is overwhelmingly dominant). In contrast, the collection from Salazac undeniably indicates that more variation was allowed within the older *Mariella* population from the *M.* (*M.*) *fallax* Zone at Salazac (62% sinistral *vs*. 38% dextral; Jattiot *et al*. 2021) than within the younger *Mariella* population from the *M.* (*S.*) *rostratum* Zone at Clansayes (93% sinistral *vs*. 7% dextral). Noteworthy, turrilitids first appear at the base of the middle Albian, where they are represented by two genera (*Proturrilitoides* Breistroffer, 1947 and *Pseudhelicoceras* Spath, 1921) that are both dextral and sinistral, unfortunately in unassessed proportions so far (Klinger and Kennedy 1978).

For the time being, one can only speculate about the reasons for the hypothetical evolutionary pattern of chiromorphogenesis in *Mariella* towards near total sinistral coiling through time and for the potentially associated selective process(es). According to Davison *et al*. (2020), chiral variation in snails is due to environment, chance or genetic factors, all of which might occur in the same taxonomic group of snails. From the genetic point of view, Abe and Kuroda (2019) recently identified the formin *Lsdia1* as the long-sought gene for snail dextral/sinistral coiling. They also show that this gene sets the chirality at the one-cell stage in *Lymnea stagnalis*, which makes it the earliest observed symmetry-breaking event linked directly to body chirality in the animal kingdom.

CONCLUSIONS

We have documented a total of 24 species (17 genera) of ammonites and one species of nautiloid from the *Mortoniceras* (*S.*) *rostratum* Zone at Clansayes. Based on morphological and biometric analyses, we discriminated two species for the heteromorphic ammonite genus *Mariella* within the *Mortoniceras rostratum* Zone. Investigations on shell chirality patterns in *Mariella* from the upper Albian of southern France led us to identify an increase in the proportion of sinistral specimens. This observed increase in the frequency of sinistral *Mariella* specimens may hypothetically be part of a global evolutionary pattern, considering that nearly all documented younger Cenomanian *Mariella* (and more generally Cenomanian turrilitids) are sinistral. Additionally, in our opinion it is clear that firm evidence for the separation of *M.* (*S.*) *rostratum* and *M.* (*S.*) *perinflatum*

as two distinct species is still lacking in the literature. Accordingly, the existence of a *Mortoniceras* (*S.*) *perinflatum* Zone above the *M.* (*S.*) *rostratum* Zone remains speculative. Finally, the observed differences in ammonite composition between Clansayes and the Montlaux and Col de Palluel sections are likely to be related to differences in environmental conditions.

Acknowledgements

The authors are indebted to Josep A. Moreno Bedmar and an anonymous reviewer for their meticulous reviews of the manuscript. Patrick Brisac and Alexis Gris are warmly thanked for their help during fieldwork. The linguistic proofreading by Jim Jenks and Shannon Brophy is gratefully acknowledged. This research received financial support from the Alexander von Humboldt-Foundation (project number 1205896-FRA-HFST-P) and we appreciate a scholarship of the first author at the University of Bremen.

REFERENCES

Abe, M. and Kuroda, R. 2019. The development of CRISPR for a mollusc establishes the formin *Lsdia1* as the long-sought gene for snail dextral/sinistral coiling. *Development*, **146** (9), 1–7.

Agassiz, L. 1847. Nomenclatoris zoologici index universalis continens nomina systematica classium, ordinum, familiarum et generum animalium omnium, tam viventium quam fossilium, segundum ordinem alphabeticum unicum disposita, adjectis homonymiis plantarum, 1135 pp. Jent & Gassmann; Soloduri.

Amédro, F. 2002. Plaidoyer pour un étage Vraconnien entre l'Albien *sensu stricto* et le Cénomanien (système Crétacé). *Académie Royale de Belgique, Classe des Sciences*, **4**, 128 pp.

Amédro, F. 2008. Support for a Vraconnian Stage between the Albian *sensu stricto* and the Cenomanian (Cretaceous System). *Carnets de Géologie / Notebooks on Geology*, *Memoir*, **2008/02**, 83 pp.

Amédro, F. and Matrion, B. 2014. L'étage Albien dans sa région-type, l'Aube (France): une synthèse dans un contexte sédimentaire global. *Carnets de Géologie / Notebooks on Geology* (5), **14**, 69–128.

Amédro, F. and Robaszynski, F. 2000. La formation des argiles silteuses de Marcoule dans les sondages ANDRA du Gard rhodanien (SE France): La limite Albien terminal ("Vraconnien")-Cénomanien au moyen des ammonites et comparaison avec les affleurements de Salazac. *Géologie Méditerranéenne*, **27** (3–4), 175–201.

Arkell, W.J. 1950. A classification of the Jurassic ammonites. *Journal of Paleontology*, **24**, 354–364.

Arnott, R.W. and Southard, J.B. 1990. Exploratory flow-duct experiments on combined-flow bed configurations, and some implications for interpreting storm-event stratification. *Journal of Sedimentary Research*, **60**, 211–219.

Avram, E., Szasz, L., Antonescu, E., Baltreš, A., Iva, M., Melinte, M., Neagu, T., Rădan, S. and Tomescu, C. 1993. Cretaceous terrestrial and shallow marine deposits in northern South Dobrogea (SE Rumania). *Cretaceous Research*, **14**, 265–305.

Bayle, É. 1878. Fossiles principaux des terrains. Explication de la Carte Géologique de la France, 4, (1), (Atlas), 158 pls. Service carte géologique; Paris.

Bermúdez, H.D., Gómez-Cruz, A. de J., Hyžný, M., Moreno-Bedmar, J.A., Barragán, R., Moreno Sánchez, M. and Vega, F.J. 2013. Decapod crustaceans from the Cretaceous (Aptian–Albian) San Gil Group in the Villa de Leyva section, central Colombia. *Neues Jahrbuch für Geologie und Paläontologie*, *Abhandlungen*, **267**, 255–272.

Blainville, H.M.D. de 1825–1827. Manuel de malacologie et de conchyliologie, 664 pp. (1825), 87 pls. (1827). Levrault; Paris and Strasbourg.

Böhm, J. 1895. Review of A. de Grossouvre: Recherches sur la craie supérieure, 2nd part. *Neues Jahrbuch für Mineralogie, Geologie und Paläontologie*, **1895**, 360–366.

Böhm, J. 1910. Review of 'Études de Paléontologie Tunisienne' by L. Pervinquiére. *Neues Jahrbuch für Mineralogie, Geologie und Paläontologie*, **1910**, 149–155.

Bréhéret, J.G. 1997. L'Aptien et l'Albien de la fosse vocontienne (des bordures au bassin). Évolution de la sédimentation et enseignements sur les événements anoxiques. *Publication de la Société Géologique du Nord*, **25**, 614 pp.

Breistroffer, M. 1936. Les subdivisions du Vraconien dans le Sud-Est de la France. *Bulletin de la Société Géologique de France*, **5** (6), 63–68.

Breistroffer, M. 1940a. Révision des ammonites du Vraconien de Salazac (Gard) et considérations générales sur ce sous-étage albien. *Travaux du Laboratoire de Géologie de l'Université de Grenoble*, **22**, 101 pp.

Breistroffer, M. 1940b. Sur la découverte de *Knemiceras* aff. *saadense* Thom. et Per. sp. dans le Vraconien de Salazac (Gard). *Compte Rendu sommaire des Séances de la Société Géologique de France*, **8**, 87–89.

Breistroffer, M. 1947. Sur les zones d'ammonites dans l'Albien de France et d'Angleterre. *Travaux du Laboratoire de Géologie de la Faculté des Sciences de Grenoble*, **26**, 17–104.

Breistroffer, M. 1953. Commentaires taxonomiques. In: Breistroffer, M. and de Villoutreys, O. (Eds.), Les ammonites albiennes de Peille (Alpes-Maritimes). *Travaux du Laboratoire de Géologie de la Faculté des Sciences de l'Université de Grenoble*, **30**, 71–74.

Brongniart, A. 1822. Sur quelques terrains de Craie hors du Bassin de Paris, pp. 80–101. In: Cuvier, G. and Brongniart, A. (Eds.), Description géologique des environs de Paris. 3rd edn., 428 pp. G. Dufour et E. d'Ocagne; Paris.

Cooper, M.R. 1990. A revision of the Scaphitidae (Cretaceous Ammonoidea) from the Cambridge Greensand. *Neues Jahrbuch für Geologie und Paläontologie*, *Abhandlungen*, **178**, 285–308.

Cooper, M.R. 1998. A revision of the Turrilitidae (Cretaceous Ammonoidea) from the Cambridge Greensand. *Neues Jahrbuch für Geologie und Paläontologie*, *Abhandlungen*, **207**, 145–170.

Cooper, M.R. and Kennedy, W.J. 1977. A revision of the Baculitidae of the Cambridge Greensand. *Neues Jahrbuch für Geologie und Paläontologie*, *Monatshefte*, **1977**, 641–658.

Cooper, M.R. and Kennedy, W.J. 1979. Uppermost Albian (*Stoliczkaia dispar* Zone) ammonites from the Angolan littoral. *Annals of the South African Museum*, **77** (10), 175–308.

Cooper, M.R. and Kennedy, W.J. 1987. A revision of the Puzosiinae (Cretaceous ammonites) of the Cambridge Greensand. *Neues Jahrbuch für Geologie und Paläontologie*, *Abhandlungen*, **174**, 105–121.

Cooper, M.R. and Owen, H.G. 2011. Evolutionary relationships within Hoplitidae (Cretaceous Ammonoidea). *Neues Jahrbuch für Geologie und Paläontologie*, *Abhandlungen*, **261**, 337–351.

Crick, G.C. 1907. The Cephalopoda from the deposit at the North End of False Bay, Zululand. *Report of the Geological Survey of Natal and Zululand*, **3**, 235–249.

Davison, A., Thomas, P. and 'Jeremy the snail' citizen scientists. 2020. Internet 'shellebrity' reflects on origin of rare mirror-image snails. *Biology Letters*, **16** (6), 20200110.

Debelmas, J., Ballesio, R., Brochier, J.-L., Fourneaux, C., Moûtier, L. and Triat, J.-M. 2004. Notice explicative, Carte géol. France (1/50 000), feuille Valréas 2e édition (890), 75 pp. BRGM; Orléans.

Delanoy, G. and Latil, J.L. 1988. Découverte d'un nouveau gisement albien dans les environs de Drap (Alpes-Maritimes, France) et description d'une riche ammonitofaune d'âge Albien terminal. *Geobios*, **21** (6), 749–771.

Diener, C. 1925. Ammonoidea neocretacea. *Fossilium Catalogus* (1: Animalia), **29**, 244 pp.

Douvillé, H. 1879. Note accompagnant la présentation de l'Atlas de t. iv de l'explication de la carte géologique de France de E. Bayle et R. Zeiller. *Bulletin de la Société Géologique de France*, **7** (3), 91–92.

Douvillé, H. 1890. Sur la classification des Cératites de la Craie. *Bulletin de la Société Géologique de France*, **18**, 275–292.

Douvillé, H. 1912. Évolution et classification des Pulchelliidés. *Bulletin de la Société géologique de France*, **11**, 285–320.

Draparnaud, J.P.R. 1805. Histoire naturelle des mollusques terrestres et fluviatiles de la France, 140 pp. Louis Colas; Paris.

Elliott, T. 1974. Interdistributary bay sequences and their genesis. *Sedimentology*, **21**, 611–622.

Ferry, S. 1999. Apport des forages ANDRA de Marcoule à la connaissance de la marge crétacée rhodanienne. In: Étude du Gard rhodanien (Ed.), Actes des Journées scientifiques CNRS-ANDRA, Bagnols-sur-Cèze, 20–21 octobre 1997, 63–91. EDP Sciences; Paris.

Ferry, S. 2017. Summary on Mesozoic carbonate deposits of the Vocontian Trough (Subalpine Chains, SE France). *Carnets de Geologie*, **2017**, 9–42.

Ferry, S. and Rubino, J.-L. 1988. Eustatisme et séquences de dépôt dans le Crétacé du Sud-Est de la France. Livret-guide de l'excursion du Groupe Français du Crétacé en fosse vocontienne (25-27 mai 1988). *GéoTrope*, **1**, 1–105.

Forbes, E. 1846. Report on the Fossil Invertebrata from southern India, collected by Mr. Kaye and Mr. Cunliffe. *Transactions of the Geological Society of London*, *series 2*, **7**, 97–174.

Gale, A.S., Bown, P., Caron, M., Crampton, J.S., Crowhurst, S.J., Kennedy, W.J., Petrizzo, M.R. and Wray, D.S. 2011. The uppermost Middle and Upper Albian succession at the Col de Palluel, Hautes-Alpes, France: An integrated study (ammonites, inoceramid bivalves, planktonic foraminifera, nannofossils, geochemistry, stable oxygen and carbon isotopes, cyclostratigraphy). *Cretaceous Research*, **32** (2), 59–130.

Gale, A.S., Kennedy, W.J., Burnett, J.A., Caron, M. and Kidd, B.E. 1996. The Late Albian to Early Cenomanian succession at Mont Risou near Rosans (Drôme, SE France): an integrated study (ammonites, inoceramids, planktonic foraminifera, nannofossils, oxygen and carbon isotopes). *Cretaceous Research*, **17** (5), 515–606.

Gale, A.S., Kennedy, W.J. and Walaszczyk, I. 2019. Upper Albian, Cenomanian and Lower Turonian stratigraphy, ammonite and inoceramid bivalve faunas from the Cauvery Basin, Tamil Nadu, South India. *Acta Geologica Polonica*, **69**, 161–338.

Gautam, J.P., Pandey, B., Jaitly, A.K., Pathak, D.B., Lehmann, J. and Tiwari, D.N. 2019. Late Albian ammonite from the Cauvery Basin, south India. *Cretaceous Research*, **102**, 12–29.

Gauthier, H. 2006. Révision Critique de la Paléontologie Française d'Alcide d'Orbigny, 6, Céphalopodes Crétacés, 292 + 662 pp. Backhuys; Leiden.

Gill, T. 1871. Arrangement of the Families of Mollusks. *Smithsonian Miscellaneous Collections*, **227**, 49 pp.

Grossouvre, A. de 1894. Recherches sur la craie supérieure, 2, Paléontologie. Les ammonites de la craie supérieure. Mémoires du Service de la Carte géologique détaillée de la France, 264 pp. Imprimiere Nationale; Paris. [misdated 1893]

Guex, J. 1967. Contribution à l'étude des blessures chez les ammonites. *Bulletin des Laboratoires de géologie, minéralogie, géophysique et du Musée géologique de l'Université de Lausanne*, **165**, 1–23.

Guex, J. 1968. Sur deux conséquences particulières des traumatismes du manteau des ammonites. *Bulletin des Laboratoires de géologie, minéralogie, géophysique et du Musée géologique de l'Université de Lausanne*, **175**, 1–8.

Guex, J., Koch, A., O'Dogherty, L. and Bucher, H. 2003. A morphogenetic explanation of Buckman's law of covaria-

tion. *Bulletin de la Société Géologique de France*, **174** (6), 603–606.

Hammer, Ø. and Bucher, H. 2005. Buckman's first law of covariation: a case of proportionality. *Lethaia*, **38** (1), 67–72.

Hartigan, J.A. and Hartigan, P.M. 1985. The dip test of unimodality. *The Annals of Statistics*, **13** (1), 70–84.

Hébert, E. and Munier-Chalmas, E.P.A. 1875. Fossiles du bassin d'Uchaux. *Annales des Sciences Géologiques, Paris*, **6**, 113–132.

Herrle, J.O. and Mutterlose, J. 2003. Calcareous nannofossils from the Aptian–Lower Albian of southeast France: palaeoecological and biostratigraphic implications. *Cretaceous Research*, **24** (1), 1–22.

Hyatt, A. 1889. Genesis of the Arietidae. *Smithsonian Contributions to Knowledge*, **673**, 239 pp.

Hyatt, A. 1894. Phylogeny of an acquired characteristic. *Proceedings of the American Philosophical Society*, **32** (143), 349–647.

Hyatt, A. 1900. Cephalopoda. In: Zittel, K.A. von 1896–1900, Textbook of Palaeontology, pp. 502–604, transl. Eastman. C.R. Macmillan; London and New York.

Jacob, C. 1905. Étude sur les ammonites et sur l'horizon stratigraphique du gisement de Clansayes. *Bulletin de la Société Géologique de France*, **5**, 399–432.

Jacob, C. 1907. Études paléontologiques et stratigraphiques sur la partie moyenne des terrains crétacés dans les Alpes Françaises et les régions voisines, 314 pp. Typographie et Litographie Allier Frères; Grenoble.

Jattiot, R., Lehmann, J., Latutrie, B., Vuarin, P., Tajika, A. and Vennin, E. 2021. Reappraisal of the latest Albian (*Mortoniceras fallax* Zone) cephalopod fauna from the classical Salazac locality (Gard, southeastern France). *Geobios*, **64**, 1–46.

Joly, B. 1993. Les Phylloceratacеae malgaches au Crétacé (Phylloceratina, Ammonoidea). *Documents des Laboratoires de Géologie de la Faculté des Sciences de Lyon*, **127**, 171 pp.

Joly, B. 2000. Les Juraphyllitidae, Phylloceratidae, Neophylloceratidae (Phylloceratacеae, Phylloceratina, Ammonoidea) de France au Jurassique et au Crétacé. *Mémoire Spécial Geobios*, **23** and *Mémoire de la Société Geologique de France*, **174**, 204 pp.

Joly, B. and Delamette, M. 2008. Les Phylloceratoidea (Ammonoidea) aptiens et albiens du bassin vocontien (Sud-Est de la France). *Carnets de Géologie / Notebooks on Geology*, **2008/04**, 60 pp.

Kennedy, W.J. 2004. Ammonites from the Pawpaw Shale (Upper Albian) in northeast Texas. *Cretaceous Research*, **25** (6), 865–905.

Kennedy, W.J. 2020. Upper Albian, Cenomanian and Upper Turonian ammonite faunas from the Fahdène Formation of Central Tunisia and correlatives in northern Algeria. *Acta Geologica Polonica*, **70** (2), 147–272.

Kennedy, W.J., Cobban, W.A., Gale, A.S., Hancock, J.M. and Landman, N.H. 1998. Ammonites from the Weno Limestone (Albian) in northeast Texas. *American Museum Novitates*, **3236**, 46 pp.

Kennedy, W.J., Cobban, W.A., Hancock, J.M. and Gale, A.S. 2005. Upper Albian and Lower Cenomanian ammonites from the Main Street Limestone, Grayson Marl and Del Rio Clay in northeast Texas. *Cretaceous Research*, **26** (3), 349–428.

Kennedy, W.J. and Delamette, M. 1994a. *Neophlycticeras* Spath, 1922 (Ammonoidea) from the Upper Albian of Ain, France. *Neues Jahrbuch für Geologie und Paläontologie*, *Abhandlungen*, **191** (1), 1–24.

Kennedy, W.J. and Delamette, M. 1994b. Lyelliceratidae and Flickiidae (Ammonoidea) from the Upper Albian of the Helvetic shelf (western Alps, France and Switzerland). *Journal of Paleontology*, **68**, 1263–1284.

Kennedy, W.J. and Fatmi, A.N. 2014. Albian ammonites from northern Pakistan. *Acta Geologica Polonica*, **64**, 47–98.

Kennedy, W.J. and Gale, A.S. 2015. Upper Albian and Cenomanian ammonites from Djebel Mrhila, Central Tunisia. *Revue de Paléobiologie*, **34**, 235–361.

Kennedy, W.J., Gale, A.S., Bown, P.R., Caron, M., Davey, R.J., Gröcke, D. and Wray, D.S. 2000. Integrated stratigraphy across the Aptian-Albian boundary in the Marnes Bleues, at the Col de Pré-Guittard, Arnayon (Drôme), and at Tartonne (Alpes-de-Haute-Provence), France: a candidate Global Boundary Stratotype Section and Boundary Point for the base of the Albian Stage. *Cretaceous Research*, **21** (5), 591–720.

Kennedy, W.J., Gale, A.S., Huber, B.T., Petrizzo, M.R., Bown, P., Barchetta, A. and Jenkyns, H.C. 2014. Integrated stratigraphy across the Aptian/Albian boundary at Col de Pré-Guittard (southeast France): A candidate Global Boundary Stratotype Section. *Cretaceous Research*, **51**, 248–259.

Kennedy, W.J., Gale, A.S., Huber, B.T., Petrizzo, M.R., Bown, P., Barchetta, A. and Jenkyns, H.C. 2017. The Global Boundary Stratotype Section and Point (GSSP) for the base of the Albian Stage, of the Cretaceous, the Col de Pré-Guittard section, Arnayon, Drôme, France. *Episodes*, **40** (3), 177–188.

Kennedy, W.J., Jagt, J.W.M., Amédro, F. and Robaszynski, F. 2008. The late late Albian (*Mortoniceras fallax* Zone) cephalopod fauna from the Bracquegnies Formation at Strépy-Thieu (Hainaut, southern Belgium). *Geologica Belgica*, **11** (1–2), 35–69.

Kennedy, W.J. and Klinger, H.C. 1979. Cretaceous faunas from Zululand and Natal, South Africa. The ammonite family Gaudryceratidae. *Bulletin of the British Museum (Natural History) Geology*, **31** (2), 121–174.

Kennedy, W.J. and Klinger, H.C. 2013. Cretaceous faunas from Zululand and Natal, South Africa. The ammonite Subfamily Desmoceratinae Zittel, 1895. *African Natural History*, **9**, 39–54.

Kennedy, W.J. and Klinger, H.C. 2014. Cretaceous faunas from Zululand and Natal, South Africa. *Valdedorsella*, *Pseudohaploceras*, *Puzosia*, *Bhimaites*, *Pachydesmoceras*, *Parapuzosia* (*Austiniceras*) and *P.* (*Parapuzosia*) of the ammonite subfamily Puzosiinae Spath, 1922. *African Natural History*, **10**, 1–46.

Kennedy, W.J. and Latil, J.L. 2007. The Upper Albian ammonite succession in the Montlaux section, Hautes-Alpes, France. *Acta Geologica Polonica*, **57** (4), 453–478.

Kennedy, W.J. and Machalski, M. 2015. A late Albian ammonite assemblage from the mid-Cretaceous succession at Annopol, Poland. *Acta Geologica Polonica*, **65** (4), 545–553.

Kennedy, W.J. and Morris, N.J. 2018. An early Cenomanian ammonite fauna from near Lindi, Tanzania. *Cretaceous Research*, **87**, 84–101.

Keupp, H. 1977. Paläopathologische Normen bei Amaltheiden (Ammonoidea) des Fränkischen Lias. *Jahrbuch der Coburger Landesstiftung*, **1977**, 263–280.

Klein, J. 2014. Lower Cretaceous Ammonites VII Hoplitoidea and Engonoceratoidea. *Fossilium Catalogus* I: Animalia, **152** (*pars*), 280 pp.

Klein, J. 2015. Lower Cretaceous Ammonites VIII Turrilitoidea – Anisoceratidae, Hamitidae, Turrilitidae, including representatives of the Upper Cretaceous species. *Fossilium Catalogus* I: Animalia, **154** (*pars*), 265 pp.

Klein, J. 2016a. Lower Cretaceous Ammonites X Scaphitoidea, including Upper Cretaceous representatives. *Fossilium Catalogus* I: Animalia, **157** (*pars*), 203 pp.

Klein, J. 2016b. Lower Cretaceous Ammonites IX Turrilitoidea 2 – Baculitidae, including Upper Cretaceous representatives. *Fossilium Catalogus* (1: Animalia), **155** (*pars*), 140 pp.

Klein, J. 2018. Lower Cretaceous Ammonites XI Acanthoceratoidea: Leymeriellidae, Brancoceratidae, Lyelliceratidae, Flickiidae, Forbesiceratidae, including Upper Cretaceous representatives. *Fossilium Catalogus* (1: Animalia), **158**, 333 pp.

Klein, J., Hoffmann, R., Joly, B., Shigeta, Y. and Vašiček, Z. 2009. Lower Cretaceous Ammonites IV. Boreophylloceratoidea, Phylloceratoidea, Lytoceratoidea, Tetragonitoidea, Haploceratoidea including the Upper Cretaceous representatives. *Fossilium Catalogus* (1: Animalia), **146**, 416 pp.

Klein, J. and Vašiček, Z. 2011. Lower Cretaceous Ammonites V Desmoceratoidea. *Fossilium Catalogus* (1: Animalia), **148**, 311 pp.

Klinger, H.C. and Kennedy, W.J. 1978. Turrilitidae (Cretaceous Ammonoidea) from South Africa, with a discussion of the evolution and limits of the family. *Journal of Molluscan Studies*, **4**, 1–48.

Kossmat, F. 1895–1898. Untersuchungen über die südindische Kreideformation. *Beiträge zur Paläontologie Österreich-Ungarns und des Orients*, **9** (1895), 97–203 (1–107); **11** (1897), 1–46 (108–153); **11** (1898), 89–152 (154–217).

Lamarck, J.-B. 1799. Prodrome d'une nouvelle classification des coquilles. *Mémoires de la Société d'Histoire Naturelle de Paris*, **1**, 63–91.

Latil, J.L. 1989. Les genres *Engonoceras* Neumayr & Uhlig, 1881 et *Hypengonoceras* Spath, 1922 dans l'Albien supérieur (Z. à *Dispar*) de Salazac, Gard, France. *Revue de Paléobiologie*, **8** (1), 51–63.

Latil, J.L. 1994. The Dispar Zone in South-East France and comments about the biozonation of Albian in the Tethyan realm: biostratigraphy and paleontology (Ammonites). *Géologie Alpine*, *Mémoire H.S.*, **20**, 67–111.

Latil, J.L., Jaillard, E., Bardet, N., Raisossadat, N. and Vincent, P. 2021. The Albian-Cenomanian transition in a shelf-basin transect: Biostratigraphy, sedimentology and paleontology of Jebel Mghila, Central Tunisia. *Cretaceous Research*, **124**, 1–35.

López-Horgue, M.A., Owen, H.G., Rodríguez-Lázaro, J., Orue-Etxebarria, X., Fernández-Mendiola, P.A. and García-Mondéjar, J. 1999. Late Albian-Early Cenomanian stratigraphic succession near Estella-Lizarra (Navarra, central northern Spain) and its regional and interregional correlation. *Cretaceous Research*, **20** (4), 369–402.

Lundgren, B. 1891. Studier öfver fossilförande lösa block. *Geologiska Foreningens i Stockholm, Förhandlingar*, **13**, 111–121.

Meek, F.B. 1876. A report on the invertebrate Cretaceous and Tertiary fossils of the upper Missouri Country. In: Hayden, F.V. (Ed.), *Report of the United States Geological Survey of the Territories*, **9**, 629 pp.

Michelin, H. 1834. Coquilles fossiles de Gérodot (Aube). *Magazine de Zoologie de Guérin – Méneville*, **3**, pls 35.

Michelin, H. 1838. Note sur une argile dépendant du Gault, observée au Gaty, commune de Gérodot, department de l'Aube. *Mémoires de la Société Géologique de France*, **3** (5), 97–103.

Monnet, C., De Baets, K. and Yacobucci, M. M. 2015. Buckman's rules of covariation. In: Klug, C., Korn, D., De Baets, K., Kruta, I. and Mapes, R.H. (Eds), Ammonoid Paleobiology: from macroevolution to paleogeography, 67–94. Springer; Dordrecht.

Morton, S.G. 1834. Synopsis of the organic remains of the Cretaceous groups of the United States. Illustrated by nineteen plates, to which is added an appendix containing a tabular view of the Tertiary fossils discovered in America, 88 pp. Key & Biddle; Philadelphia.

Mosavinia, A., Lehmann, J. and Wilmsen, M. 2014. Late Albian ammonites from the Aitamir Formation (Koppeh Dagh, northeast Iran). *Cretaceous Research*, **50**, 72–88.

Neumayr, M. 1875. Die Ammoniten der Kreide und die Systematik der Ammonitiden. *Zeitschrift der Deutschen Geologischen Gesellschaft*, **27**, 854–942.

Nowak, J. 1908. Untersuchungen über Cephalopoden der oberen Kreide in Polen: I. Teil Genus *Baculites* Lamarck. *Bulletin international de l'Académie des Sciences de Cracovie*, *Classe des Sciences Mathématiques et Naturelles B*, **1908**, 326–353.

Nowak, J. 1916. Über die bifiden Loben der oberkretazischen Ammoniten und ihre Bedeutung für die Systematik. *Bulletin international de l'Académie des Sciences de Cracovie*, *Classe des Sciences Mathématiques et Naturelles B*, **1915**, 1–13.

Orbigny, A. d' 1840–1842. Paléontologie française. Terrains Crétacés. I: Céphalopodes, 662 pp., 148 pls. Masson; Paris.

Orbigny, A. d' 1850. Prodrome de Paléontologie stratigraphique universelle des animaux mollusques et rayonnés faisant suite au cours élémentaire de paléontologie et géologie stratigraphique, vol. I, 394 pp., vol. II, 427 pp. Masson; Paris.

Owen, H.G. 1984a. The Albian stage: European province chronology and ammonite zonation. *Cretaceous Research*, **5** (4), 329–344.

Owen, H.G. 1984b. Albian stage and substage boundaries. *Bulletin of the Geological Society of Denmark*, **33**, 183–189.

Owen, H.G. 1999. Correlation of Albian European and Tethyan ammonite zonations and the boundaries of the Albian Stage and substages: some comments. *Scripta Geologica*, special issue **3**, 129–149.

Parkinson, J. 1811. Organic Remains of a Former World, 3, 479 pp. J. Robson; London.

Pervinquière, L. 1907. Étude de paléontologie tunisienne – 1. Céphalopodes des terrains secondaires. Carte géologique de Tunisie, 438 pp. De Rudeval; Paris.

Pervinquière, L. 1910. Sur quelques ammonites du Crétacé algérien. *Mémoires de la Société Géologique de France, Paléontologie*, **17**, 86 pp.

Petrizzo, M.R., Huber, B.T., Gale, A.S., Barchetta, A. and Jenkyns, H.C. 2012. Abrupt planktic foraminiferal turnover across the Niveau Kilian at Col de Pre-Guittard (Vocontian Basin, southeast France): new criteria for defining the Aptian/Albian boundary. *Newsletters on Stratigraphy*, **45**, 55–74.

Pictet, F.J. 1854. Céphalopodes. In: Traité de Paléontologie, 2nd edition, 2, pp. 583–716. J.-B. Baillière; Paris.

Pictet, F.J. and Campiche, G. 1858–64. Description des fossiles du terrain Crétacé des environs de Sainte-Croix. *Matériaux pour la paléontologie Suisse*, **1**, 1–380 (1858–60); **2**, 1–752 (1861–64).

Pictet, F.J. and Roux, W. 1847–1854. Description des mollusques fossiles qui se trouvent dans les Grès Verts des environs de Genève. *Mémoires de la Société de Physique et d'Histoire Naturellle de Genève*, **11**, 257–412. [also published independently with the same title, described as Première Livraison, Céphalopodes, 136 pp. Fick; Geneva]

R Core Team. 2021. R: A language and environment for statistical computing. R Foundation for Statistical Computing, Vienna, Austria. http://www.r-project.org/.

Reboulet, S., Giraud, F. and Proux, O. 2005. Ammonoid abundance variations related to changes in trophic conditions across the Oceanic Anoxic Event 1d (Latest Albian, SE France). *Palaios*, **20**, 121–141.

Reboulet, S., Szives, O., Aguirre-Urreta, B., Barragán, R., Company, M., Frau, C., Kakabadze, M.V., Klein, J., Moreno-Bedmar, J.A., Lukeneder, A., Pictet, A., Ploch, I., Raisossadat, S.N., Vašíček, Z., Baraboshkin, E.J. and Mitta, V.V. 2018. Report on the 6th International Meeting of the IUGS Lower Cretaceous Ammonite Working Group, the Kilian Group (Vienna, Austria, 20th August 2017). *Cretaceous Research*, **91**, 100–110.

Renz, O. 1968. Die Ammonoidea im Stratotyp des Vraconnien bei Sainte-Croix (Kanton Waadt). *Schweizerische Paläontologische Abhandlungen*, **87**, 99 pp.

Robaszynski, F., Amédro, F., González-Donoso J.M and Linares, D. 2008. The Albian (Vraconnian)–Cenomanian boundary at the western Tethyan margins (Central Tunisia and southeastern France). *Bulletin de la Société Géologique de France*, **179** (3), 245–266.

Rubino, J.-L. and Delamette, M. 1985. La sédimentation de la plateforme à l'Albien sur la marge nord de la Téthys (Europe). In: Réunion special de la Société Géologique de France, Résume des Communications, p. 45. Institute de Géologie du Bassin d'Aquitaine; Bordeaux.

Schlotheim, E.F.B. von 1820. Die Petrefactenkunde auf ihrem jetzigen Standpunkte durch die Beschreibung seiner Sammlung versteiner und fossiler Überreste des Thier- und Pflanzenreichs der Vorweletrläutert, 437 pp. Becker; Gotha.

Scholz, G. 1973. Sur l'âge de la faune d'Ammonites au Château près de St-Martin-en-Vercors (Drôme) et quelques considérations sur l'évolution des Turrilitidés et des Hoplitidés vracono-cénomaniens. *Géologie Alpine*, **49**, 119–129.

Scholz, G. 1979. Die Ammoniten des Vracon (Oberalb, *dispar*-Zone) des Bakony-Gebirges (Westungarn) und eine Revision der wichtigsten Vracon-Arten der westmediterranen Faunenprovinz. *Palaeontographica Abteilung A*, **165**, 136 pp.

Seeley, H.G. 1865. On Ammonites from the Cambridge Greensand. *Annals and Magazine of Natural History*, **16** (3), 225–247.

Sharifi, J., Tajika, A., Mohammadabadi, A. and Abkuh, M.H.T. 2021. First discovery of nautilids from the Albian-Cenomanian succession of the Koppeh Dagh Basin, NE Iran. *Swiss Journal of Palaeontology*, **140** (14), 1–12.

Shimizu, S. 1934. Ammonites. In: Shimizu, S. and Obata, T. (Eds), Cephalopoda, 137 pp. Iwanami's lecture series of Geology and Palaeontology; Tokyo. [In Japanese]

Sornay, J. 1950. Étude stratigraphique sur le Crétacé supérieur de la Vallée du Rhône entre Valence et Avignon et des régions voisines, 254 pp. Allier; Grenoble.

Sowerby, J. 1812–1822. The Mineral Conchology of Great Britain, 1, pls 1–9 (1812), pls 10–44 (1813), pls 45–78 (1814), pls 79–102 (1815); 2, pls 103–114 (1815), pls 115–150 (1816), pls 151–186 (1817), pls 187–203 (1818); 3, pls 204–221 (1818), pls 222–253 (1819), pls 254–271 (1820), pls 272–306 (1821); 4, pls 307–318 (1821), pls 319–383 (1822). The Author; London.

Sowerby, J. de C. 1823–1846. The Mineral Conchology of Great Britain (continued), 4, pls 384–407 (1823); 5, pls 408–443 (1823), pls 444–485 (1824), pls 486–603 (1825); 6, pls 504–544 (1826), pls 545–580 (1827), pls 581–597 (1828), pls 598–609 (1829); 7, pls 610–618 (1840), pls 619–623 (1841), pls 624–628 (1843), pls 629–643 (1844), pls 644–648 (1846). The Author; London.

Spath, L.F. 1921. On Cretaceous Cephalopoda from Zululand. *Annals of the South African Museum*, **12**, 217–321.

Spath, L.F. 1922. On Cretaceous Ammonoidea from Angola, collected by Professor J.W. Gregory, D. Sc., F.R.S. *Transactions of the Royal Society of South Africa*, **53**, 91–160.

Spath, L.F. 1923–1943. A Monograph of the Ammonoidea of the Gault, (1923) 1, pp. 1–72, pls 1–4; (1925) 2, pp. 73–110, pls 5–8; 3, pp. 111–146, pls 9–12; (1926) 4, pp. 147–186, pls 13–16; (1927) 5, pp. 187–206, pls 17–20; (1928) 6, pp. 207–266, pls 21–24; (1930), 7, pp. 265–311, pls 25–30; (1931) 8, pp. 313–378, pls 30–36; (1932) 9, pp. 779–410, pls 37–42; (1933) 10, pp. 411–442, pls 43–48; (1934) 11, pp. 443–496, pls 49–56; (1937) 12, pp. 497–540, pls 57, 58; (1939) 13, pp. 541–608, pls 59–64; (1941) 14, pp. 609–668, pls 65–72; (1942) 15, pp. 669–720; (1943) 16, pp. 721–787 et i–x. Palaeontographical Society; London.

Spath, L.F. 1927. Revision of the Jurassic fauna of Kach (Cutch). *Memoirs of the Geological Survey of India*, *Palaeontologica Indica*, *N.S.*, **9** (Memoir 2, part 1), 1–71.

Szives, O. 2007. Albian stage. In: Szives, O. (Ed.), Csontos, L., Bujtor, L., Fosy, I., Aptian-Campanian Ammonites of Hungary. *Geologica Hungarica*, *Series Palaeontologica*, **57**, 75–122.

Tajika, A., Kürsteiner, P., Pictet, A., Jattiot, R., Lehmann, J. and Klug, C. 2018a. Ammoniten (Ammonoidea). In: Kürsteiner, P. and Klug, C. (Eds), Fossilien im Alpstein. Kreide und Eozän der Nordostschweiz, 238–284. Appenzeller Verlag; Schwellbrunn.

Tajika, A., Kürsteiner, P., Pictet, A., Lehmann, J., Tschanz, K., Jattiot, R. and Klug, C. 2017. Cephalopod associations and palaeoecology of the Cretaceous (Barremian–Cenomanian) succession of the Alpstein, northeastern Switzerland. *Cretaceous Research*, **70**, 15–54.

Tajika, A., Tschanz, K. and Klug, C. 2018b. New Albian ammonite faunas from Semelenberg (Alpstein, Switzerland) and their paleoecology. *Swiss Journal of Palaeontology*, **137** (1), 65–76.

Thomel, G. 1992. Ammonites du Cénomanien et du Turonien du Sud-Est de la France, 1, 422 pp.; 2, 383 pp. Serre; Nice.

Wandelt, J. and Nagy, L.M. 2004. Left-right asymmetry: more than one way to coil a shell. *Current Biology*, **14** (16), R654–R656.

Westermann, G. 1966. Covariation and taxonomy of the Jurassic ammonite *Sonninia adicra* (Waagen). *Neues Jahrbuch für Geologie und Paläontologie*, *Abhandlungen*, **124**, 289–312.

Whitehouse, F.W. 1927. Additions to the Cretaceous ammonite fauna of eastern Australia. *Memoir of the Queensland Museum*, **9**, 109–120.

Wiedmann, J. 1962. Ammoniten aus der Vascogotischen Kreide (Nordspanien) I. Phylloceratina, Lytoceratina. *Palaeontographica Abteilung A*, **118** (4–6), 119–237.

Wiedmann, J. 1965. Origin, limits and systematic position of *Scaphites*. *Palaeontology*, **8**, 397–453.

Wiedmann, J. 1966. Stammesgeschichte und system der posttriadischen ammonoideen; ein überblick. *Neues Jahrbuch für Geologie und Paläontologie*, *Abhandlungen*, **125**, 49–79; **127**, 13–81.

Wiedmann, J. 1973. The Albian and Cenomanian Tetragonitidae (Cretaceous Ammonoidea), with special reference to the Circum-Indic species. *Eclogae Geologicae Helvetiae*, **66** (3), 585–616.

Wiedmann, J. and Dieni, I. 1968. Die Kreide Sardiniens und ihre Cephalopoden. *Palaeontographia Italica*, **64**, 1–171.

Wilmsen, M., Berensmeier, M., Fürsich, F.T., Schlagintweit, F., Hairapetian, V., Pashazadeh, B. and Majidifard, M.R. 2020. Mid-Cretaceous biostratigraphy (ammonites, inoceramid bivalves and foraminifers) at the eastern margin of the Anarak Metamorphic Complex (Central Iran). *Cretaceous Research*, **110**, 104411.

Wright, C.W. and Kennedy, W.J. 1984. The Ammonoidea of the Lower Chalk, part 1, 126 pp. Palaeontographical Society; London.

Wright, C.W. and Kennedy, W.J. 1994. Evolutionary relationships among Stoliczkaiinae (Cretaceous ammonites) with an account of some species from the English *Stoliczkaia dispar* Zone. *Cretaceous Research*, **15** (5), 547–582.

Wright, C.W. and Kennedy, W.J. 1995. The Ammonoidea of the Lower Chalk, part 4, 295–319. Palaeontographical Society; London.

Wright, C.W. and Kennedy, W.J. 1996. The Ammonoidea of the Lower Chalk, part 5, 320–403. Palaeontographical Society; London.

Wright, C.W. and Wright, E.V. 1951. A survey of the fossil Cephalopoda of the Chalk of Great Britain, 40 pp. Palaeontographical Society; London.

Zittel, K.A. Von 1884. Handbuch der Paläontologie. 1. Abteilung Paläozoologie. 2 Lieferung. 3. Cephalopoda, 329–522. R. Oldenbourg; Münich and Leipzig.

Zittel, K.A. Von 1895. Grundzüge der Paläontologie (Paläozoologie), 972 pp. R. Oldenbourg; Münich and Leipzig.

Manuscript submitted: 19th August 2021
Revised version accepted: 22nd November 2021

PLATE 1

1-4 – *Hyporbulites seresitensis* (Pervinquière, 1907). 1-3 – UBGD 293051; 4 – UBGD 293052.

5-9 – *Tetragonites timotheanus* (Pictet in Pictet and Roux, 1847). 5, 6 – UBGD 293040; 7-9 – UBGD 293041.

10, 11 – *Anagaudryceras* sp., UBGD 293055.

12-25 – *Desmoceras* (*Desmoceras*) *latidorsatum* (Michelin, 1838). 12-14 – UBGD 293045; 15, 16 – UBGD 293046; 17, 18 – UBGD 293047; 19, 20 – UBGD 293048; 21, 22 – UBGD 293050; 23 – UBGD 293049; 24, 25 – UBGD 293043.

Scale bar is 10 mm.

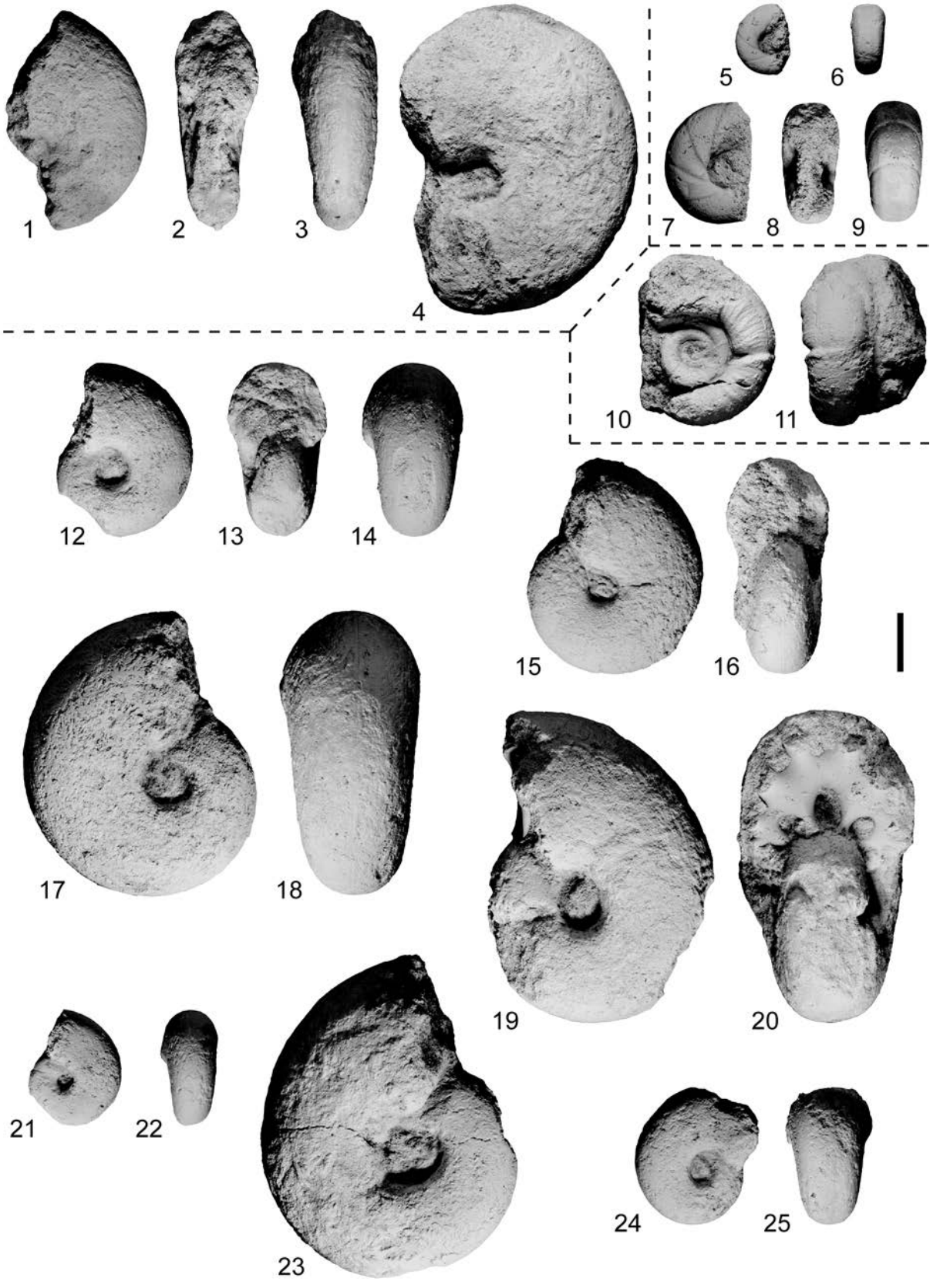
1
2
3
4
5
6
7
8
9
10
11
12
13
14
15
16
17
18
19
20
21
22
23
24
25

PLATE 2

1-9 – *Puzosia* (*Puzosia*) *mayoriana* (d'Orbigny, 1841). 1, 2 – UBGD 293001; 3 – UBGD 293006; 4-6 – UBGD 293005; 7-9 – UBGD 293007.

Scale bar is 10 mm.


1
*?
2
?*
3
4
*
5
6
7
*
8
9

PLATE 3

1-8 – *Puzosia* (*Puzosia*) *mayoriana* (d'Orbigny, 1841). 1-3 – UBGD 293008; 4, 5 – UBGD 293012; 6-8 – UBGD 293013.

9-15 – *Callihoplites* cf. *cratus* (Seeley, 1865). 9-11 – UBGD 293056; 12, 13 – UBGD 293060; 14, 15 – UBGD 293058.

16-19 – *Callihoplites tetragonus* (Seeley, 1865), UBGD 293287.

20-24 – *Lepthoplites* cf. *cantabrigiensis* Spath, 1925. 20, 21 – UBGD 293061; 22, 23 – UBGD 293062.

25-28 – *Discohoplites* cf. *valbonnensis* (Hébert and Munier-Chalmas, 1875), UBGD 293063.

29-32 – *Arrhaphoceras* (*Arrhaphoceras*) *substuderi* Spath, 1928. 29 – UBGD 293053; 30-32 – UBGD 293054.

Scale bar is 10 mm.

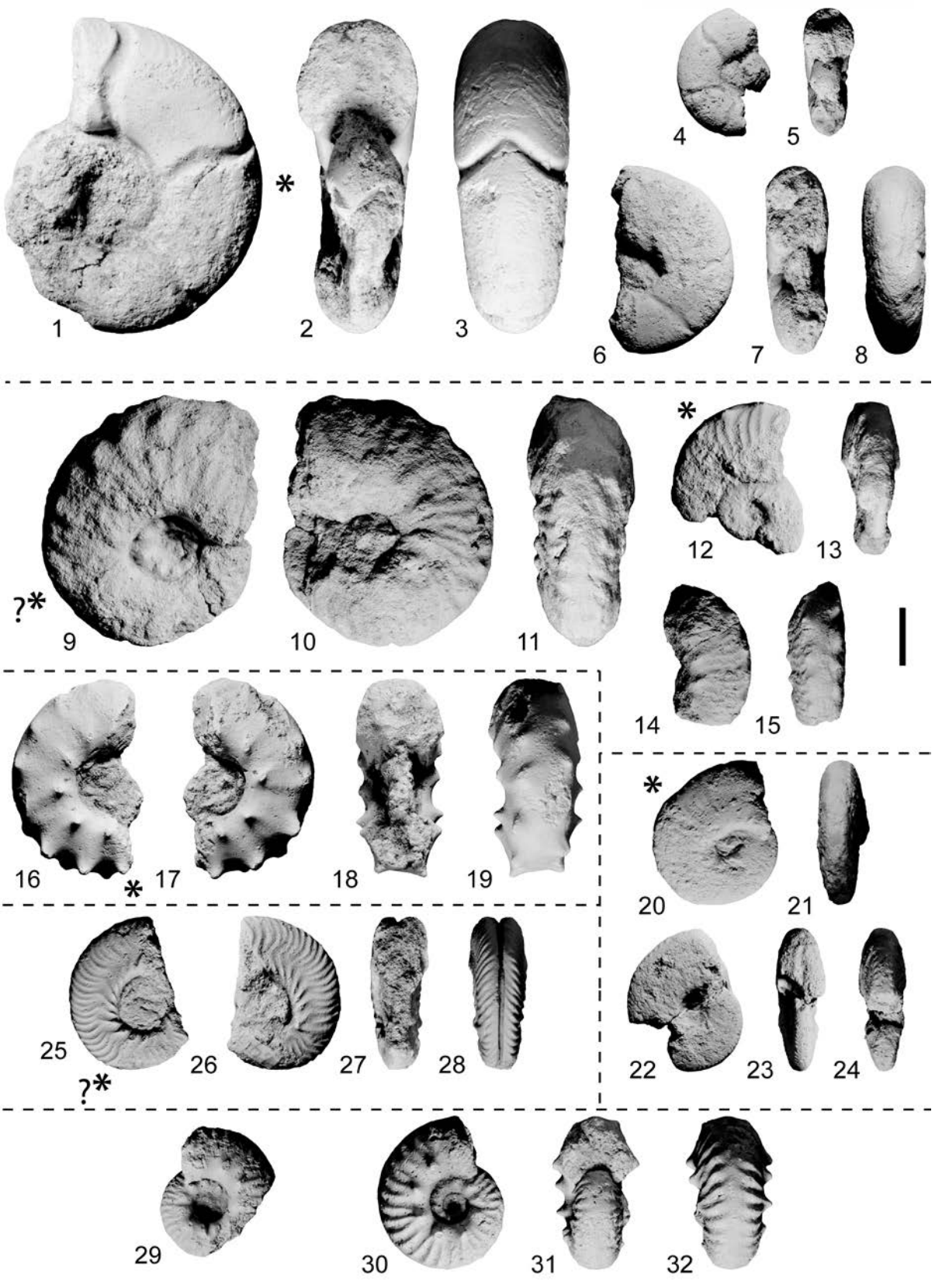
1
*
2
3
4
5
6
7
8
?*
9
10
11
*
12
13
14
15
16
*
17
18
19
*
20
21
22
23
24
25
?*
26
27
28
29
30
31
32

PLATE 4

1-12 – *Stoliczkaia* (*Stoliczkaia*) *dispar* (d'Orbigny, 1841). 1, 2 – UBGD 293021; 3, 4 – UBGD 293020; 5-7 – UBGD 293017; 8, 9 – UBGD 293018; 10-12 – UBGD 293019.

Scale bar is 10 mm.


1
*
2
3
*
4
5
*?
6
7
8
*?
9
10
*?
11
12

PLATE 5

1-23 – *Stoliczkaia* (*Stoliczkaia*) *dispar* (d'Orbigny, 1841). 1-3 – UBGD 293024; 4-6 – UBGD 293023; 7-9 – UBGD 293022; 10-12 – UBGD 293025; 13-15 – UBGD 293034; 16, 17 – UBGD 293037; 18-20 – UBGD 293035; 21-23 – UBGD 293036.

Scale bar is 10 mm.

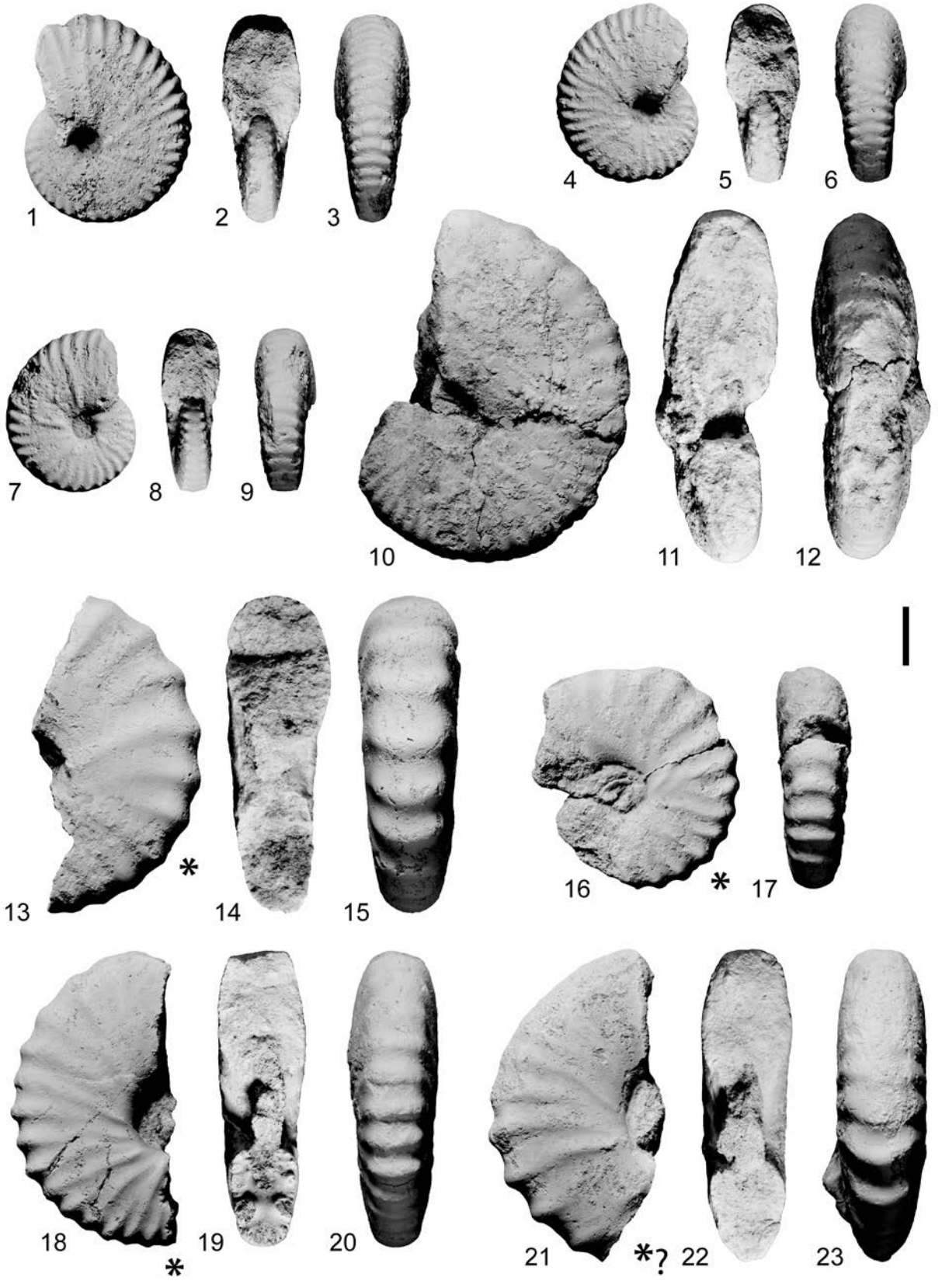
1
2
3
4
5
6
7
8
9
10
11
12
13
*
14
15
16
*
17
18
*
19
20
21
*?
22
23

PLATE 6

Mortoniceras (*Subschloenbachia*) *rostratum* (J. Sowerby, 1817), UBGD 293118.

Scale bar is 10 mm.


*
1

PLATE 7

1, 2 – *Mortoniceras* (*Subschloenbachia*) *rostratum* (J. Sowerby, 1817), UBGD 293118.

Scale bar is 10 mm.

1

2

PLATE 8

1-4 – *Mortoniceras* (*Subschloenbachia*) *rostratum* (J. Sowerby, 1817), UBGD 293117.

Scale bar is 10 mm.

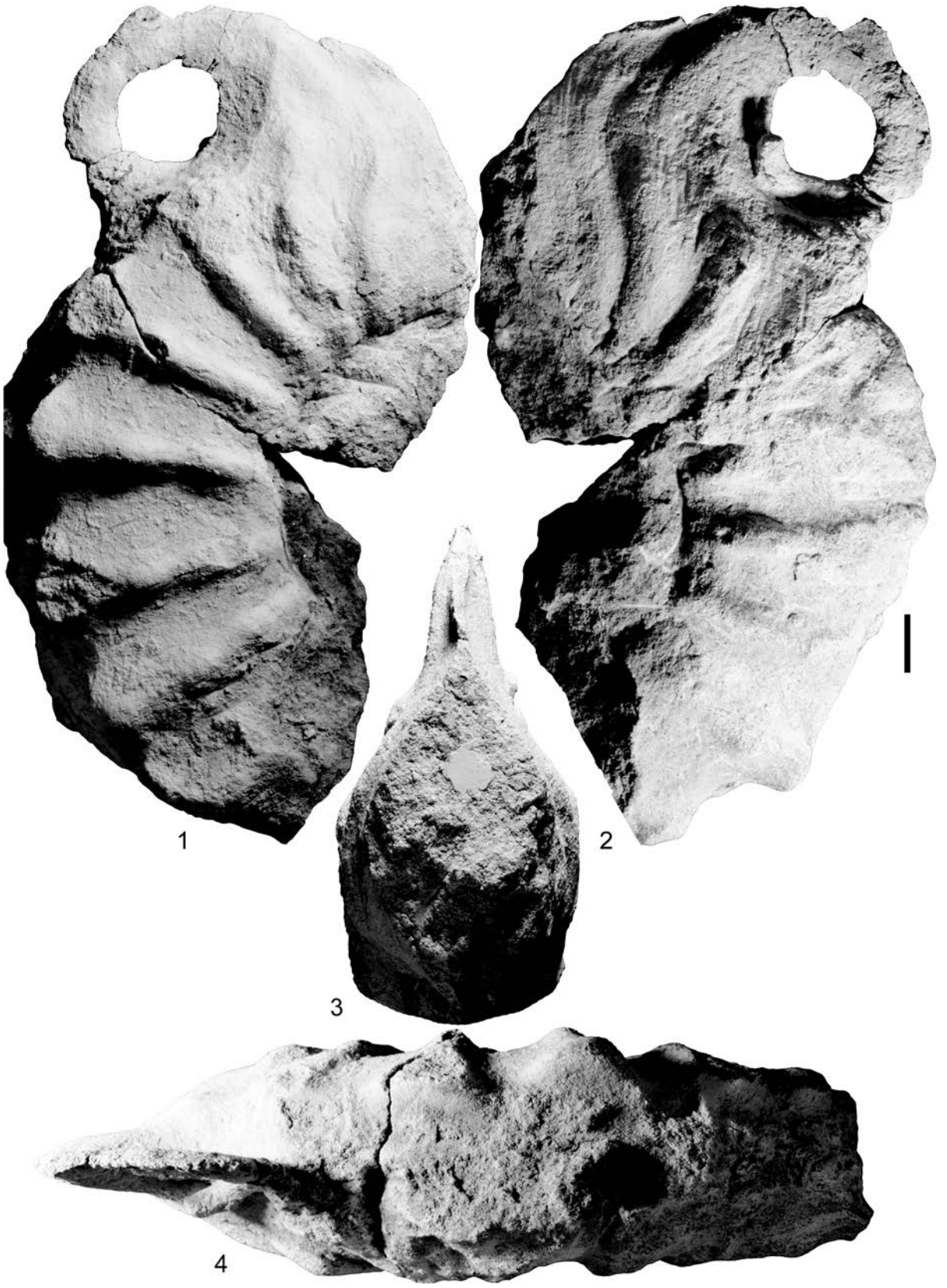
1
2
3
4

PLATE 9

1-4 – *Mortoniceras* (*Subschloenbachia*) *rostratum* (J. Sowerby, 1817). 1, 2 – UBGD 293118; 3, 4 – UBGD 293117.

Scale bar is 10 mm.

1

2

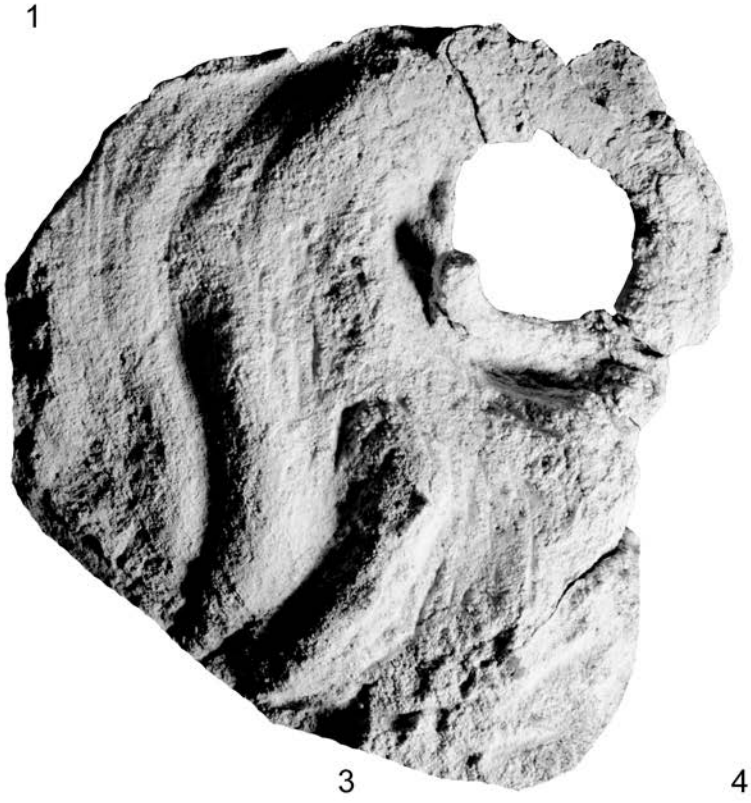

3

4

PLATE 10

1-3 – *Mortoniceras* (*Subschloenbachia*) *rostratum* (J. Sowerby, 1817), UBGD 293119.

Scale bar is 10 mm.

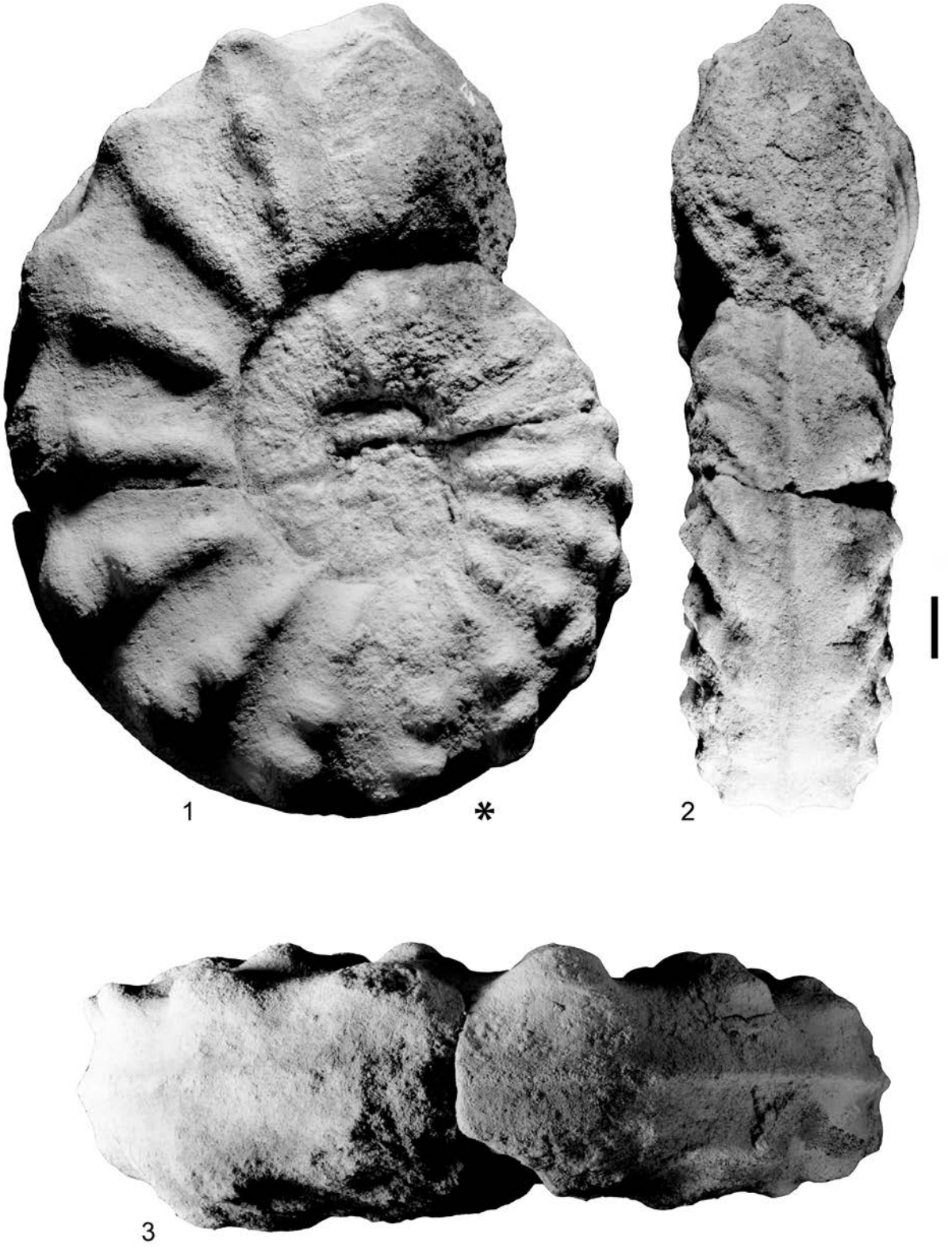
1
*
2
3

PLATE 11

1-8 – *Mortoniceras* (*Subschloenbachia*) *rostratum* (J. Sowerby, 1817). 1-3 – UBGD 293114; 4-6 – UBGD 293107; 7, 8 – UBGD 293106.

Scale bar is 10 mm.

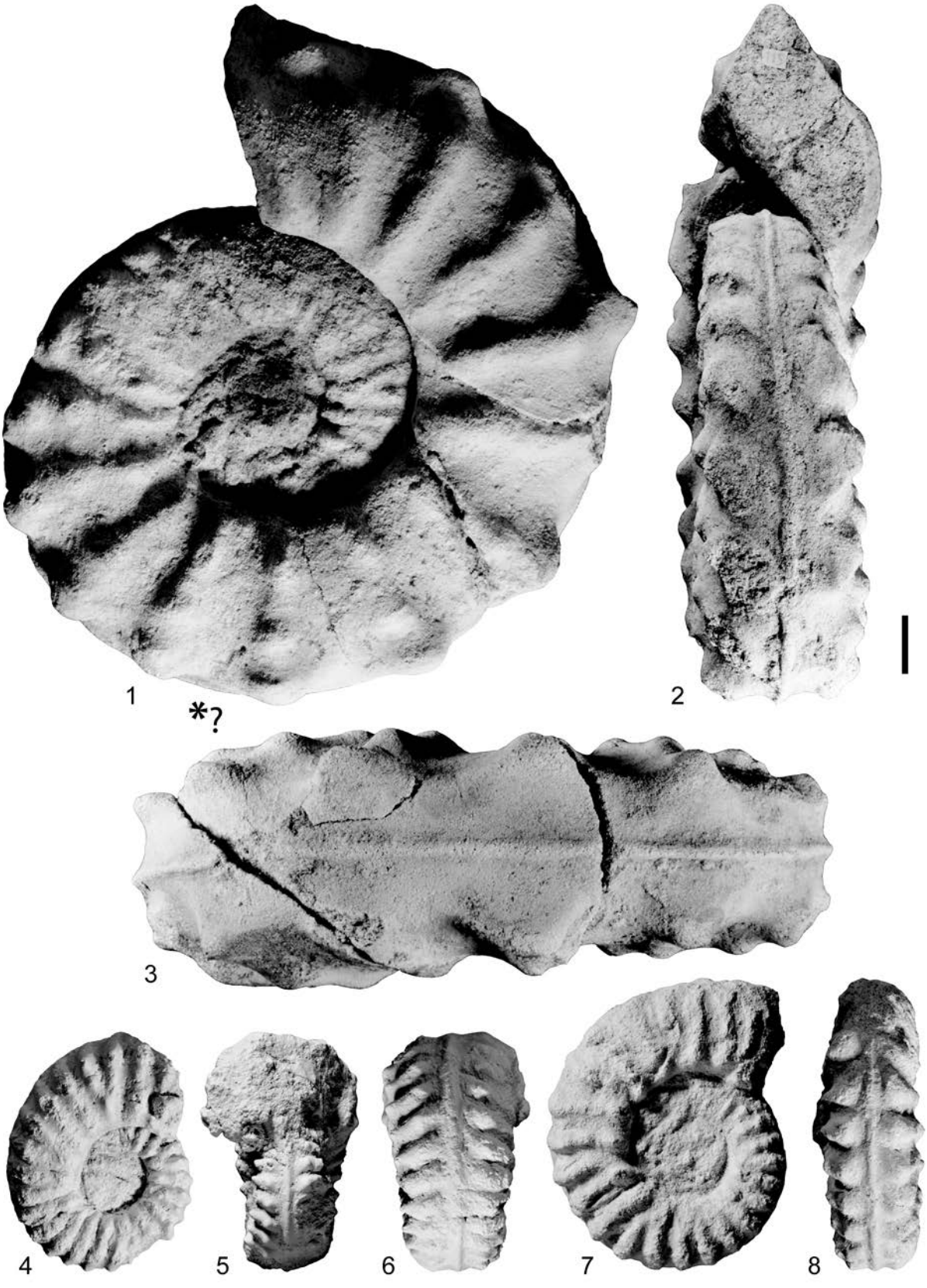
1
*?
2
3
4
5
6
7
8

PLATE 12

1-4 – *Mortoniceras* (*Subschloenbachia*) *rostratum* (J. Sowerby, 1817). 1, 2 – UBGD 293113; 3, 4 – UBGD 293110.

Scale bar is 10 mm.

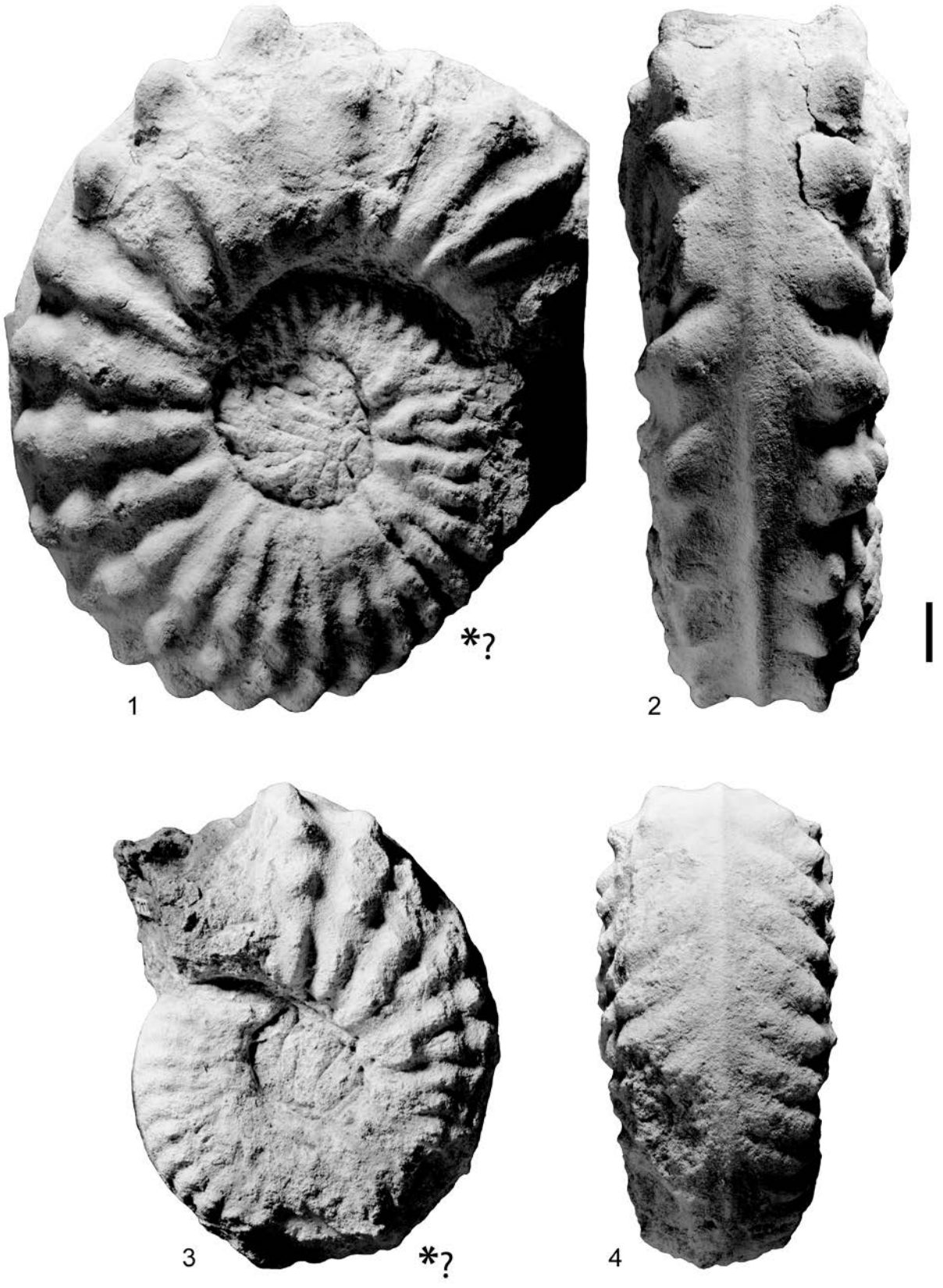
*?
1
2
3
*?
4

PLATE 13

1-15 – *Mortoniceras* (*Subschloenbachia*) *rostratum* (J. Sowerby, 1817). 1-3 – UBGD 293104; 4-6 – UBGD 293103; 7-9 – UBGD 293100; 10-12 – UBGD 293109; 13-15 – UBGD 293108.

Scale bar is 10 mm.

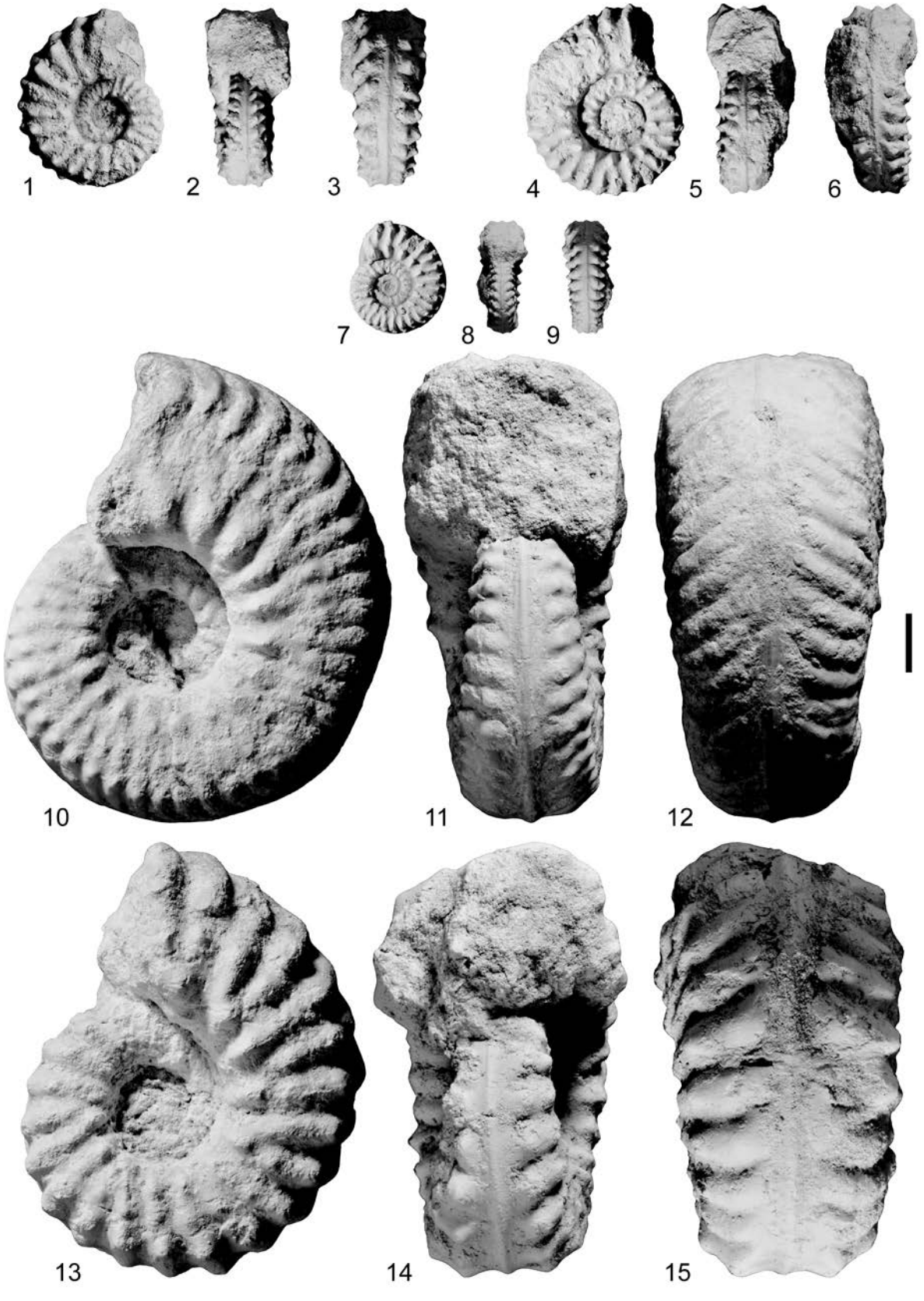
1
2
3
4
5
6
7
8
9
10
11
12
13
14
15

PLATE 14

1-13 – *Scaphites hugardianus* d'Orbigny, 1842. 1-3 – UBGD 293064; 4, 5 – UBGD 293065; 6, 7 – UBGD 293066. 8, 9 – UBGD 32632 (specimen from the *Mortoniceras fallax* Zone at Salazac; original of Jattiot *et al*. 2021, fig. 19O-P); 10, 11 – UBGD 32638 (specimen from the *Mortoniceras fallax* Zone at Salazac; original of Jattiot *et al*. 2021, fig. 19Q-R); 12, 13 – UBGD 32639 (specimen from the *Mortoniceras fallax* Zone at Salazac; original of Jattiot *et al*. 2021, fig. 19S-T).

14-30 – *Scaphites meriani* Pictet and Campiche, 1861. 14, 15 – UBGD 293067; 16-19 – UBGD 293072; 20-22 – UBGD 293070; 23-26 – UBGD 293073; 27-30 – UBGD 293074.

Scale bar is 10 mm.

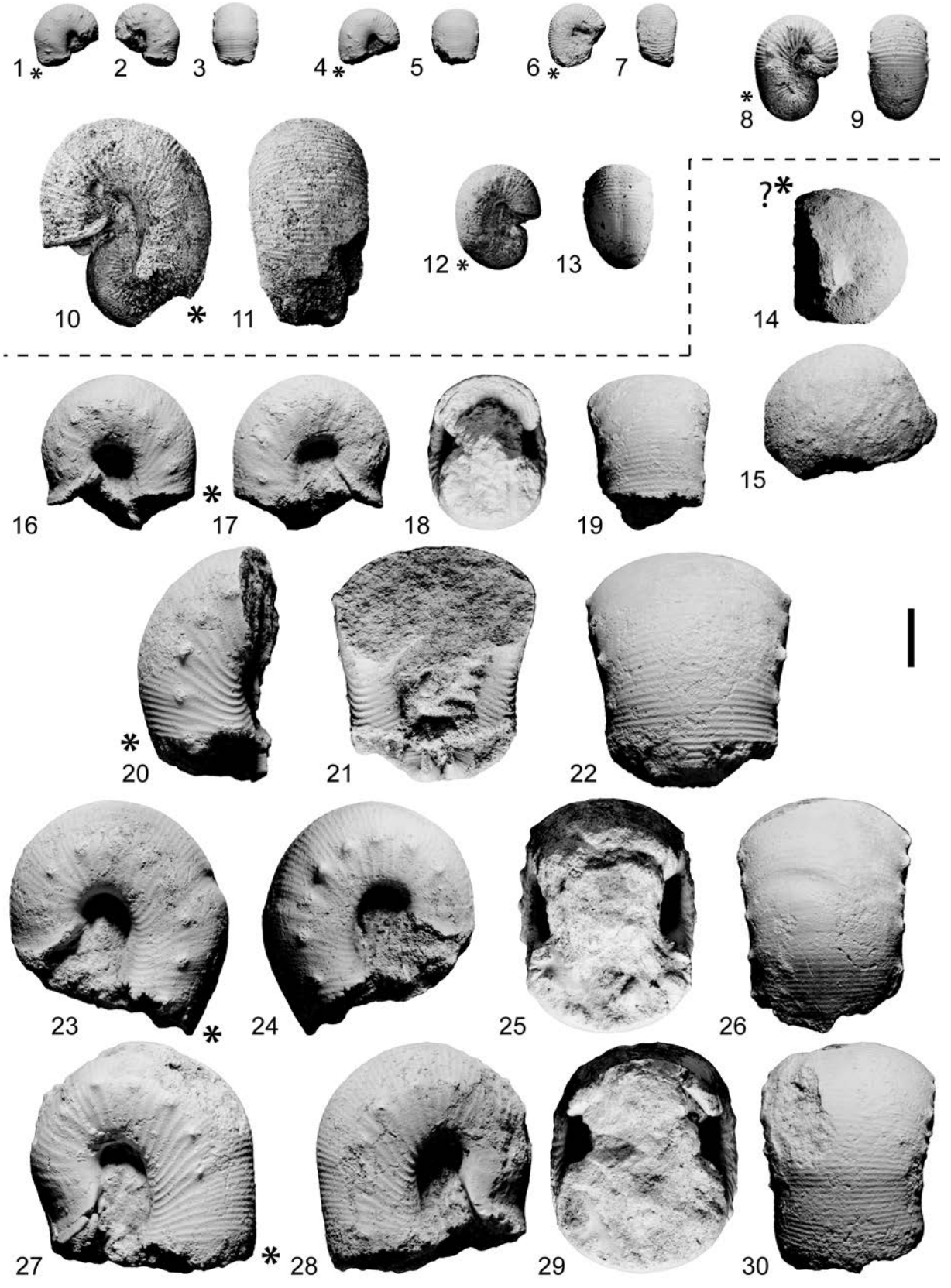
1 *
2
3
4 *
5
6 *
7
* 8
9
10 *
11
12 *
13
?*
14
15
16
* 17
18
19
* 20
21
22
23 *
24
25
26
27 *
28
29
30

PLATE 15

1-8 – *Mariella* (*Mariella*) *miliaris* (Pictet and Campiche, 1861). 1, 2 – UBGD 293186; 3-5 – UBGD 293205; 6-8 – UBGD 293241.

9-40 – *Mariella* (*Mariella*) *bergeri* (Brongniart, 1822). 9 – UBGD 293194; 10, 11 – UBGD 293197; 12 – UBGD 293195; 13 – UBGD 293207; 14 – UBGD 293212; 15, 16 – UBGD 293211; 17-19 – UBGD 293218, arrow indicates a very minor disruption in the arrangement of the tubercles; 20 – UBGD 293213; 21 – UBGD 293223; 22 – UBGD 293217; 23-25 – UBGD 293235; 26, 27 – UBGD 293243; 28 – UBGD 293253; 29-31 – UBGD 293248; 32, 33 – UBGD 293246; 34, 35 – UBGD 293256; 36-38 – UBGD 293247; 39, 40 – UBGD 293224, arrows indicate very minor disruptions in the arrangement of the tubercles.

Scale bar is 10 mm.

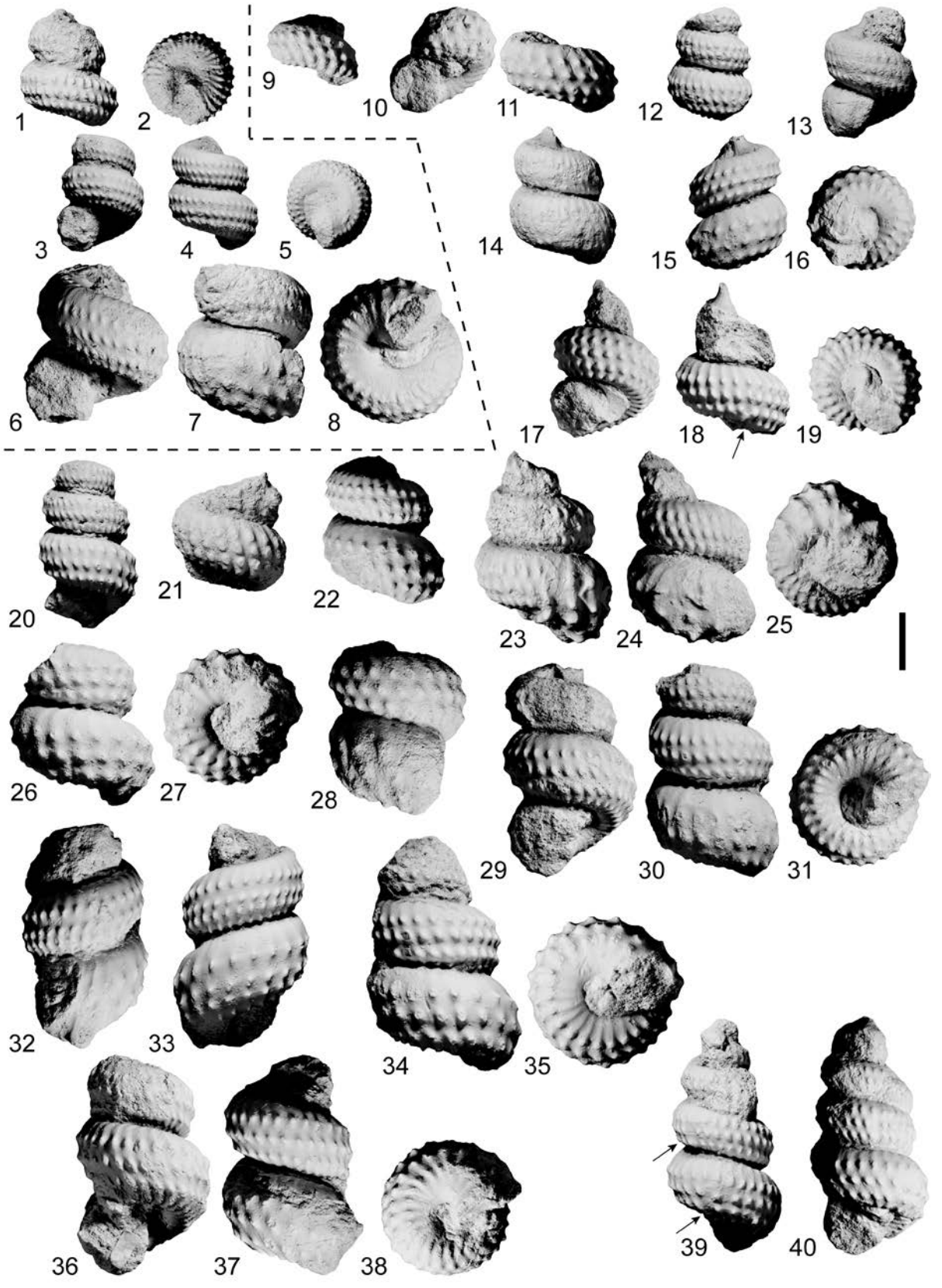
1
2
9
10
11
12
13
3
4
5
14
15
16
6
7
8
17
18
19
20
21
22
23
24
25
26
27
28
29
30
31
32
33
34
35
36
37
38
39
40

PLATE 16

1-19 – *Mariella* (*Mariella*) *bergeri* (Brongniart, 1822). 1-3 – UBGD 293261; 4 – UBGD 293258; 5-8 – UBGD 293215; 9-12 – UBGD 293255; 13, 14 – UBGD 293270; 15 – UBGD 293260; 16, 17 – UBGD 293263; 18, 19 – UBGD 293268.

Scale bar is 10 mm.

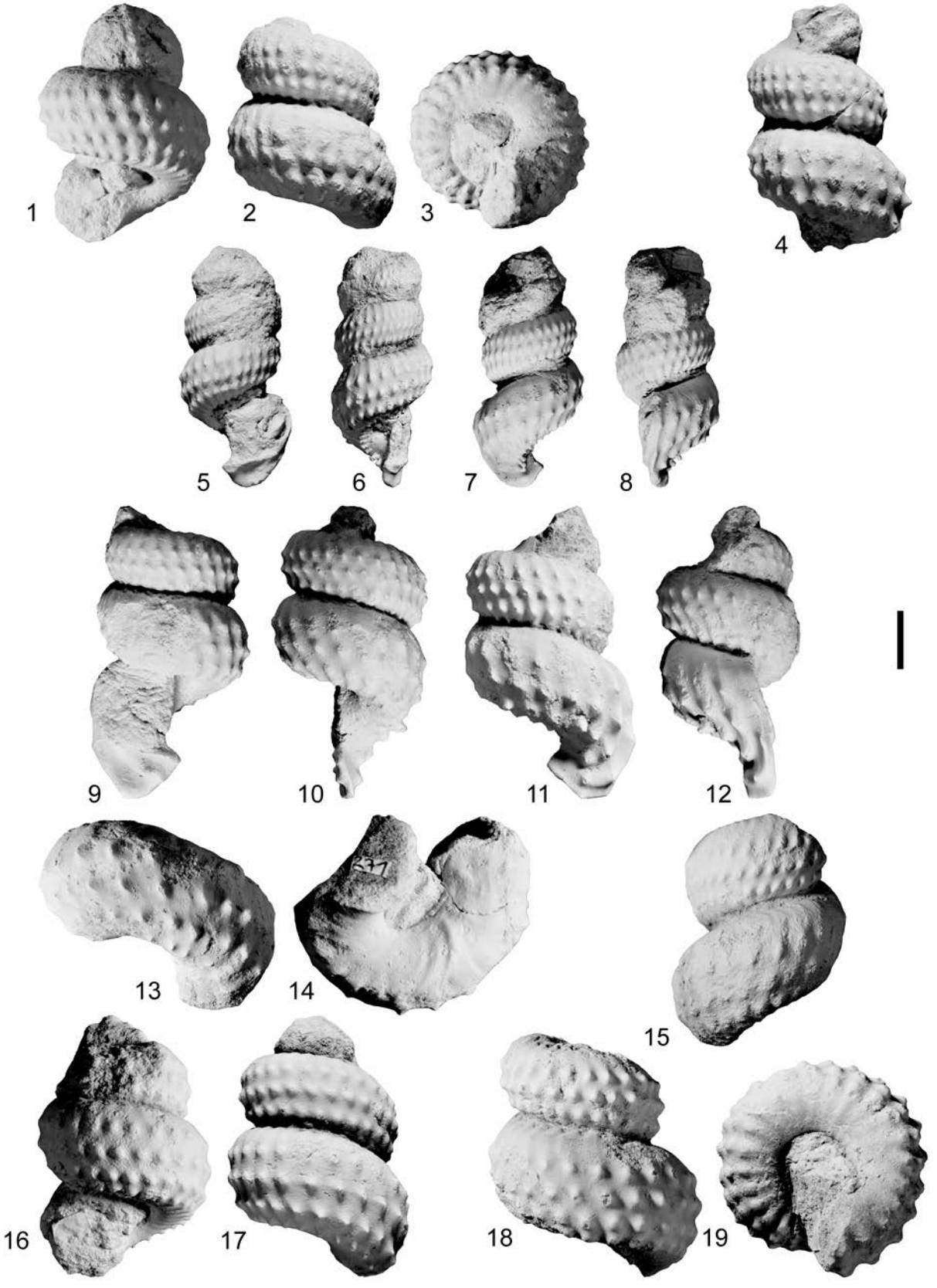
1
2
3
4
5
6
7
8
9
10
11
12
13
14
15
16
17
18
19

PLATE 17

1-20 – *Mariella* (*Mariella*) *bergeri* (Brongniart, 1822). 1-3 – UBGD 293259; 4-6 – UBGD 293249; 7 – UBGD 293245; 8, 9 – UBGD 293262; 10 – UBGD 293273; 11 – UBGD 293266; 12 – UBGD 293267; 13-15 – UBGD 293264; 16 – UBGD 293271; 17, 18 – UBGD 293274; 19, 20 – UBGD 293275.

Scale bar is 10 mm.

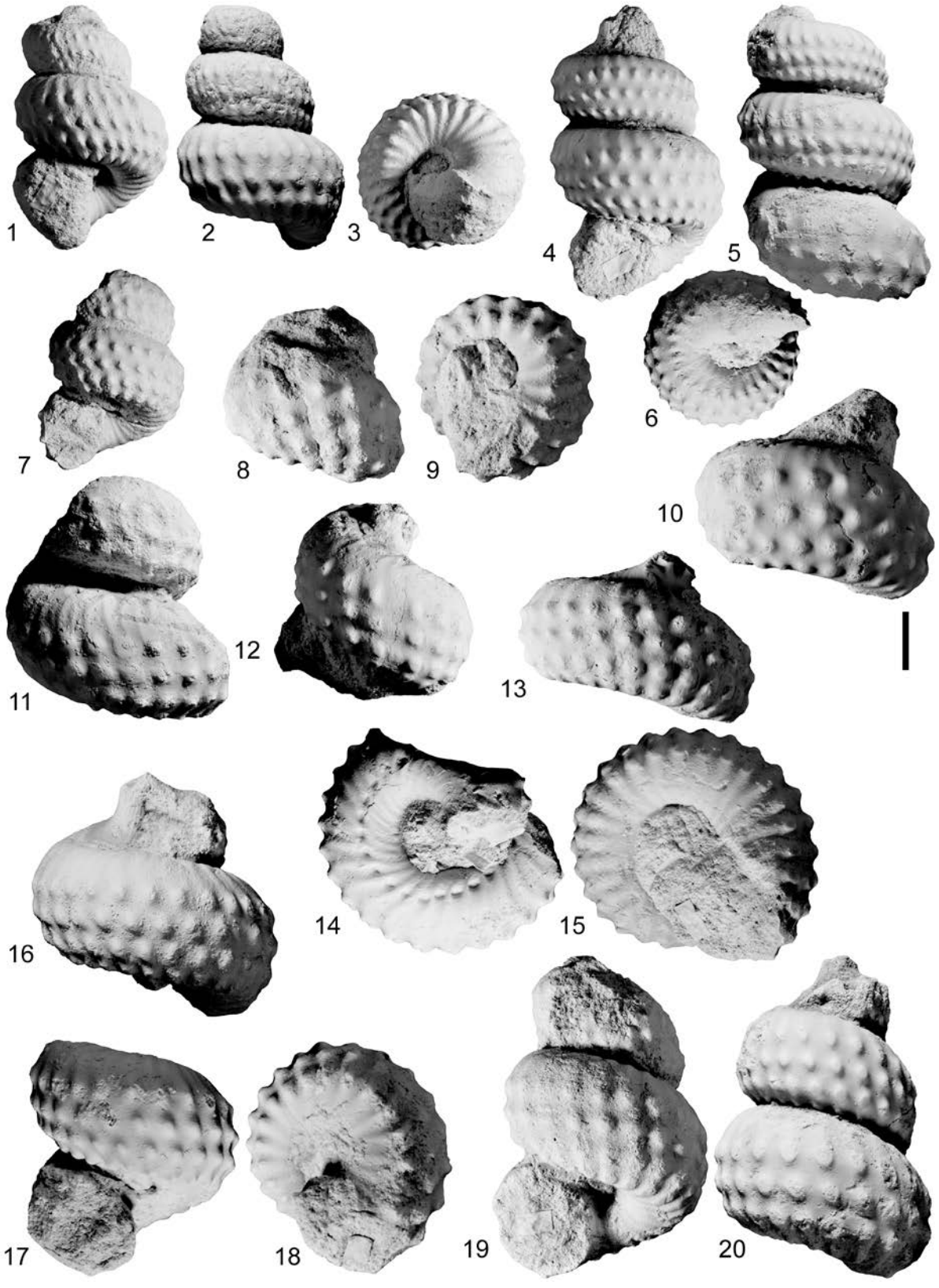
1
2
3
4
5
6
7
8
9
10
11
12
13
14
15
16
17
18
19
20

PLATE 18

1-6 – *Mariella* (*Mariella*) *bergeri* (Brongniart, 1822). 1-3 – UBGD 293281; 4 – UBGD 293282; 5, 6 – UBGD 293276.

7-9 – *Mariella* (*Mariella*) *miliaris* (Pictet and Campiche, 1861), UBGD 293280.

10, 11 – *Mariella* sp. 2, UBGD 293192.

12 – *Mariella* sp. 1, UBGD 293294.

Scale bar is 10 mm.

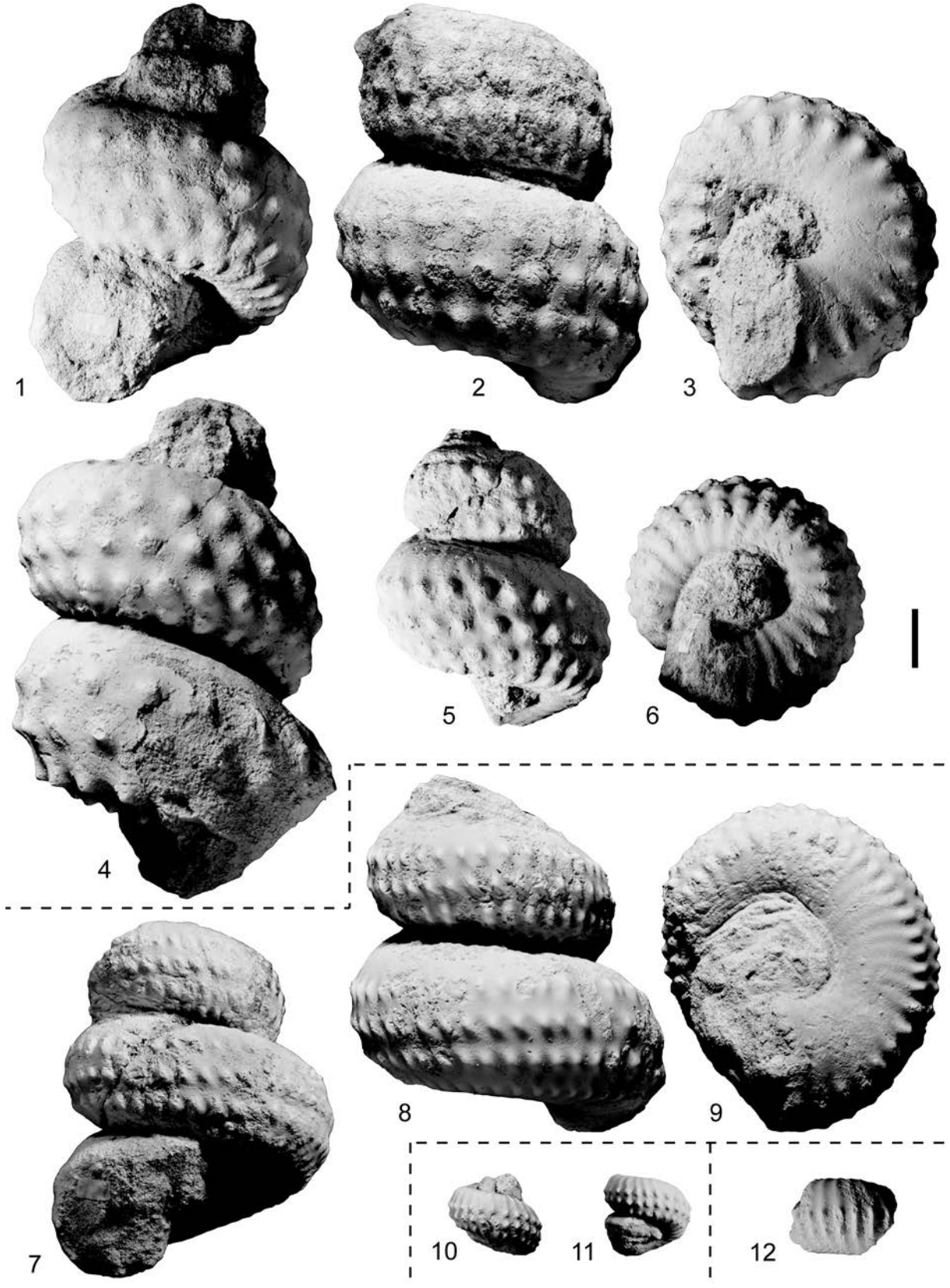
1
2
3
4
5
6
7
8
9
10
11
12

PLATE 19

1-10 – *Anisoceras armatum* (J. Sowerby, 1817). 1, 2 – UBGD 293090; 3, 4 – UBGD 293092; 5, 6 – UBGD 293091; 7, 8 – UBGD 293088; 9, 10 – UBGD 293093.

Scale bar is 10 mm.

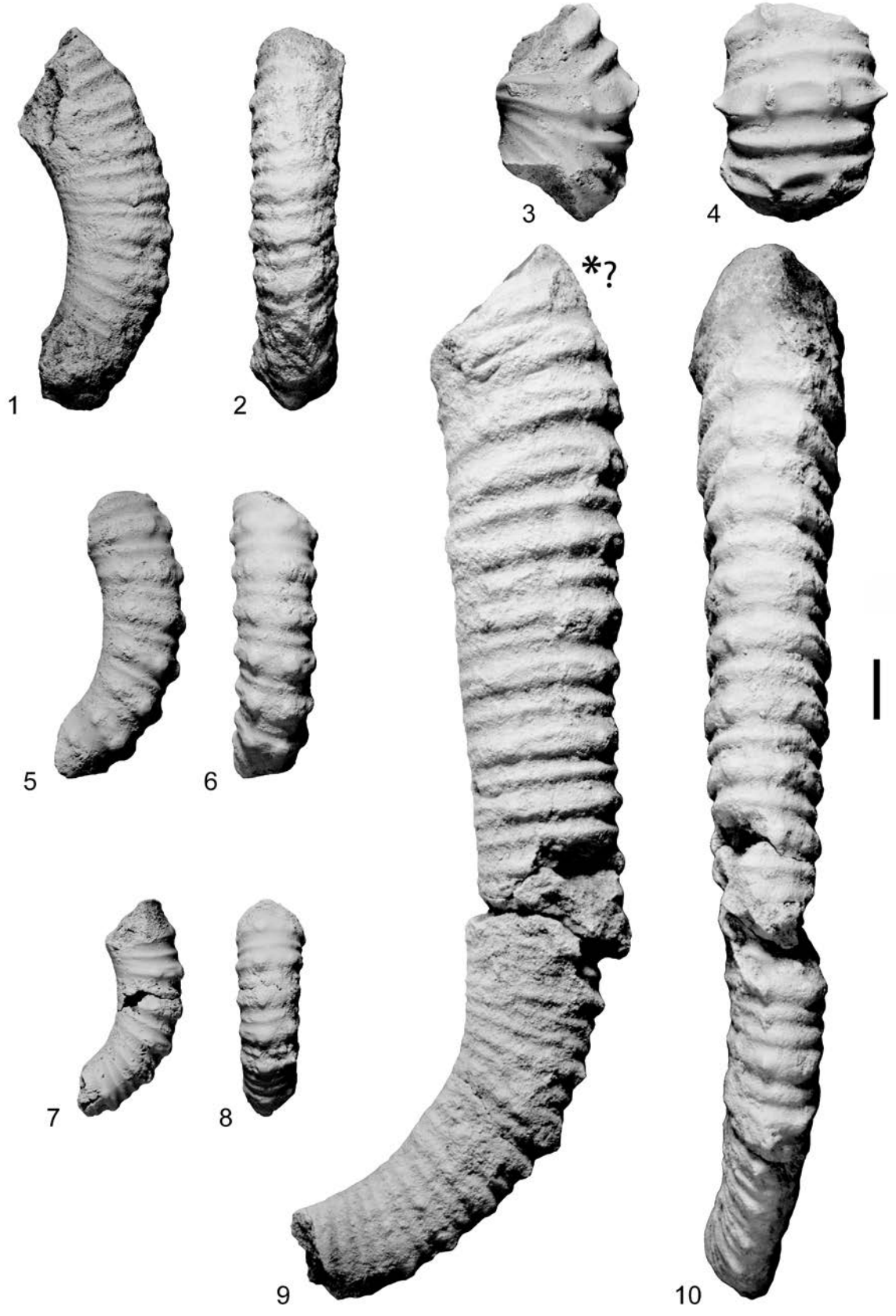
1
2
3
4
*?
5
6
7
8
9
10

PLATE 20

1-3 – *Anisoceras perarmatum* Pictet and Campiche, 1861, UBGD 293075.

Scale bar is 10 mm.

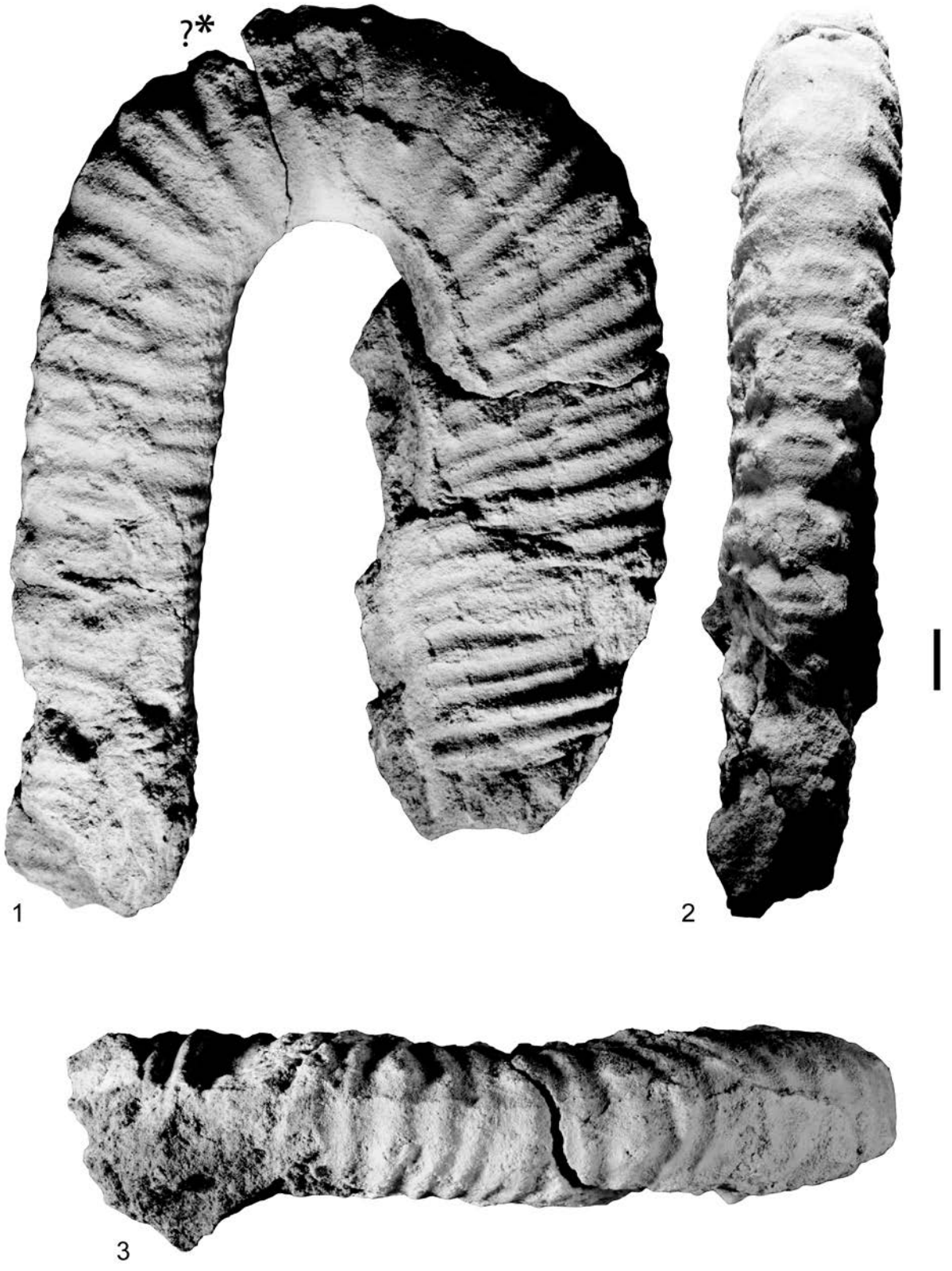
?*
1
2
3

PLATE 21

1-8 – *Anisoceras perarmatum* Pictet and Campiche, 1861. 1-3 – UBGD 293076; 4 – UBGD 293082; 5, 6 – UBGD 293079; 7, 8 – UBGD 293080.

Scale bar is 10 mm.

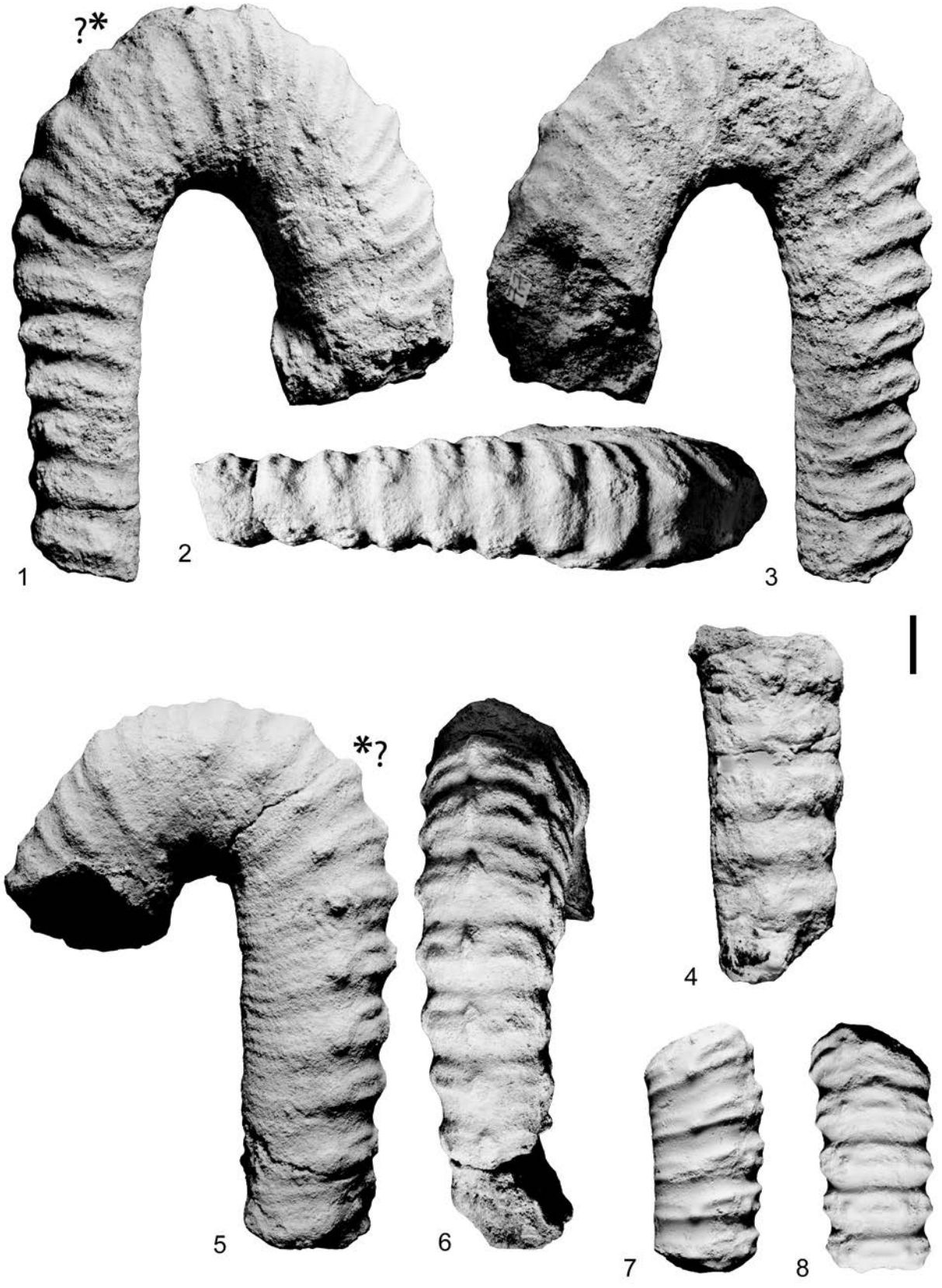
?*
1
2
3
*?
4
5
6
7
8

PLATE 22

1-7 – *Anisoceras* sp. 1-3 – UBGD 293077; 4, 5 – UBGD 293078; 6 – UBGD 293085; 7 *pars* – UBGD 293098.

Scale bar is 10 mm.

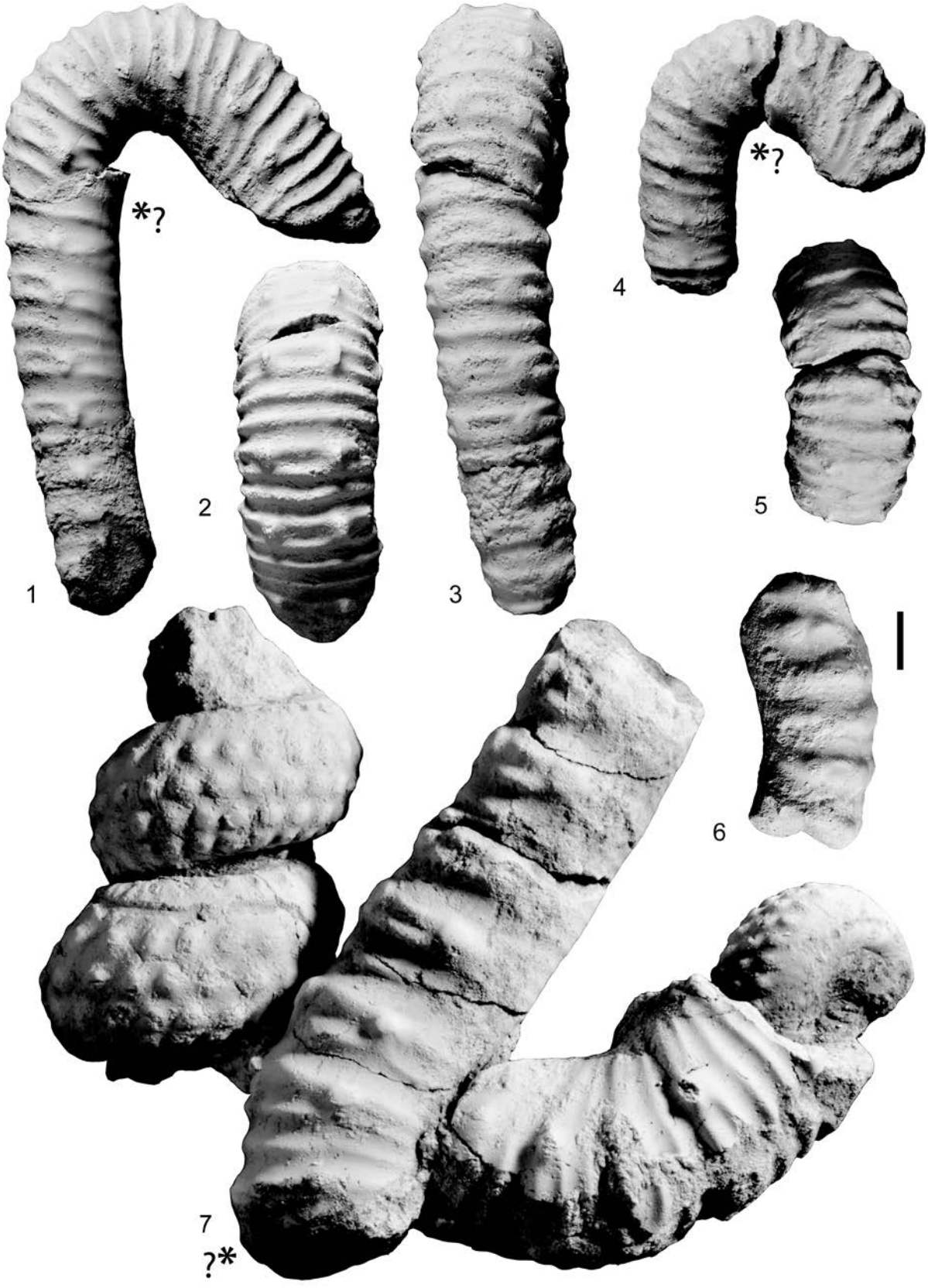
*?
1
2
3
*?
4
5
6
7
?*

PLATE 23

1-4 – *Anisoceras pseudoelegans* Pictet and Campiche, 1861. 1, 2 – UBGD 293094; 3, 4 – UBGD 293095.

5-7 – *Idiohamites elegantulus* Spath, 1939. 5 – UBGD 293150; 6, 7 – UBGD 293149. Figures 5-7 are X 0.75.

8-16 – *Lechites* (*Lechites*) *gaudini* (Pictet and Campiche, 1861). 8-10 – UBGD 293147; 11-13 – UBGD 293146; 14-16 – UBGD 293145.

17-19 – *Lechites* (*Lechites*) *moreti* Breistroffer, 1936, UBGD 293148.

Scale bar is 10 mm.

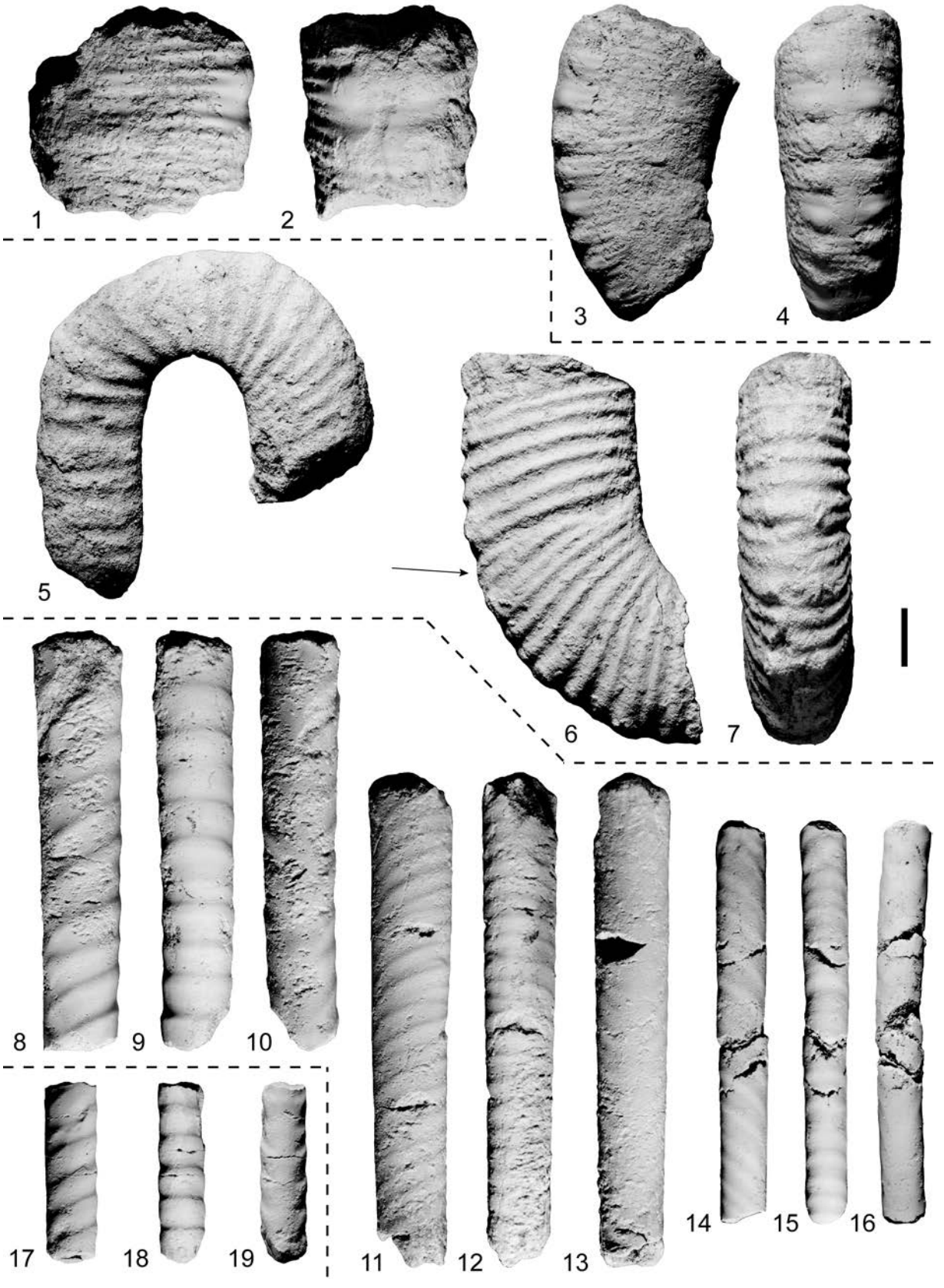
1
2
3
4
5
6
7
8
9
10
11
12
13
14
15
16
17
18
19

PLATE 24

1-23 – *Hamites virgulatus* Brongniart, 1822. 1-3 – UBGD 293155; 4, 5 – UBGD 293156; 6-8 – UBGD 293157; 9-11 – UBGD 293158; 12-14 – UBGD 293159; 15, 16 – UBGD 293171; 17, 18 – UBGD 293172; 19, 20 – UBGD 293178; 21, 22 – UBGD 293179; 23 – UBGD 293180.

24-31 – *Hamites duplicatus* Pictet and Campiche, 1861. 24-26 – UBGD 293181; 27-29 – UBGD 293182; 30, 31 – UBGD 293183.

32-35 – *Hamites venetzianus* Pictet in Pictet and Roux, 1847. 32, 33 – UBGD 293160; 34, 35 – UBGD 293161.

36-41 – *Hamites* sp. 36, 37 – UBGD 293152; 38 – UBGD 293153; 39-41 – UBGD 293154.

Scale bar is 10 mm.

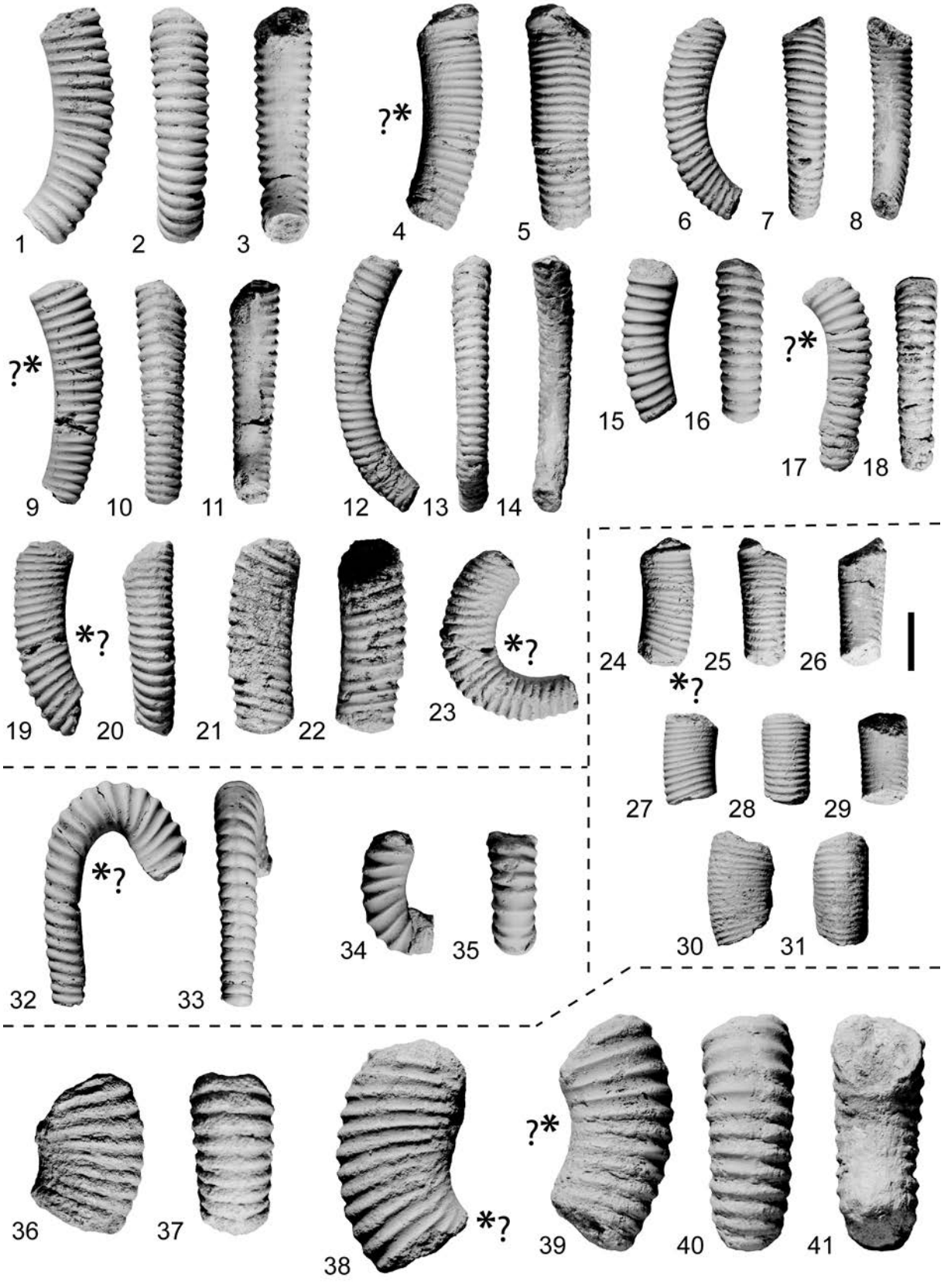
1
2
3
?*
4
5
6
7
8
?*
9
10
11
12
13
14
15
16
?*
17
18
*?
19
20
21
22
*?
23
24
25
26
*?
27
28
29
30
31
*?
32
33
34
35
36
37
*?
38
?*
39
40
41

PLATE 25

1-8 – *Eutrephoceras sublaevigatum* (Pervinquière, 1907). 1, 2 – UBGD 293290; 3-5 – UBGD 293291; 6, 7 – UBGD 293292; 8 – UBGD 293293.

Scale bar is 10 mm.

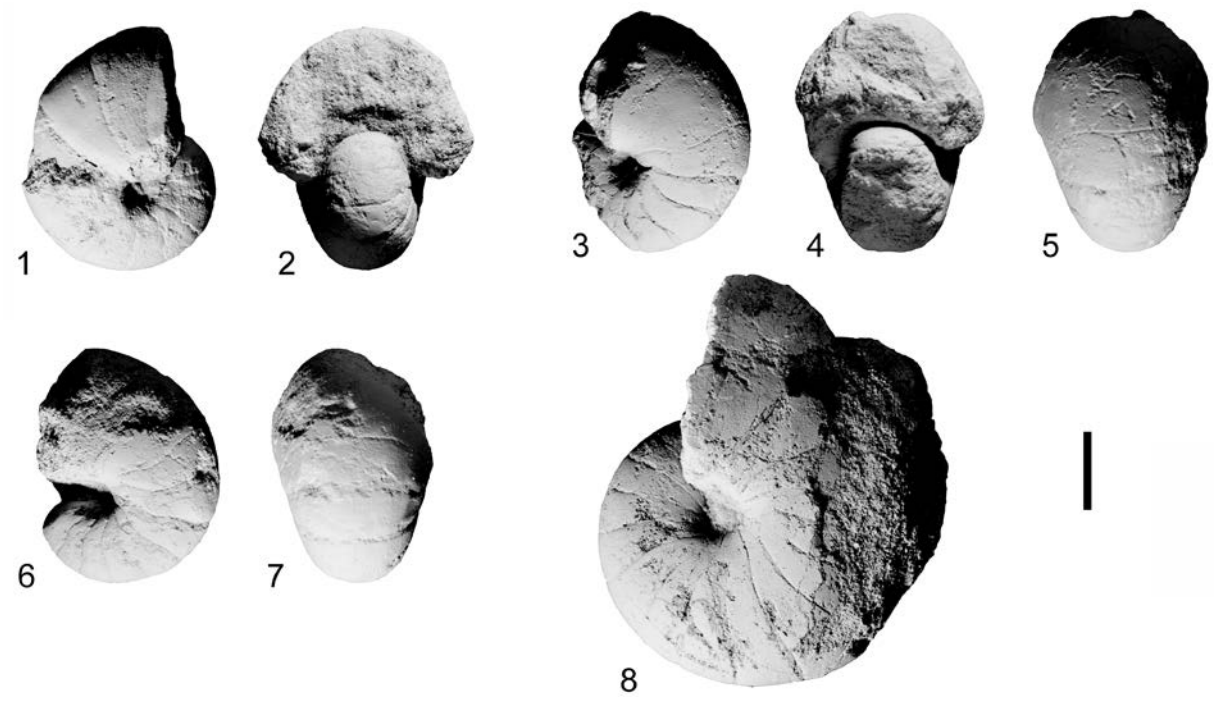
1
2
3
4
5
6
7
8